Role of Protein Kinase R in the immune response to tuberculosis

Robin Smyth

Thesis submitted to the University of Ottawa
in partial fulfillment of the requirements for the
MSc degree in Microbiology and Immunology

Department of Biochemistry, Microbiology and Immunology
Faculty of Medicine
University of Ottawa

University of Ottawa

PREFACE

Chapter 3 of this thesis has been published as an original research article in *Frontiers in Microbiology*:

Smyth, R., Berton, S., Rajabalee, N., Chan, T., Sun, J. 2021. Protein Kinase R restricts the intracellular survival of *Mycobacterium tuberculosis* by promoting selective autophagy. *Front. Microbiol.* 11: 613963. doi: 10.3389/fmicb.2020.613963. PMID: 33552025.

The specific contributions of each author to this paper are listed below:

Robin Smyth: Conceived, designed, and performed the experiments; analyzed the data; wrote and edited the manuscript.

Stefania Berton: Performed the western blot shown in Fig. 19B in this thesis; reviewed the manuscript.

Nusrah Rajabalee: Assisted with the generation of PKR overexpressing cells and qRT-PCR experiments; reviewed the manuscript.

Therese Chan: Performed preliminary trials of the bacterial survival experiment shown in Fig. 12; reviewed the manuscript.

Jim Sun: Conceived and designed the experiments; analyzed the data; wrote and edited the manuscript.

ABSTRACT

Tuberculosis (TB) is a deadly infectious lung disease caused by the pathogenic bacterium *Mycobacterium tuberculosis* (Mtb). The identification of macrophage signaling proteins exploited by Mtb during infection will enable the development of alternative host-directed therapies (HDT) for TB. HDT strategies will boost host immunity to restrict the intracellular replication of Mtb and therefore hold promise to overcome antimicrobial resistance, a growing crisis in TB therapy. Protein Kinase R (PKR) is a key host sensor that functions in the cellular antiviral response. However, its role in defense against intracellular bacterial pathogens is not clearly defined. Herein, we demonstrate that expression and activation of PKR is upregulated in macrophages infected with Mtb. Immunological profiling of human THP-1 macrophages that overexpress PKR (THP-PKR) showed increased production of IP-10 and reduced production of IL-6, two cytokines that are reported to activate and inhibit IFNγ-dependent autophagy, respectively. Indeed, sustained expression and activation of PKR reduced the intracellular survival of Mtb, an effect that could be enhanced by IFNγ treatment. We further demonstrate that the enhanced anti-mycobacterial activity of THP-PKR macrophages is mediated by a mechanism dependent on selective autophagy as indicated by increased levels of LC3-II that colocalize with intracellular Mtb. Consistent with this mechanism, inhibition of autophagolysosome maturation with bafilomycin A1 abrogated the ability of THP-PKR macrophages to limit replication of Mtb, whereas pharmacological activation of autophagy enhanced the anti-mycobacterial effect of PKR overexpression. As such, PKR represents a novel and attractive host target for development of HDT for TB, and our data suggest value in the design of more specific and potent activators of PKR.

ACKNOWLEDGEMENTS

First and foremost, I would like to extend a huge thank you to my supervisor, Dr. Jim Sun, for his continued support throughout my Master's degree. He was always available to help me when I needed it, yet still encouraged me to be independent. Thanks to him, I was able to acquire invaluable research experience in a supportive and engaging environment. The work presented in this thesis would not be possible without him.

I would also like to thank my fellow lab members for their feedback and support, with a special thanks to our research associate Dr. Stefania Berton. Stefania was always kind and patient when teaching me research techniques or explaining new scientific concepts to me. I would also like to thank Nusrah Rajabalee, not only for training me but also for her continued moral support and always being willing to accompany me on a coffee break!

Next, I would like to thank my Thesis Advisory Committee members, Dr. Subash Sad and Dr. Vanessa D'Costa, for their guidance and invaluable feedback during my graduate studies. I would also like to acknowledge financial support from Ontario Graduate Scholarship (OGS) and the University of Ottawa.

Finally, I would like to thank my family – especially my parents, Scott and Judy Smyth – for their endless support and encouragement. I would also like to thank my partner for being my #1 fan and never getting mad at me for running late when an experiment took longer than I had anticipated!

TABLE OF CONTENTS

LIST OF ABBREVIATIONS

2-AP – 2-aminopurine

AECs – Airway epithelial cells

AMPK – AMP-dependent protein kinase

AMs – Alveolar macrophages

APCs – Antigen-presenting cells

ATG – Autophagy-related protein

ATP – Adenosine triphosphate

A.U – Arbitrary units

BCG – Bacillus Calmette-Guérin

BEPP – 1*H*-benzimidazole1-ethanol,2,3-dihydro-2-imino-*a*-(phenoxymethyl)-3-(phenylmethyl)-,monohydrochloride

BSA – Bovine serum albumin

CCL – Chemokine (C-C motif) ligand

CFU – Colony forming units

cGAS – Cyclin GMP-AMP synthase

CI – Cell Index

CLRs – C-type lectin receptors

CML – Chronic myelogenous leukemia

CR – Complement receptors

DCs – Dendritic cells

DC-SIGN – Dendritic cell-specific adhesion molecule-3-grabbing non-integrin

DHBDC – 3-(2,3-dihydrobenzo[b][1,4]dioxin-6-yl)-5,7-dihydroxy-4H-chromen-4-one

DMEM – Dulbecco's Modified Eagle Medium

DosR – Dormancy survival regulator

dsDNA – Double stranded DNA

dsRBD – dsRNA binding domain

dsRBM – dsRNA binding motifs

dsRNA – Double-stranded RNA

ECMV – Encephalomyocarditis virus

EIF2α – Eukaryotic initiation factor-2 alpha subunit

Eis – Enhanced intracellular survival

EMB – Ethambutol

ERK – Extracellular-signal-regulated kinase

ESAT-6 – 6-kDa early secretory antigenic target

ESCRT – Endosomal sorting complex required for transport

ESX-1 – 6-kDa early secretory antigenic target secretion system-1

FADD – Fas-associated protein with death domain

FDA – Food and Drug Administration

GAP – GTPase activating protein

GCN2 – General control non-depressible 2

GFP – Green fluorescent protein

GTP – Guanosine triphosphate

HDT – Host-directed therapy

HIV – Human immunodeficiency virus

HRS – Hepatocyte growth factor-regulated tyrosine kinase substrate

HSV-1 – Herpes Simplex Virus-1

IκBα – Inhibitory κB alpha

IFNγ – Interferon gamma

IGRA – Interferon Gamma Release Assay

IKK – IκB kinase

IL – Interleukin

INH – Isoniazid

IP-10 – Interferon gamma-induced protein 10

IRF-3 – Interferon regulatory factor 3

ISGF3 – Interferon-stimulated gene factor 3

ISRE – Interferon-stimulated response element

JNK – c-Jun N-terminal kinase

LAM – Lipoarabinomannan

LC3 – microtubule-associated proteins 1A/B light chain 3B

Lipopolysaccharide – LPS

LTBI – Latent TB infection

ManLAM – Mannose-capped lipoarabinomannan

MAPK – Mitogen-activated protein kinase

MCP-1 – Monocyte chemoattractant protein-1

MDA5 – Melanoma differentiation-associated gene 5

MDC – Minimum detectable concentration

MDMs – Monocyte-derived macrophages

MDR-TB – Multidrug resistant TB

MEFs – Mouse embryonic fibroblasts

Met-tRNAi – Initiator methionyl transfer RNA

MHC – Major histocompatibility complex

MKK – MAPK kinase

MLKL – Mixed lineage kinase domain-like pseudokinase

MOI – Multiplicity of infection

MR – Mannose receptor

mRNA – messenger RNA

Mtb – *Mycobacterium tuberculosis*

mTOR – Mammalian target of rapamycin

NADPH – Nicotinamide adenine dinucleotide phosphate

Ndk – Nucleoside diphosphate kinase

NF-κB – Nuclear factor kappa-light-chain enhancer of activated B cells

NK – Natural killer

NLRP3 – NOD-like receptor family pyrin domain containing 3

NO – Nitric oxide

NTM – Non-tuberculosis mycobacteria

NTZ – Nitazoxanide

PAMPs – Pathogen-associated molecular patterns

PBS – Phosphate buffered saline

PCR – Polymerase chain reaction

PERK – PKR-like endoplasmic reticulum kinase

PI3K – Phosphoinositide 3-kinase

PI3P – Phosphatidylinositol 3-phosphate

PKR – Interferon-induced, double-stranded RNA-activated protein kinase (Protein Kinase R)

PMA – Phorbol ester 13-phorbol-12-myristate acetate

Poly(I:C) – Polyinosinic:polycytidylic acid

PPM1A – Protein phosphatase Mg^{2+}/Mg^{2+}-dependent-1A

PRRs – Pattern recognition receptors

p-S403 – Phosphorylated serine 403

p-T446 – Phosphorylated threonine 446

PtpA – Protein-tyrosine phosphatase A

PZA – Pyrazinamide

qRT-PCR – Quantitative real-time polymerase chain reaction

RD1 – Region of difference 1

RIF – Rifampicin

RIG-I – Retinoid acid-inducible gene I

RIPK – Receptor-interacting serine/threonine protein kinase

RLU – Relative light units

ROS – Reactive oxygen species

RPMI – Roswell Park Memorial Institute

RTCA – Real-time cell analyzer

SapM – Secreted acid phosphatase

SEM – Standard error of the mean

Ser – Serine

sgRNA – Single guide RNA

SodA – Superoxide dismutase

STAT – Signal transducer and activator of transcription

STING – Stimulator of interferon genes

TB – Tuberculosis

TBK-1 – Tank-binding kinase-1

TBS-T – Tris buffered saline solution containing 0.5% tween-20

TGF-β – Transforming growth factor beta

THP-ΔPKR – THP-1 cells with a PKR knockout

THP-Ø – THP-1 cells expressing empty pMSCVpuro vector

THP-PKR –THP-1 cells overexpressing PKR

Thr – Threonine

TIRAP – Toll/interleukin-1 receptor domain-containing adapter protein

TLRs – Toll-like receptors

TNFα – Tumour necrosis factor alpha

TST – Tuberculin skin test

ULK – UNC-51-like autophagy activating kinase

V-ATPase – Vacuolar-$H(^{+})$-ATPase

WHO – World Health Organization

XDR-TB – Extensively drug-resistant TB

LIST OF FIGURES

3LIST OF TABLES

1. INTRODUCTION

1.1 Tuberculosis: Past, present, and future

1.1.1 History and epidemiology

Tuberculosis (TB) is an infectious respiratory disease caused by the pathogenic bacterium *Mycobacterium tuberculosis* (Mtb). Archeologists have found evidence of TB disease in human remains from 9,000 years ago (1), and genetic studies suggest that an early progenitor of Mtb infected primitive human ancestors 3 million years ago (2). By the 18th century, TB had become epidemic in Europe and North America. It is estimated that during the 16th -19th centuries, TB was responsible for approximately 25% of adult deaths in Europe, with comparable rates in North America (3). In 1943, following the discovery of antibiotics, Selman Waksman identified streptomycin as an anti-TB therapeutic (4), which was successfully used to cure a TB patient for the first time in 1949 (5).

Despite the development of antibiotics, TB remains the leading cause of infectious disease-related deaths worldwide. According to the World Health Organization (WHO) approximately one-quarter of the world's population is infected with Mtb, although only about 10% of these individuals will develop active TB disease and will be capable of transmitting the bacteria (6). In 2018, an estimated 10 million people globally fell ill with TB, with a global average of 130 new cases per 100,000 population (6). TB occurs in people of both sexes across all age groups, but men aged 15 years or older have the highest burden, accounting for 57% of total TB cases in 2018 (6). Women accounted for 32% and children aged less than 15 years old accounted for 11% (6). Risk factors for TB include malnutrition, overcrowding, poor sanitation, air pollution, and co-infection with diseases such as human immunodeficiency

virus (HIV) (7). Consequently, TB incidence rates vary tremendously between countries, with developing countries having the highest rates. Indeed, many developed countries such as Canada have fewer than 5 new cases per 100,000 population annually, whereas this incidence rate exceeds 500 in some developing countries (6). According to WHO, four countries accounted for half of the total global TB cases in 2018: India (27%), China (9%), Indonesia (8%), and the Philippines (6%) (6).

Although Canada has one of the lowest TB incidence rates in the world, the incidence rates among foreign-borne and Indigenous populations in Canada are comparable to certain developing countries. For instance, in 2016, the rate of TB in the foreign-born population was 26 times the rate in the Canadian-born non-Indigenous population (8). Although the TB incidence rate was only 4.8 cases per 100,000 population for Canada overall, the incidence rate in Nunavut was 142.9 cases per 100,000 population (8). Inadequate housing, food insecurity, and inequitable access to health care services are contributing factors to the high TB incidence rates in Nunavut (9).

1.1.2 *Mycobacterium tuberculosis*

Mtb is a non-motile, rod-shaped bacterium that was first isolated by Robert Koch in 1882 (10). The bacilli have a diameter of 0.3 – 0.5 μm and a length that can range from 1.5 – 4.0 μm (11, 12). Mtb is an obligate aerobe and humans are the sole reservoir. As a facultative intracellular pathogen, Mtb primarily resides in the replicative niche of host phagocytes. Hiding within phagocytes allows Mtb to avoid detection by circulating immune cells and provides a barrier to anti-TB drugs (13). Mtb is a slow-growing bacterium with a generation time of 16 – 20 hours (12).

Mtb is a highly successful human pathogen due to its unique cell wall structure and large repertoire of virulence proteins (14). The cell wall of Mtb is unique due to its high lipid and mycolic acid content. Mtb produces multiple unique and specialized glycolipids, including phthiocerol dimycocerosates, trehalose-6,-6-dimycolate, and phenolic glycolipids that contribute to its overall virulence by triggering or manipulating host cell receptors (14). Mycolic acids account for 50% of the dry weight of the Mtb cell wall and confer resistance to chemical injury, impermeability to hydrophilic drugs, and resistance to dehydration (15). The success of Mtb as a human pathogen can also be attributed to its mode of human-to-human transmission through airborne droplets, and it has a very low infectious dose, with an estimated median infective dose of 1 to 10 bacilli (16).

1.1.3 Clinical manifestation and diagnosis

Primary TB disease, which refers to the immediate onset of active TB disease following infection, occurs in approximately 5% of Mtb-infected individuals, although the risk is much higher in persons with severe immunocompromising conditions such as HIV-AIDs and children under 5 years of age (17). Individuals with active TB disease are contagious and symptomatic. Common symptoms include a persistent cough, chest pain, fever, night sweats, fatigue, weight loss, and lack of appetite. In approximately 90% of infected individuals, a structure known as a granuloma will successfully contain the infection. These individuals are said to have latent TB infection (LTBI) (17). A granuloma is an organized aggregate of immune cells, with pro-inflammatory cells in the center and anti-inflammatory cells along the periphery. The granuloma forms as a last-ditch effort to control Mtb growth and “wall off” infection from the rest of the body. Individuals with LTBI are asymptomatic

and non-contagious. However, roughly 5 – 10% of individuals with LTBI will progress to active TB infection later in life (17). This reactivation of Mtb infection is referred to as secondary TB disease, and the causes of Mtb reactivation remain elusive.

There are multiple tools for detecting Mtb infection, however it is important to distinguish between tools that identify LTBI versus active TB disease. The tuberculin skin test (TST) and Interferon Gamma Release Assay (IGRA) are the two tests available for identifying LTBI. For the TST, the patient is injected intradermally with tuberculin, a purified protein derivative extracted from Mtb. If the patient is infected with Mtb, tuberculin challenge will trigger a cell-mediated immune response, which will cause swelling at the injection site within 48 to 72 hours. The TST is a commonly used screening tool since it is low-cost and easy to perform. However, exposure to non-tuberculosis mycobacteria (NTM) or vaccination with the Bacillus Calmette-Guérin (BCG) vaccine can result in a positive result, since tuberculin is not specific to Mtb (18). The second test for LTBI is the IGRA. For this test, a blood sample is taken from the patient and *in vitro* tests are performed to measure the release of interferon gamma (IFNγ) from T cells following stimulation by Mtb antigens. The specific antigens used for this test are encoded by the region of difference 1 (RD1) locus, a genomic region required for full virulence of Mtb (19). BCG and most NTM do not possess the RD1 locus in their genome and consequently do not produce these RD1-encoded antigens (20). As such, the IGRA has a higher specificity than the TST. Importantly, neither the TST nor the IGRA can distinguish between LTBI or active TB disease. Therefore, if an individual has a positive result from a TST or IGRA, further steps must be taken to make a clinical diagnosis of active TB disease. If active TB disease is suspected, a chest x-ray can be performed as a screening tool. Chest X-rays are used to detect lung abnormalities such as cavities, lesions, and edema that

can arise due to active pulmonary TB disease. Abnormal chest X-rays are suggestive of TB disease but are not specific. As such, clinical identification of Mtb in the patient's sputum must occur for a diagnosis of active TB disease.

There are 3 methods used to detect Mtb in the sputum: sputum smear microscopy, sputum culture, or nucleic acid amplification. Sputum microscopy and culture both rely on visual identification of bacteria. Given the slow rate of Mtb growth, time is a major limitation in sputum culture, and results in delayed initiation of anti-TB therapy. As such, nucleic acid amplification tests such as the Xpert MTB/RIF assay are becoming more popular for TB diagnostics (21). Xpert MTB/RIF uses an automated polymerase chain reaction to specifically amplify Mtb nucleic acids present in the sputum sample, which is a much faster and more sensitive approach than sputum smear (22). Overall, molecular tests allow for rapid and accurate diagnosis of active TB disease, however they are costlier to perform than sputum smears or sputum cultures.

1.1.4 Vaccination

Currently, the only licensed vaccine for TB is BCG. The BCG vaccine was made by sub-culturing *Mycobacterium bovis* to produce an attenuated strain that may confer cross immunity to Mtb. The BCG vaccine was first administered in 1921 and continues to be administered in many countries nearly 100 years later. However, the efficacy of BCG is highly variable (0 to 80%) (23, 24), and only provides limited protection in adults (23). Meta-analyses have shown that BCG vaccination offers protection against active TB disease in children, including severe extrapulmonary TB disease (23, 25). Since children under 5 years old have high morbidity and mortality to TB (26), the BCG vaccine is invaluable for this age group. As

such, BCG vaccination is common practice in developing countries with higher rates of active TB disease. However, it is uncommon for BCG to be administered in developed countries due to its uncertain efficacy in adults. There are four potential explanations for the variability in BCG efficacy. First, it is speculated that exposure to NTM confers some resistance to Mtb and therefore BCG will not be effective in certain NTM-exposed individuals (27). Alternatively, some reports have shown that concurrent parasite infection may reduce the protective immune response to BCG vaccination (28). It is also possible that genetic variation in BCG strains can influence the protective efficacy (29, 30). Lastly, it has been speculated that genetic variations in human populations may contribute to the variability in BCG efficacy (31).

As such, development of an effective TB vaccine is highly desirable and a major focus in the TB research community. Currently, there are 16 preventative vaccine candidates being tested in clinical trials and 5 therapeutic vaccine candidates, which are designed to be administered alongside existing TB drugs to prevent reactivation in active TB cases (32).

1.1.5 Antibiotic therapy & resistance

There are four first-line antibiotics used for TB treatment. These four drugs are isoniazid (INH), rifampicin (RIF), ethambutol (EMB), and pyrazinamide (PZA). INH binds and inhibits InhA, an enzyme that contributes to the biosynthesis of mycolic acids, thus inhibiting mycobacterial cell wall synthesis (33, 34). RIF inhibits protein synthesis by binding to the β-subunit of the RNA polymerase, resulting in inhibition of messenger RNA (mRNA) elongation (35). EMB inhibits cell wall synthesis by interfering with the biosynthesis of arabinogalactan and lipoarabinomannan, although the underlying molecular mechanism remains unclear (36). The exact target and mechanism of action of PZA also remains elusive,

although it is reported to disrupt the Mtb plasma membrane and energy metabolism (37). The standard treatment regimen for drug-susceptible TB is all four first-line drugs for 2 months, followed by INH and PYZ for an additional 4 months. As such, the lengthy duration of treatment and the associated side effects often result in reduced patient compliance, which has contributed to the development of antibiotic-resistant TB. Treatment of antibiotic-resistant TB requires up to two years of treatment time and the use of second-line TB drugs, including fluoroquinolones (ciprofloxacin, ofloxacin, levofloxacin, and moxifloxacin), injectable aminoglycosides (kanamycin, amikacin, and streptomycin), ethionamide/prothionamide, *p*-aminosalicylic acid, cycloserine, and the injectable polypeptide capreomycin. However, second-line TB drugs are associated with increased morbidity and the risk of more severe side-effects compared to first-line TB drugs (38).

Drug resistant TB is defined as either multidrug resistant TB (MDR-TB) or extensively drug-resistant TB (XDR-TB). MDR-TB is defined as resistance to the first-line TB antibiotics RIF and INH, while XDR-TB is defined as resistance to RIF and INH, in addition to any fluoroquinolone and at least one of the three injectable aminoglycosides. Globally, about 500,000 drug resistant TB cases emerge every year, and it is estimated that 5% of all active TB cases are MDR-TB, with 6.2% of these cases estimated to be XDR-TB (6).

One of the contributing factors to the challenge of TB treatment is the location of Mtb during infection. Mtb is often contained within nonvascularized granulomas, which makes it difficult for antibiotics to reach the bacteria (13). Indeed, RIF is reported to ineffectively penetrate pulmonary granulomas (39). Furthermore, as an intracellular pathogen, Mtb often remains hidden within phagocytes such as alveolar macrophages. As such, an effective anti-TB drug must be able to exit the blood into granulomas and penetrate Mtb-containing immune cells (40). Once the antibiotics have entered the granuloma and the Mtb-containing

phagocytes, they must then be able to penetrate the cell wall of Mtb, which is notoriously impermeable to antibiotics due to its thick mycolic acid layer and hydrophobic properties (41). In addition, the Mtb cell wall contains efflux pumps that actively expel antibiotics that enter the bacteria. Indeed, there are 18 transporters reported to decrease antibiotic susceptibility of mycobacterial species (42).

Another hurdle for TB treatment is the ability of Mtb to remain dormant within phagocytes. Studies in the mouse model have shown that the hypoxic environment in the granuloma core triggers the phosphorylation of an Mtb response regulator known as dormancy survival regulator (DosR) (43). DosR then activates a set of 48 genes that allow the bacteria to transition into a dormant state (44). DosR is also induced in response to nitric oxide (NO) and nutrient starvation, and *in vitro* studies show that it is induced in Mtb contained within macrophages (45). The dormant state is characterized by low metabolic activity, rendering Mtb resistant to many antibiotics that target metabolically active bacteria (46). The presence of dormant Mtb at any given time during infection renders it very difficult for bactericidal antibiotics to eliminate the bacteria.

Genetic mutation also contributes to the antibiotic resistance of Mtb. Mutations that confer antibiotic resistance usually result in modification of the bacterial target upon which the antibiotic acts, or an enzymatic defect that prevents a pro-drug from being converted into an active drug. As an example of the former, there are multiple reported mutations in the *rpoB* gene encoding RNA polymerase that provide resistance to RIF (47). The mutations hinder the binding of RIF to RNA polymerase, thus blocking the drug's ability to inhibit RNA synthesis. As an example of the latter, INH-resistant Mtb are reported to have mutations in several genes required for the conversion of the pro-drug into the active form, including the enzymes KatG and InhA (48).

The increasing incidence of antibiotic-resistant TB means that the development of novel TB therapeutics is urgently needed. However, only two new anti-TB drugs have been FDA approved in the last 50 years. These new TB drugs are bedaquiline and pretomanid. The efficacy of these drugs in MDR-TB patients appears promising in clinical trials (49, 50). However, there are already reports of bedaquiline-resistant TB (51), one of the most recently approved TB therapeutics. As such, alternative treatment strategies must be explored that consider the problem of antibiotic resistance.

1.1.6 Host-directed therapy

Host-directed therapy (HDT) is a treatment strategy that aims to boost the host immune response to Mtb rather than targeting the bacterium itself, thus circumventing the development of antibiotic resistance. Many HDTs are being explored for use as adjuvants alongside current TB antibiotics to enhance efficacy or shorten the treatment duration.

Due to the antibacterial effects of the vitamin D pathway, targeting this pathway is frequently explored as an HDT strategy for TB (52). In fact, vitamin D supplementation is the furthest along the pipeline of TB HDTs in clinical trials, due in part to the low risks associated with vitamin supplementation (53). Vitamin D supplementation can lead to the production of cathelicidin antimicrobial peptide by macrophages, which enhances the response of these phagocytes to Mtb infection in 3 different ways: it is toxic to Mtb, it activates phagosome maturation, and it enhances autophagosome formation (54–56). However, there are inconsistencies among clinical trial outcomes. Although some trials have demonstrated that vitamin D supplementation results in clinical and radiological improvements (57), other studies have not shown a difference in Mtb sputum conversion rates or clinical outcome (58,

59). Discrepancies among trial outcomes may be due to variations in vitamin D administration and dosage, differences in endogenous levels of vitamin D among participants, genetic differences in the vitamin D receptor, or confounding variables such as sunlight exposure (53).

Although the granuloma can be advantageous for the host by preventing dissemination of Mtb, it also impedes TB therapeutics from reaching Mtb contained within the granuloma core (60). Granulomas therefore contribute to the lengthy treatment duration required for current TB antibiotics. As such, HDTs that target tumour necrosis factor alpha (TNFα), a cytokine that is crucial for the formation and maintenance of granulomas, are currently being explored in clinical trials (61). Etanercept, a soluble TNFα receptor antagonist, has been shown to disrupt granuloma integrity in Mtb-infected mice, which leads to more rapid and enhanced bacterial clearance following INH and RIF treatment, in addition to a reduction in lung pathology (62). Indeed, a phase I clinical trial using etanercept as an adjunctive therapy during the initial treatment stage of HIV-associated TB accelerated sputum culture conversion in participants (63).

In active TB disease, excessive and prolonged activation of the inflammatory response often leads to tissue pathology and disease progression. As such, many HDT strategies aim to reduce chronic, non-productive inflammation (64). One such HDT strategy is the use of non-steroidal anti-inflammatory drugs, which inhibit cyclooxygenase enzymes to limit the production of pro-inflammatory mediators such as prostaglandins. For example, a phase II clinical trial investigated Aspirin as an adjunct to dexamethasone during early TB treatment in adult TB meningitis (65). Aspirin was observed to reduce brain infarcts and related deaths through a mechanism dependent on inhibition of thromboxane-A2 and increased levels of protectins (65).

Following phagocytosis by macrophages, Mtb can inhibit phagosome acidification to evade degradation by pH-sensitive lysosomal enzymes (discussed in section 1.3.1). Abelson tyrosine kinase has been demonstrated to control phagosome acidification by regulating the proton pump vacuolar-H($^{+}$)-ATPase (V-ATPase) (66). Imatinib is an Abelson tyrosine kinase inhibitor that was developed for treatment of chronic myelogenous leukemia (CML). Imatinib therapy was observed to increase the number of circulating monocytes with acidified lysosomes in CML patients (66). In the same study, it was also shown that treatment of macrophages with sera collected from patients receiving imatinib reduced the intracellular survival of Mtb. Therefore, tyrosine kinase inhibitors offer the potential for being repurposed for TB HDT (67).

Mtb promotes the formation of lipid bodies in macrophages. It is hypothesized that the fatty acids derived from such lipid bodies provide a crucial energy source to Mtb, thus promoting an energy-rich niche for the bacteria within the macrophage (67). As such, inhibition of macrophage lipid body synthesis has been suggested as an HDT. Statins are a group of medications commonly used to prevent or treat atherosclerosis due to their ability to lower cholesterol levels in the blood (68). In addition, statins are known for their ability to limit lipid accumulation by inhibiting HMG-CoA reductase enzymes that are essential in lipid metabolism (68). Importantly, statins have been shown to limit Mtb growth in macrophages (69–71). As such, there is growing interest in repurposing statins for use as TB HDT.

In summary, there are many drugs that have shown promising potential for use as TB HDT in clinical and pre-clinical trials. However, all current TB HDT strategies focus on either repurposing currently approved drugs, or have unknown host targets. As such, to truly advance the TB HDT field, we must identify novel host targets that can be modified with therapeutics

and understand their roles in TB defense. This will enable the discovery of completely new and more specific pharmaceutical compounds to treat TB.

1.2 Immune response to *M. tuberculosis*

1.2.1 Innate immune response

Mtb infection begins upon inhalation of airborne droplets containing the bacteria. These droplets are expelled from active TB patients when they talk, cough, or sneeze. Following inhalation of Mtb, the bacteria contact the respiratory mucosa as they travel along the airway. Airway epithelial cells (AECs) form the epithelium and function as an initial barrier to prevent bacterial invasion. AECs express pattern recognition receptors (PRRs) such as Toll-like receptors (TLRs) and C-type lectin receptors (CLRs) that recognize pathogen-associated molecular patterns (PAMPs) on the surface of Mtb. Upon recognition of Mtb, AECs attempt to kill the bacteria by secreting numerous antibacterial substances such as defensins, cathelicidin, hepcidin, reactive oxygen species (ROS), and NO (72). In addition, AECs produce pro-inflammatory cytokines and chemokines such as interleukin (IL)-8 and monocyte chemoattractant protein-1 (MCP-1) to recruit phagocytes to the site of infection (73). The lamina propria is situated beneath the epithelium and contains resident immune cells including mucosal-associated invariant T cells. AECs can present Mtb antigens to these T cells and stimulate them to produce IFNγ, TNFα, and granzyme, factors that may contribute to early Mtb clearance and activation of macrophages (74).

If AECs are unsuccessful in clearing the infection, Mtb will continue to travel down the respiratory tract until the bacteria reach the alveoli. The alveoli contain resident alveolar macrophages (AMs) and dendritic cells (DCs) that recognize and phagocytose the bacteria.

These phagocytes express various PRRs that allow for the internalization of non-opsonized Mtb, including CLRs (e.g. mannose receptor (MR), dendritic cell-specific adhesion molecule-3-grabbing non-integrin (DC-SIGN), dectin-1), Fc receptors (e.g. FcγR), CD14, and scavenger receptors (e.g. MARCO, SR-A1, CD36, SR-B1). Phagocytosis of Mtb by macrophages occurs predominantly through the MR, which recognizes mannose-containing biomolecules that are abundant in the cell envelope of Mtb (75). These mannose-containing biomolecules include lipoarabinomannan (LAM) and its mannosylated form (ManLAM) (76). Studies have shown that interactions of Mtb with the MR can have negative consequences for the host. Indeed, ManLAM recognition by MR leads to inhibition of phagosome-lysosome fusion in the macrophage and triggers the production of anti-inflammatory cytokines (77, 78). Furthermore, recognition of mannose residues by MR reduces the antibacterial activities of macrophages by inhibiting the production of NO and oxygen radicals, in addition to blocking Mtb-induced apoptosis (78). As such, Mtb may exploit its mannosylated cell surface biomolecules and interact with MR to promote its intracellular survival within macrophages. Indeed, it has been shown that antibody-coated Mtb, which bind the FcγR rather than the MR, traffic to the lysosome and do not evade phagolysosome fusion (79). In addition, complement receptors (CR) such as CR3 play a role in phagocytosis of opsonized Mtb (80). Complement cleavage fragment C3b and its inactive form C3bi opsonize Mtb via covalent linkages, which leads to CR3-mediated phagocytosis of the bacteria (81). CR3 deficiency reduces the ability of macrophages to phagocytose Mtb, however it does not impair the antibacterial effector mechanisms of the macrophages or impact the survival of intracellular Mtb (82). In addition, CR4 is particularly abundant on macrophages and is hypothesized to play an important role in mediating Mtb uptake in the early stages of infection (83, 84). Indeed, CR4 and the MR are

the most highly expressed PRRs on AMs (85). Phagocytes also express PRRs that recognize Mtb or Mtb products and activate receptor-mediated signalling pathways that alter gene expression profiles of the infected immune cells (86). These PRRs include TLRs such as TLR2, TLR4, and TLR9. Overall, Mtb is not recognized by one single PRR on phagocytes but rather by numerous receptors that induce a network of coordinated signalling pathways (86).

Following phagocytosis of Mtb, AMs employ bactericidal mechanisms in attempt to kill Mtb. These mechanisms include sequestration of essential nutrients/metals, delivery of toxic metals to the Mtb phagosome, phagosome acidification, and autophagy (discussed in section 1.3). In addition, AMs produce ROS, reactive nitrogen intermediates, proteases, and antimicrobial peptides. However, AMs also attempt to limit lung tissue injury inflicted by inflammatory mediators and are thus considered to be immunoregulatory cells with low bactericidal ability (87, 88). Indeed, AMs have poor antigen presentation capabilities and produce cytokines such as IL-10 and transforming growth factor beta (TGF-β), which inhibit pro-inflammatory responses and suppress T cell activation (89, 90). As such, while AMs serve to eliminate routinely encountered microbes, they often fail to do so for Mtb (90). Furthermore, Mtb produces many virulence factors that allow it to evade or counteract macrophage defenses (discussed in section 1.3). Progression of disease is thus largely determined by the ability of AMs to kill Mtb. If the antibacterial response of AMs is adequate, the host will achieve early clearance of Mtb without initiation of the adaptive immune response. However, if the AMs fail to control the infection, they provide a niche for Mtb replication and dissemination (91).

Infected AMs release chemokines such as chemokine (C-C motif) ligand (CCL)-2, CCL3, CCL4, CCL5, and interferon gamma-induced protein 10 (IP-10) that recruit peripheral immune cells to the site of infection (92). The recruited immune cells include neutrophils, natural killer (NK) cells, and peripheral blood mononuclear cells. In bronchoalveolar lavage and sputum collected from active TB patients, neutrophils are the most abundant cell type (93). Interestingly, one study found that individuals in contact with active TB cases were less likely to be infected with Mtb if they had higher peripheral blood neutrophil counts (94). Activation of neutrophils by Mtb and pro-inflammatory cytokines triggers neutrophil degranulation. Neutrophils release proteases, hydrolyses, antimicrobial peptides, and oxidants that kill Mtb. Neutrophils also release pro-inflammatory cytokines such as TNFα, IL-1β, and IFNγ. However, the effectors released by neutrophils do not discriminate between Mtb and host tissue, therefore neutrophils may be a cause of necrotic lung pathology and disease severity in pulmonary TB patients. Indeed, matrix metalloproteinases released by neutrophils can lead to severe tissue destruction (95, 96). As such, whether neutrophils play an overall beneficial or harmful role during Mtb infection remains controversial. NK cells are also recruited to the lungs during Mtb infection. NK cells recognize Mtb cell wall components such as mycolic acids via their natural cytotoxicity receptor NKp44 (97). NK cells can directly restrict Mtb growth by producing granules containing perforin, granulysin, and granzyme (98). Furthermore, NK cells can recognize and lyse Mtb-infected macrophages (99). NK cells can also indirectly inhibit intracellular Mtb growth by enhancing phagolysosome fusion in macrophages through the release of IFNγ and IL-22 (100, 101). The chemokines released by AMs and AECs also recruit peripheral blood mononuclear cells to the lung. For example, C-C chemokine receptor type 2 (CCR2)-expressing monocytes are recruited to the infection site

via CCL2 (102), where they can then differentiate into DCs, macrophages, or remain as inflammatory monocytes (103). These monocytes produce pro-inflammatory cytokines such as IL-1α, IL-1β, and TNFα, which assist in bacterial control (104). However, although these monocytes can assist with Mtb clearance, they can also be permissive for cell-to-cell transmission of Mtb (105).

DCs are the innate immune cells that bridge the innate and adaptive immune response during Mtb infection. While some reports have demonstrated a crucial role of DCs in activating adaptive immunity (106), other studies have found that Mtb uses DCs as a replicative niche and impairs their ability to activate T cells (107, 108). DCs express many PRRs that can recognize Mtb. Among them, the most well-known receptor is DC-SIGN, which recognizes LAM on the cell wall of Mtb (109). Following phagocytosis of Mtb, DCs express the chemokine receptor CCR7 (108). This allows the DCs to be guided to the mediastinal lymph nodes by following a gradient of chemokines including CCL-19 and CCL-21 (108). CCL-21 is expressed by the lymphatic endothelium, directing the initial migration of DCs, while both CCL-19 and CCL-21 are expressed by lymph node resident cells (110). DCs in CCR7 knockout mice have an impaired ability to migrate to the draining lymph nodes, resulting in delayed priming of Mtb-specific T cells (111).

1.2.2 Adaptive immune response

Antigen-presenting cells (APCs) such as DCs and macrophages migrate to the draining lymph node and prime T cells at around 14 days post-infection in the mouse model (108). Although DCs are recognized to be essential for the induction of T cell responses, it is now known that Mtb-infected $CCR2^{+}$ inflammatory monocytes also migrate to the lymph node to

assist with T cell priming (112, 113). A study demonstrated that depletion of $CCR2^+$ cells in mice significantly reduces the appearance of Mtb in the lymph node and delays $CD4^+$ T cell priming (112). On the other hand, depletion of DCs had no impact on delivery of Mtb to the lymph node but dramatically reduced $CD4^+$ T cell priming. Altogether, the findings from this study suggest that migratory $CCR2^+$ monocytes are required for trafficking of Mtb to the lymph node, where DCs then phagocytose the bacteria and present the Mtb antigens to naïve $CD4^+$ T cells on major histocompatibility complex (MHC)-II molecules (114).

$CD4^+$ T cells are an essential component of the adaptive immune response to Mtb infection. The importance of $CD4^+$ T cells during Mtb infection is exemplified by the heightened susceptibility of HIV patients to TB disease (115). Initiation of T cell activation is delayed during Mtb infection in comparison to other intracellular bacteria (116). Indeed, antigen-specific $CD4^+$ T cells are not detected in the lungs until 2-3 weeks post-Mtb infection in the mouse model (117). This delay in the $CD4^+$ T cell response is believed to be a major reason for the host's failure to control the infection. The delay in activation of $CD4^+$ T cells could be due to a variety of factors, the most accepted being the ability of Mtb to inhibit apoptosis and antigen presentation by APCs (118). The main effector function of $CD4^+$ T cells is the secretion of IFNγ, which activates macrophages and enables them to exert their bactericidal functions. Indeed, mouse studies have demonstrated that IFNγ is essential for macrophage activation and the killing of intracellular Mtb (119). In mouse macrophages, IFNγ reduces Mtb burden by inducing NO production (119). However, stimulation of NO production is not believed to play a role in the control of Mtb burden in human macrophages due to their limited ability to produce NO (120). Nevertheless, IFNγ remains a crucial cytokine for control of Mtb in humans, as evidenced by increased susceptibility to Mtb in individuals

with genetic defects in IFNγ signaling (121). This could be due to other antimicrobial pathways induced by IFNγ, such as autophagy or apoptosis (122, 123). Although $CD4^+$ T cells play a critical role in restricting Mtb growth, studies suggest $CD4^+$ T cells can also harm the host by contributing to lung pathology. For example, a cohort study of individuals co-infected with HIV and TB revealed a positive correlation between increased numbers of $CD4^+$ T cells and the likelihood of cavitary TB (124). Individuals with cavitary TB are more infectious compared to active TB patients without lung cavities (125), therefore the lung pathology arising from $CD4^+$ T cell responses may facilitate bacterial transmission.

$CD8^+$ T cells also play a role in the adaptive immune response to Mtb. These cells recognize Mtb antigen presented on MHC-I molecules. As such, $CD8^+$ T cells may be important in recognizing Mtb that escapes the phagosome, since antigen presentation on MHC-II occurs via the phagosome maturation pathway (126). Upon recognition of Mtb antigens presented on MHC-I, $CD8^+$ T cells release cytokines that assist in controlling Mtb, including IL-2, IFNγ, and TNFα. In addition, these T cells release perforin and granulysin to lyse infected macrophages (127). However, the relative contributions of these effector functions during Mtb infection are unknown.

Humoral immunity was not previously believed to play a role during Mtb infection. However, there is a growing body of evidence to suggest that B cell and antibody responses contribute to the immune response to Mtb. Antibodies for Mtb proteins have been observed in the sera of TB patients (128), and passive transfer of monoclonal antibodies specific for Mtb cell wall components provides some protection in mice (129). Furthermore, Mtb-infected mice that are deficient in B cells have elevated neutrophil recruitment and exacerbated lung pathology (130). B cells have also been shown to produce cytokines such as type I IFN (IFNα

and IFNβ) that influence macrophage polarization towards an anti-inflammatory phenotype (131). These findings suggest that B cells can limit inflammatory responses during Mtb infection. However, whether this anti-inflammatory effect of B cells is ultimately beneficial or harmful to the host remains unknown.

1.2.3 Tuberculosis granuloma

The accumulation of innate and adaptive immune cells in the lung results in the formation of granulomas **(Figure 1)**, the hallmark pathological structure of Mtb infection. The core of the granuloma is composed of infected AMs and epithelioid cells, which provide nutritional support to Mtb. Progressive layers of immune cells including neutrophils, DCs, and NK cells surround the infected macrophages. The outer layers of the granuloma contain B lymphocytes, $CD4^+$ and $CD8^+$ T cells that form a cellular wall to prevent the spread of Mtb (132). Pro-inflammatory cytokines such as TNFα, IFNγ, and IL-12 are required for granuloma formation and stability and also assist in limiting Mtb growth (119, 133, 134). As such, granulomas allow for both physical containment and immunological restraint of Mtb growth.

Importantly, there is heterogeneity between granulomas within the same host, with each individual granuloma having its own trajectory (135). Some granulomas are capable of eliminating all bacteria (referred to as granuloma sterilization), whereas others contain Mtb growth but do not eliminate the bacteria, resulting in stable granulomas that may remain for decades (135, 136). Cynomolgus macaques are a commonly used model to study TB granulomas since the granulomas in these non-human primates closely mimic those found in humans (137, 138). Recent studies in these primates have shown that there are both progressing and healed lesions within the same animal, with nearly all animals being capable

of sterilizing at least a subset of granulomas (139). Thus, even within the same host, the number of viable Mtb found in individual granulomas varies considerably. Indeed, some granulomas in Mtb-infected cynomolgus macaques were observed to have 0 colony forming units (CFU) per granuloma (sterilized granuloma), while other granulomas within the same animal had approximately 1 million CFU per granuloma (139). Overall, the presence of granulomas is insufficient to control Mtb infection. Rather, the ability of all granulomas to control Mtb growth is what determines the outcome of infection (135).

Some granulomas are unable to control bacterial growth. Under this circumstance, infected cells become necrotic, triggering the release of bacteria and an inflammatory response. Overtime, the inflammation results in large caseating granulomas and fibrotic scarring that contribute to tissue injury. If the granuloma fails to contain the infection, the granuloma's caseous necrotic center liquefies and cavitates, allowing infected cells and bacteria to exit the granuloma and disseminate (60) **(Figure 1)**. The resulting lung cavities are the hallmark of pulmonary TB disease. At this stage of infection, the individual is said to have active TB disease and is both symptomatic and contagious. Infectious Mtb can spill into the airways and be transmitted to other humans when the infected individual coughs, sneezes, or speaks. Mtb can also enter the host's bloodstream and spread to virtually any organ, including the brain.

The granuloma also creates challenges to treating TB disease. Layers of immune cells sequester Mtb within the granuloma core and help to shield the bacteria from antibiotics (13). Furthermore, granulomas are heterogenous with respect to their vascularization. Indeed, vascularization in the granuloma core is gradually destroyed as it begins to necrotize from the centre outwards (13). The reduced vascular supply in some granulomas impedes drug delivery and can also result in reduced oxygen levels in the granuloma (140). The resulting hypoxic

environment in the granuloma core triggers Mtb to enter a dormant state, rendering Mtb resistant to many antibiotics that target metabolically active bacteria (43, 46).

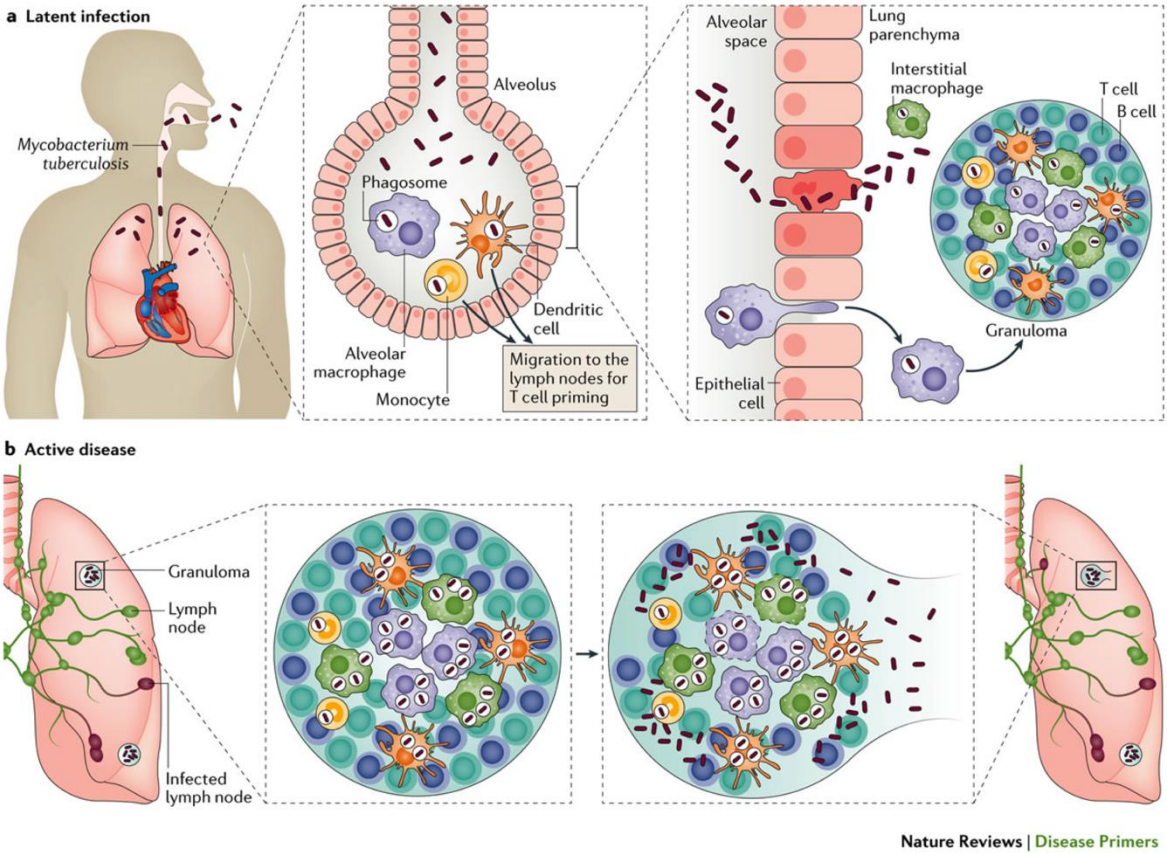
a Latent infection
Mycobacterium tuberculosis
Alveolus
Phagosome
Dendritic cell
Alveolar macrophage
Monocyte
Migration to the lymph nodes for T cell priming
Alveolar space
Lung parenchyma
Interstitial macrophage
T cell
B cell
Granuloma
Epithelial cell
b Active disease
Granuloma
Lymph node
Infected lymph node
Nature Reviews | Disease Primers

Figure 1. Progression of *M. tuberculosis* infection. Mtb bacilli are transmitted in airborne droplets after an individual with active tuberculosis (TB) disease coughs, sneezes, or speaks. Inhaled Mtb travel to the lung alveoli where they are phagocytosed by resident alveolar macrophages (AMs) and dendritic cells (DCs). These phagocytes exert antibacterial processes to degrade internalized Mtb, such as the phagosome maturation process. AMs and DCs also release cytokines and chemokines that recruit peripheral immune cells such as monocytes. DCs and monocytes migrate to the draining lymph nodes to prime T cells, which then travel to the site of infection. The accumulation of lymphocytes and innate immune cells triggers the formation of a granuloma, which functions to physically and immunologically restrict Mtb growth. If the granuloma successfully contains the infection, the individual is said to have latent TB infection and remains asymptomatic and non-contagious. If the granuloma fails to contain Mtb infection, the caseous necrotic center liquefies and cavitates, allowing infected cells and bacteria to exit the granuloma and disseminate through the host. At this stage, the individual is said to have active TB disease and can transmit the bacteria to other hosts. Figure from Pai et al. (369), reprinted with permission from Springer Nature.

1.2.4 Regulation of inflammation in tuberculosis

An inflammatory Th1 response is crucial for containment of Mtb. Indeed, too little inflammation can delay the activation of innate and adaptive immunity, thus impairing bacterial control (118). However, uncontrolled inflammation impairs cellular immunity and damages lung tissue. The severe lung pathology resulting from over-exuberant inflammation causes lung cavitation and promotes transmission of Mtb (118). As such, inflammation must be tightly regulated by pro- and anti-inflammatory cytokines.

TLRs play an important role in modulating the inflammatory response during Mtb infection. TLRs are expressed by a wide variety of cells, including AMs, DCs, neutrophils, lymphocytes, and alveolar epithelial cells. Mtb is primarily detected by TLR2, TLR4, and TLR9 (141). Genetic variants in TLR2 are associated with TB susceptibility and underline the predominant role of TLR2 during Mtb infection (142). TLR2 is expressed on the cell surface and can function alone or as a heterodimer with TLR1 or TLR6. Interestingly, TLR4-deficient mice infected with BCG have shown increased local inflammation, indicating that TLR4 plays a modulatory role in inflammation during mycobacterial infections (143). TLR9 is expressed intracellularly on endosomes and recognizes unmethylated CpG found in mycobacterial DNA (144). Recognition of Mtb PAMPs by different TLRs results in the recruitment of distinct adapter proteins that activate signaling cascades such as nuclear factor kappa-light-chain-enhancer of activated B cells (NF-κB) and mitogen-activated protein kinase (MAPK) pathways. Activation of the NF-κB pathway is of particular importance to the inflammatory response. Once in the nucleus, NF-κB drives production of multiple pro-inflammatory cytokines that play a critical role in controlling Mtb infection.

Important pro-inflammatory cytokines during Mtb infection include TNFα, IL-12, IL-18, IFNγ, IL-1β, and IL-6. TNFα is primarily produced by macrophages but can also be secreted by other immune cells such as lymphocytes. TNFα mediates inflammation by stimulating the production of IL-1, IL-6, and early chemokine production. This cytokine also assists in macrophage activation and can induce apoptosis of Mtb-infected human AMs, thus assisting in the control of Mtb (145, 146). TNFα-deficient mice have increased susceptibility to Mtb and succumb to infection within 2 – 3 weeks (147). Furthermore, TNFα-deficient mice have inhibited granuloma formation (61). The importance of TNFα during Mtb infection is also demonstrated by the increased susceptibility to TB in individuals receiving anti-TNFα neutralization therapy for autoimmune diseases. There is a significant correlation between reactivation of LTBI in patients undergoing these therapies (148, 149). Production of IL-12 by macrophages and DCs is also essential for survival of Mtb-infected mice (150, 151). IL-12 triggers the release of IFNγ by T cells, thus initiating the Th1 response (152). Similarly, IL-18 is believed to optimize the production of IFNγ by T cells, since total IFNγ production by $CD4^+$ and $CD8^+$ T cells is decreased in IL-18-deficient mice (153–155). Mice deficient in IL-18 are susceptible to Mtb and have an accumulation of monocytes, neutrophils, and inflammatory chemokines in the lung (154). As such, IL-18 may play a critical role in preventing the recruitment of permissive monocytes and neutrophils to the lung. IFNγ is the chief cytokine in Mtb immunity due its role in activating macrophages. After it is secreted by T cells, IFNγ activates antibacterial mechanisms of macrophages including phagosome maturation, ROS production, apoptosis, and autophagy (119, 122, 123). IFNγ knockout mice succumb to Mtb infection (119), and humans with defective IFNγ signalling have a high susceptibility to mycobacterial infections and poor prognosis (121, 156). IL-1β is another pro-

inflammatory cytokine critical for survival during Mtb infection (157). IL-1β regulates a number of processes important for control of Mtb infection, including phagosome maturation and limiting type I IFN production (90, 158). IL-6 can also have a proinflammatory effect during Mtb infection. IL-6 induces differentiation of cytotoxic T cells and is required for survival in mice following high dose challenge with Mtb (159). However, IL-6 can also be beneficial for Mtb, since it has been shown to antagonize the antibacterial effects of IFNγ in macrophages (160). Indeed, Mtb is reported to induce production of IL-6 by infected macrophages to inhibit IFNγ-mediated autophagy (161).

To avoid tissue injury, inflammation must be tightly regulated during Mtb infection. IL-10 and TGF-β are important cytokines that limit inflammation during Mtb infection. IL-10 is produced by monocytes, macrophages, DCs, and T regulatory cells. This cytokine inhibits the production of chemokines and pro-inflammatory cytokines such as IL-12 and IFNγ by APCs (162). IL-10 also inhibits cell recruitment, generation of oxidants, and T cell activation (163). Furthermore, IL-10 is reported to inhibit autophagy (164) and interfere with phagosome maturation in human macrophages (165). TGF-β is produced by most immune cells, including lymphocytes, macrophages, monocytes, and DCs. This cytokine is believed to inhibit T cell proliferation and the antibacterial activity of monocytes, since T cells and monocytes from TB patients co-cultured with TGF-β inhibitors exhibit restored T cell proliferation and enhanced monocytic control of Mtb (166). In addition, TGF-β induces IL-10 production and synergizes with it to inhibit IFNγ production (167).

1.3 Interplay between *M. tuberculosis* and host macrophages

1.3.1 Phagosome maturation

Macrophages are powerful antibacterial cells equipped with multiple processes that degrade invading bacteria. Given that bacteria reside in host membrane-derived vacuoles called phagosomes, the maturation process of the phagosome is the main process responsible for degrading the bacteria. Phagosome maturation is a series of membrane fusion and fission events that occur through the recruitment of endosomes. Endosome recruitment is coordinated by guanosine triphosphate (GTP) binding proteins such as RABs as well as phospholipids such as phosphatidylinositol 3-phosphate (PI3P). PI3P on the nascent phagosome's surface recruits a component of the nicotinamide adenine dinucleotide phosphate (NADPH) oxidase complex. NADPH oxidase then generates microbicidal ROS to assist with bacterial killing. Early endosomes containing RAB5 are recruited by the nascent phagosome and provide the phagosome with V-ATPase. V-ATPase pumps hydrogen ions into the phagosome, gradually reducing the phagosomal pH over the course of maturation. Next, late endosomes containing RAB7 provide the phagosome with proteases, antimicrobial peptides, and more V-ATPase. In the final stage of phagosome maturation, the late phagosome fuses with the lysosome to form the phagolysosome. The lysosome membrane also contains V-ATPase and the final pH of the phagolysosome is ~4.5. The lysosome chloride channel CLC-7 is also believed to contribute to this decrease in pH (168). The lysosome provides hydrolytic enzymes including glycosidases, lipases, DNases, and proteases such as cathepsins (169). These enzymes autoactivate in the acidic environment of the phagolysosome and degrade the pathogen. The final phagolysosome is an extremely hostile environment capable of killing most pathogens. As such, to survive within macrophages, Mtb uses a variety of virulence proteins and lipids

to manipulate the phagosome maturation pathway and block phagolysosome fusion **(Figure 2)**.

Shortly after phagocytosis of Mtb and before the progression of phagosome maturation, the macrophage undergoes an oxidative burst. During the oxidative burst, ROS are rapidly released to degrade the internalized bacteria. However, Mtb can counteract the oxidative burst by inhibiting NADPH oxidase **(Figure 2)**. NADPH is composed of two integral membrane subunits that form flavocytochrome b558 and a trimeric cytosolic complex. The assembled complex requires the recruitment of GTP-bound RAC1/2 to activate its catalytic activity (170). Mtb secretes possible conserved protein CpsA, which inhibits the recruitment of flavocytochrome b558 complex to the phagosome (171). Furthermore, Mtb secretes the virulence factor nucleoside diphosphate kinase (Ndk), which inhibits the final activation step of NADPH oxidase by functioning as a GTPase activating protein (GAP) to inactivate RAC1 (172). Mtb also secretes enzymes that scavenge ROS, such as superoxide dismutase (SodA), and the catalase KatG (173, 174). Nevertheless, individuals with mutations in NADPH oxidase develop chronic granulomatous disease, and are more susceptible to TB (175). Therefore, although Mtb inhibits NADPH oxidase and secretes ROS scavenging enzymes, inhibition of ROS production must be imperfect.

To block phagosome maturation, Mtb inhibits the recruitment of early endosomal proteins involved in membrane trafficking and protein complex assembly by interfering with the production of PI3P **(Figure 2)**. PI3P located in the phagosome membrane recruits endosomal proteins and is required for proper fusion with endocytic vesicles. ManLAM, a component of the Mtb cell envelope, has been shown to impair PI3P activity, thus leading to phagosome maturation arrest (176). Furthermore, Mtb inhibits phagosome maturation through secreted acid phosphatase (SapM), a lipid phosphatase that hydrolyzes PI3P and removes it

from the phagosome (177). Mtb also inhibits phagosome maturation by promoting interactions with early endosomes. One mechanism utilized by Mtb is to impair RAB functioning. For example, Mtb secretes Ndk, which possesses GAP activity towards RAB proteins (178). Indeed, Ndk has been shown to inactivate both RAB5 and RAB7, thus inhibiting phagosome maturation and fusion with lysosomes in macrophages (178). In addition to secreted virulence factors, Mtb also has components in its cell envelope that assist with inhibition of phagosome maturation. Indeed, the envelope glycolipid phosphatidylinositol mannoside promotes early endosome fusion by altering RAB programming (179).

Mtb also inhibits recruitment of late endosomes and lysosomes by interfering with processes downstream of PI3P. Hepatocyte growth factor-regulated tyrosine kinase substrate (HRS) is an important PI3P binding protein that is usually localized to early endosomes. HRS recruits the endosomal sorting complex required for transport (ESCRT), which directs phagosomes to the lysosome. Mtb secreted ESAT-6-like protein EsxH binds HRS and inhibits ESCRT activity, leading to impaired phagosome maturation and inhibition of MHC-II presentation (180, 181).

Finally, Mtb can prevent phagosome acidification by disrupting recruitment of V-ATPase **(Figure 2)**, the proton pump responsible for reducing the intraphagosomal pH (182). Mtb secretes protein-tyrosine phosphatase A (PtpA), which binds subunit H of the V-ATPase (183). At the same time, PtpA is able to dephosphorylate VPS33B, a key vacuolar sorting protein that is essential for phagosome-lysosome fusion (184). Both dephosphorylation of VPS33B and binding of PtpA to subunit H were shown to be required for intracellular survival of Mtb and inhibition of phagosome acidification (183, 184). Collectively, the multiple virulence proteins produced by Mtb ensure that it can survive and replicate freely in an immature phagosome **(Figure 2)**.

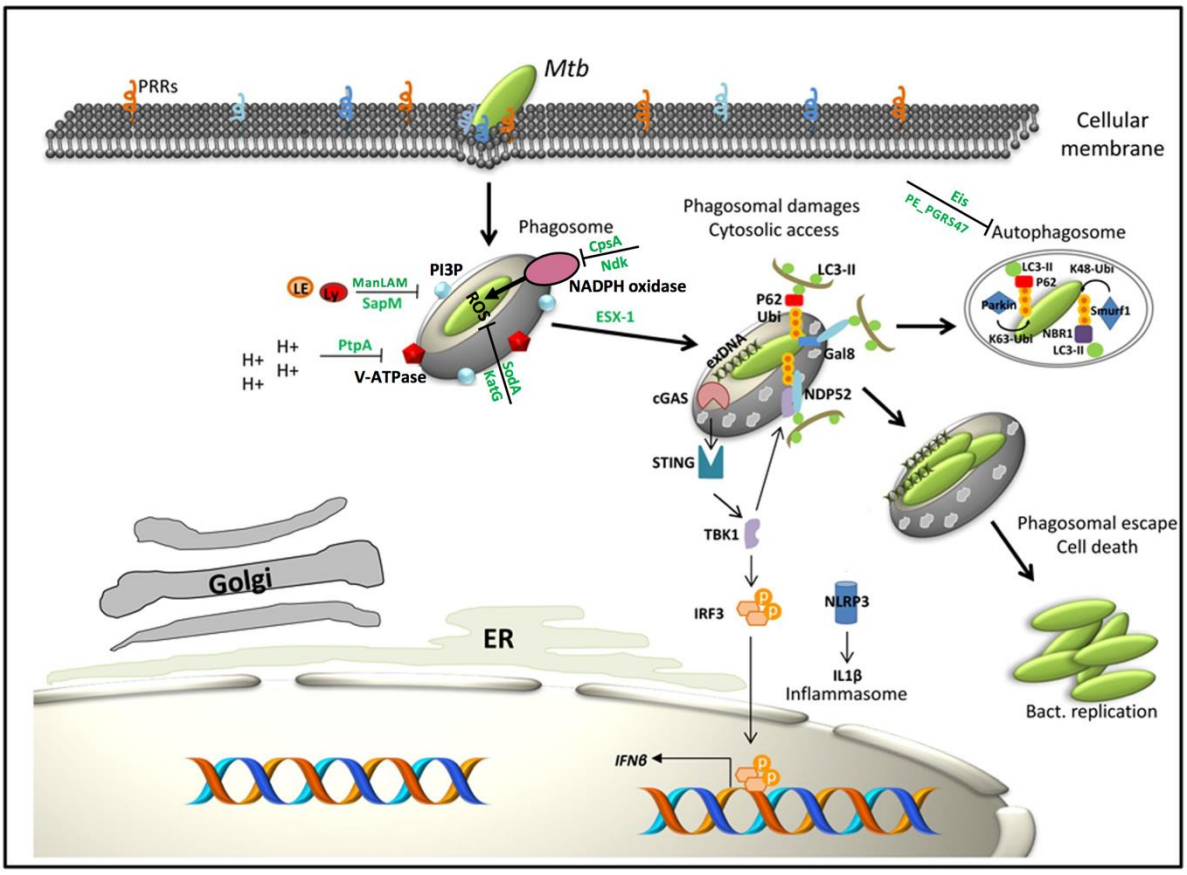
Mtb
PRRs
Cellular membrane
Phagosome
CpsA
Ndk
PI3P
NADPH oxidase
ROS
LE
Ly
ManLAM
SapM
ESX-1
H+
H+
H+
H+
PtpA
V-ATPase
SodA
KatG
Phagosomal damages
Cytosolic access
Eis
PE_PGRS47
Autophagosome
LC3-II
P62
Ubi
exDNA
Gal8
cGAS
NDP52
STING
TBK1
IRF3
NLRP3
IL1β
Inflammasome
IFNß
Golgi
ER
LC3-II
K48-Ubi
P62
Parkin
Smurf1
K63-Ubi
NBR1
LC3-II
Phagosomal escape
Cell death
Bact. replication

Figure 2. Virulence factors and cell wall lipids allow *M. tuberculosis* to escape degradation following phagocytosis. *M. tuberculosis* (Mtb) is recognized by a variety of pattern recognition receptors (PRRs) on the macrophage cell surface, leading to internalization of the bacteria. Phosphatidylinositol 3-phosphate (PI3P) on the nascent phagosome surface recruits early endosomes and a component of the NADPH oxidase complex. However, the Mtb cell wall component mannose-capped lipoarabinomannan (ManLAM) and secreted acid phosphatase (SapM) impair PI3P activity. NADPH oxidase functions to produce ROS to kill phagosomal bacteria, however Mtb secretes CpsA and nucleoside diphosphate kinase (Ndk) to interfere with NADPH assembly or activation. Furthermore, Mtb secretes protein-tyrosine phosphatase A (PtpA), which prevents phagosome acidification by impairing vacuolar-$H^{(+)}$-ATPase (V-ATPase) activity and inhibiting fusion with the lysosome (Ly). Mtb can also perforate the phagosome through its ESX-1 system, triggering the release of Mtb and extracellular bacterial DNA (exDNA) into the cytosol. Cytosolic Mtb DNA is recognized by the DNA sensor cyclin GMP-AMP synthase (cGAS). This interaction leads to the transcription of IFNβ and promotes the delivery of bacilli to the ubiquitin-mediated selective autophagy pathway. E3 ubiquitin-protein ligase SMURF1 and parkin ubiquitinate Mtb. p62 and NDP52 are target-specific autophagy receptors that form a bridge between LC3-II and ubiquitinated Mtb, allowing sequestration of Mtb within the autophagosome. However, Mtb virulence proteins such as enhanced intracellular survival (Eis) and PE_PGRS47 can inhibit the autophagy pathway. Once Mtb has escaped degradation by inhibiting phagosome maturation or autophagy, the bacteria can replicate freely within the macrophage until the cell bursts. Mtb can also activate the NLRP3 inflammasome through its ESX-1 system, thus triggering macrophage pyroptosis and IL-1β production. Figure adapted from Queval et al. (370) and reprinted under the Creative Commons Attribution License (CC BY).

1.3.2 Escape from phagosome

Unlike a few other bacteria pathogens such as *Listeria monocytogenes* and *Francisella tularensis* that are known to escape from the phagosome into the host cell cytoplasm, Mtb was classically considered a strictly intra-phagosome pathogen. However, this view has changed with the advent of new high-resolution imaging technology. Using cryo-electron microscopy, van der Wel et al. reported that Mtb can be found in the cytosol of infected macrophages (185). While this result was originally controversial, multiple studies by independent groups have confirmed its validity (186, 187). Mtb perforates the phagosome to escape into the host cell cytosol, a process that requires its 6-kDa early secretory antigenic target (ESAT-6) secretion system-1 (ESX-1) (Figure 2). ESAT6, one of the proteins secreted by the ESX-1 system, has been shown to be crucial for phagosome rupture (185). However, the exact mechanism for phagosome damage remains unknown, and whether ESAT6 can directly lyse the phagosome membrane remains controversial (188). Nevertheless, mycobacterial mutants defective in ESAT6 are unable to perforate the phagosome and have reduced membrane lytic activity (185, 186, 189). Perforation of the phagosome is beneficial for the success of Mtb since such a strategy allows it to escape the hostile phagosome environment and allows for direct delivery of its arsenal of virulence proteins to disrupt host signaling pathways in the cytosol.

An unintended consequence of phagosome escape by Mtb is the release of bacterial DNA into the cytosol, which can be sensed by the innate cytosolic surveillance pathway (190) (Figure 2). Specifically, cyclin GMP-AMP synthase (cGAS) is a cytosolic DNA sensor that has been shown to recognize Mtb DNA (191). Upon binding Mtb double stranded DNA (dsDNA), cGAS synthesizes the secondary messenger cyclic GMP-AMP, which in turn activates stimulator of interferon genes (STING). Activated STING dimerizes and activates tank-binding kinase-1 (TBK-1), which then phosphorylates the transcription factor interferon

regulatory factor-3 (IRF-3). Phosphorylated IRF-3 then dimerizes and translocates to the nucleus, where it induces IFNβ production (Figure 2). Type I IFN have been postulated to be harmful to the host, since they are associated with disease progression of TB and have been shown to antagonize the production and activity of IL-1β, a critical cytokine in the anti-TB response (104, 192). Nevertheless, recognition of Mtb by cGAS is an important host-pathogen interaction in Mtb-infected macrophages, since it promotes the delivery of bacilli to the ubiquitin-mediated selective autophagy pathway (193, 194) (Figure 2).

1.3.3 Autophagy

Autophagy was originally described as a homeostatic process that generates nutrients by degrading cytoplasmic constituents. Autophagy is activated by amino acid deprivation, serum starvation, growth factor deprivation, hypoxia, and exposure to certain toxins. However, it was later discovered that autophagy can be activated by intracellular pathogens (122). It is now known that autophagy plays an important role in immunity. In addition to organelles and proteins, the autophagy pathway can degrade targeted pathogens in a process termed xenophagy (122, 195). Nonselective autophagy refers to turnover of bulk cytoplasm during starvation, whereas selective autophagy specifically targets damaged or surplus organelles as well as intracellular pathogens (196). Autophagy is a relevant defense mechanism in macrophages infected with Mtb, since it can target and degrade cytosolic Mtb after it escapes the phagosome via ESX-1 (193) (Figure 2). Ubiquitination of cytosolic bacteria is required to mark them as cargo for autophagic degradation (197), and it is now understood that recognition of extracellular Mtb DNA is required for this ubiquitination event. The cytosolic DNA sensor cGAS binds cytosolic Mtb dsDNA and activates the

STING/TBK1/IRF-3 pathway, which results in ubiquitination of Mtb (193, 194). Specific E3 ubiquitin ligases that have been observed to ubiquitinate Mtb include E3 ubiquitin-protein ligase SMURF1 and parkin (198, 199) (Figure 2).

The initiation stage of autophagy requires the UNC-51-like autophagy activating kinase (ULK1) complex, which is comprised of ULK1/2, autophagy-related protein (ATG)13, FIP100, and ATG101. Under basal conditions, mammalian target of rapamycin (mTOR) inactivates this complex, preventing the initiation of autophagy. During stress conditions, mTOR is inhibited and autophagy is activated. The second stage of autophagy is membrane nucleation and phagophore formation, which requires the class III phosphoinositide-3 kinase (PI3K) complex, ATG14, beclin-1, and ATG9. The third stage of autophagy is phagophore elongation. During this stage, microtubule-associated proteins 1A/B light chain 3B (LC3) is recruited to the site of phagophore formation and is cleaved by ATG4 to form cytosolic LC3-I (200). The sequential actions of ATG7 (E1-like activating enzyme), ATG3 (E2-like activating enzyme), and the ATG12-5-16L1 complex (E3-like ligase) lead to the conjugation of phosphatidylethanolamine to LC3-I, thus forming LC3-II (201). LC3-II is required for phagophore elongation, expansion, and closure and is found on both outer and inner membranes (Figure 2). The selectivity of the autophagy process is ensured by target-specific autophagy receptors that form a bridge between LC3-II and the ubiquitinated cargo. Thus far, p62 and NDP52 are the autophagy receptors that have been determined to target Mtb (193) (Figure 2). The phagophore closes to form a double-membrane organelle called the autophagosome. The next stage of autophagy is autophagosome-lysosome fusion, which requires lysosomal integral membrane protein-2, SNARE proteins, and RAB proteins such as RAB5 and RAB7 (202, 203). Finally, lysosomal hydrolases degrade the contents inside the formed autophagolysosome, which not only include Mtb but also p62 and LC3-II.

In addition to STING and TBK1, AMP-dependent protein kinase (AMPK) and MAPKs have also been shown to activate autophagy (193). AMPK is activated by cell stress or low adenosine triphosphate (ATP) levels and phosphorylates tuberous sclerosis complex-2 and regulatory-associated protein of mTOR. These downstream effectors inhibit mTOR activity, thus indirectly promoting autophagy (204, 205). AMPK can also directly activate autophagy by phosphorylating ULK1 (206). MAPKs such as c-Jun N-terminal kinase (JNK) and p38 can also activate autophagy through indirect actions to stimulate beclin-1 (207–209). Importantly, IFNγ induces selective autophagy of Mtb in macrophages through the activation of both JNK and p38 (161).

While selective autophagy is clearly required to control Mtb infection, Mtb can counteract this by inhibiting multiple processes in the autophagy pathway. Mtb secretes proteins that can block autophagy, including PE_PGRS47 and enhanced intracellular survival (Eis) (Figure 2). Macrophages infected with a PE_PGRS47 knockout strain of Mtb had increased LC3-I to LC3-II conversion, increased colocalization of Mtb with LC3, and reduced bacterial survival (210). Another group observed that macrophages infected with an Eis knockout strain of Mtb displayed increased formation of autophagosomes both *in vitro* and *in vivo*, as well as elevated ROS generation, which rendered the cells highly sensitive to autophagy activation (211). Notably, Eis can acetylate a JNK-specific phosphatase, which can lead to the inactivation of JNK (212). Since JNK is required for activation of beclin-1, Eis may indirectly block autophagy by preventing activation of beclin-1. Alternatively, Eis may block autophagy by upregulating IL-10, a cytokine that has been shown to inhibit autophagy (164). Interestingly, Mtb is also reported to upregulate IL-6 in order to block IFNγ-dependent autophagy (161). Specifically, IL-6 was observed to antagonize autophagy-inducing effects

of IFNγ by preventing the phosphorylation of JNK and p38. Although autophagy is distinct from the phagosome maturation pathway, autophagosome-lysosome fusion relies on some of the same machinery as late phagosome-lysosome fusion. As such, certain Mtb effectors that block phagolysosome formation can also block autophagolysosome formation. In fact, Mtb selectively blocks the autophagic flux in macrophages by preventing the recruitment of RAB7 (213). In addition, initiation of autophagy depends on PI3P, which is also important for phagosome maturation. As such, the Mtb virulence proteins and membrane components discussed in section 1.3.1 that impair PI3P accumulation are also likely to impair autophagy. Indeed, ManLAM coated beads have been observed to block LC3 trafficking (214).

Autophagy is significantly inhibited during Mtb infection as less than 10% of Mtb bacilli are found within late autophagosomes (213). Consistent with this, enhanced induction of autophagy in Mtb-infected macrophages allows for progressive elimination of the bacteria (215), decreased Mtb burden (122), and improved control of inflammation (216). Moreover, mice deficient in ATG5 have higher bacillary burden, increased lung pathology, and increased mortality compared to autophagy-competent mice (193, 217). Interestingly, current TB antibiotics that should only target the bacteria have been shown to activate host-cell autophagy. The first-line antibiotics PYZ and INH activate autophagy in Mtb-infected macrophages, and inhibition of autophagy reduces the effectiveness of these drugs (218). In addition, it was recently shown that the newly approved anti-TB drug bedaquiline also activates autophagy (219). Due to the antibacterial role of autophagy in macrophages and its synergy with existing anti-TB antibiotics, therapeutic activation of autophagy is a promising HDT strategy against TB (220, 221).

1.3.4 Macrophage cell death

The mode of cell death of Mtb-infected macrophages greatly influences the extent of inflammation, and consequently, disease outcome. Apoptosis of Mtb-infected macrophages is a critical defense mechanism and offers many advantages to the host. Indeed, this programmed "cell suicide" of macrophages results in Mtb containment within apoptotic bodies, which can then be phagocytosed and killed by activated macrophages in a process termed efferocytosis. Following engulfment of Mtb-containing apoptotic bodies, the activated macrophages exert bactericidal mechanisms that result in enhanced bacterial killing (222). The apoptotic bodies can also be taken up by DCs to facilitate the priming of antigen-specific T cells and stimulation of adaptive immunity (223). Importantly, apoptosis of Mtb-infected cells limits inflammation and tissue damage (224). In fact, studies have shown that engulfment of apoptotic bodies stimulates the production of anti-inflammatory cytokines IL-10 and TGF-β (225, 226). However, Mtb can inhibit macrophage apoptosis and remain hidden inside the phagocyte (227). Mtb blocks apoptosis by producing virulence factors such as NADH-quinone oxidoreductase subunit G, SodA, Eis, and Ndk, which function to neutralize or interfere with the production of ROS (172, 211, 228, 229). Mtb also produces phosphatases such as PtpA to inhibit macrophage apoptosis by dephosphorylating host GSK3α (230). Interestingly, Mtb also exploits host phosphatases to block apoptosis. Indeed, Mtb infection triggers increased expression of the host protein phosphatase Mg^{2+}/Mg^{2+}-dependent-1A (PPM1A), which inhibits macrophage apoptosis by inactivating JNK signaling (231). The current paradigm is that attenuated Mtb strains induces macrophage apoptosis, whereas virulent Mtb strains block apoptosis and induce necrosis once the bacteria have proliferated to a high intracellular load (224). Necrotic cell death results in cell lysis that permits Mtb to spread to neighboring cells.

Furthermore, necrosis results in the release of pro-inflammatory mediators that can cause tissue damage and lung cavitation, thus harming the host and promoting bacterial transmission. While necrosis was previously regarded as an unregulated type of cell death, it is now known that programmed necrotic pathways exist, namely pyroptosis and necroptosis.

Pyroptosis occurs following the activation of cytosolic inflammasomes that differ based on their activating ligands. All inflammasome cascades lead to the activation of caspase-1, which cleaves pro-IL-1β and pro-IL-18 into their active forms. Capase-1 also activates gasdermin D, which forms pores in the cell membrane that permit the release of IL-β and IL-18 from the cell. The release of IL-1β and IL-18 triggers inflammation, and the pores allow ion flux across the cell membrane which leads to osmotic swelling and cell lysis. NOD-like receptor family pyrin domain containing 3 (NLRP3) is the predominant inflammasome activated during Mtb infection (232, 233) (Figure 2), although the specific ligand remains elusive (234). Pyroptosis activation was previously believed to be an essential process in the host response to Mtb infection, since mice deficient in IL-1β signaling succumb to Mtb infection (235). However, it was later discovered that IL-1β is produced independently of caspase-1 during Mtb infection (157). In fact, pyroptosis is now believed to be harmful to the host and beneficial to Mtb. Indeed, a recent report by Beckwith and colleagues showed that Mtb ESAT-6 could directly damage the macrophage plasma membrane, triggering potassium ion efflux, an essential upstream event of NLRP3 activation by Mtb (236).

Mtb can also induce macrophage necroptosis. Indeed, time-lapse microscopy has shown that pyroptosis and necroptosis are the predominant forms of cell death in Mtb-infected macrophages, whereas apoptotic cell death is the dominant cell death pathway in uninfected bystander cells (236). Mtb induces macrophage necroptosis by utilizing its outer membrane

channel protein CpnT to secrete its toxic C-terminal domain (237). This secreted C-terminal domain, termed tuberculosis necrotizing toxin, depletes cellular NAD^+, which activates receptor-interacting serine/threonine protein kinase (RIPK)-3 and mixed lineage kinase domain-like pseudokinase (MLKL), two proteins that form a complex along with RIPK1 and Fas-associated protein with death domain (FADD) to induce necroptosis (238). The necroptosis pathway triggers the oligomerization of MLKL, which is believed to subsequently permeabilize the cell membrane (239). Similar to pyroptosis, necroptosis results in cell lysis and triggers an inflammatory response. Since inflammatory cell death pathways promote tissue pathology and bacterial dissemination, both necroptosis and pyroptosis are harmful to the host and beneficial to Mtb.

1.3.5 Activation of autophagy as a strategy for host-directed therapy

Activation of autophagy has been demonstrated to be critical for mouse survival during Mtb infection (193, 217), yet this pathway is substantially inhibited in Mtb-infected macrophages (213). Since the ability of macrophages to control Mtb infection largely influences disease progression, activation of macrophage autophagy is one of the most frequently suggested strategies for TB HDT (221). One proposed strategy to induce autophagy is by activating AMPK, which promotes autophagy by inhibiting mTOR and phosphorylating ULK1/2. For example, the antihyperglycemic drug metformin promotes macrophage autophagy by activating the expression of AMPK and has been shown to inhibit Mtb growth, reduce inflammation, and prevent lung damage (240). Importantly, retrospective analysis of clinical trial data revealed that metformin treatment of individuals with type-II diabetes and TB disease is correlated with fewer lung cavities, lower proportion of participants with

advanced TB disease, and improved sputum culture conversion rate 2 months post-treatment initiation (240).

Many autophagy-inducing small molecules have been explored for HDT against TB. For example, the cancer chemotherapeutic gefitinib targets epidermal growth factor receptor and induces autophagy to enhance intracellular Mtb clearance in macrophages and *in vivo* (241). The mucolytic agent ambroxol has also been shown to induce autophagy both *in vitro* and *in vivo*, promoting Mtb clearance in murine macrophages (242). Furthermore, ambroxol potentiated rifampicin activity in a murine model of Mtb infection (242). Rapamycin is another autophagy-activating drug that has been suggested as a candidate for TB HDT (243). Although it is used as an immunosuppressant in patients undergoing organ transplantation, this compound activates autophagy by inhibiting mTOR (244) and has been shown to increase the lifespan of Mtb-infected mice when the animals are fed rapamycin late in life (245).

Importantly, autophagy induction via small molecules can also be effective in reducing survival of drug-resistant Mtb strains. For example, a study that screened U.S Food and Drug Administration (FDA)-approved drugs demonstrated that the anti-convulsant drug carbamazepine induces autophagy in an mTOR-independent pathway by depleting inositol triphosphate and activating AMPK (246). In the same study, carbamazepine was shown to reduce bacterial burden, improve lung pathology, and stimulate adaptive immunity in mice infected with a highly virulent MDR-Mtb strain. Carbamazepine also induced autophagic killing of Mtb in primary human macrophages and stimulated autophagy in the zebrafish model to enhance clearance of *Mycobacterium marinum*.

Altogether, these studies highlight the promising potential of autophagy induction as a strategy for HDT against TB. There are multiple pre-approved drugs that can activate autophagy and have shown success in limiting Mtb survival in pre-clinical trials. However,

these compounds are repurposed drugs that have multiple targets and effects in the host. As such, it is hard to discern whether their effects on Mtb survival are solely due to autophagy activation. The field of TB HDT is lacking novel host targets and new therapeutics that can specifically target the autophagy pathway.

1.4 Protein Kinase R

1.4.1 Function and mechanism of activation

Interferon-induced, double-stranded RNA-activated protein kinase, also known as protein kinase R (PKR), is a serine-threonine kinase encoded by the *EIF2AK2* gene located on chromosome 2 (247). PKR is 551 amino acids in length and is ubiquitously and constitutively expressed in vertebrate cells. PKR is one of four kinases that phosphorylate the alpha subunit of eukaryotic initiation factor-2 (EIF2α). The other three EIF2α kinases are heme-regulated inhibitor, PKR-like endoplasmic reticulum kinase (PERK), and general control non-depressible 2 (GCN2), which are activated by heme depletion, endoplasmic reticulum stress, and amino acid starvation, respectively (248). Phosphorylation of serine 51 (Ser51) on EIF2α results in inhibition of protein translation **(Figure 3)**. In addition to controlling translation, PKR can also regulate signal transduction pathways, thus impacting transcription and cellular processes such as apoptosis and inflammation. Although the canonical role of PKR is in the antiviral response, PKR also functions in the response to non-viral pathogens.

The canonical activator of PKR is viral double-stranded RNA (dsRNA) (249). However, synthetic and cellular dsRNA can also activate PKR. Furthermore, recent studies

have revealed that PKR can be activated by bacterial dsRNA (250, 251). PKR has a C-terminal kinase domain and an N-terminal dsRNA binding domain (dsRBD) **(Figure 3)**. The dsRBD consists of two dsRNA binding motifs (dsRBM1 and dsRBM2), both of which are required for the high-affinity interaction with dsRNA. During basal conditions, PKR exists in a monomeric latent state. Recognition and binding of dsRNA by the dsRBMs triggers PKR homodimerization and subsequent autophosphorylation (252) **(Figure 3)**. PKR is autophosphorylated at multiple serine and threonine residues, including Ser242, Ser83, Thr88, Thr89, Thr90, Thr255, Thr258, Thr446, and Thr451 (253). Thr446 and Thr451 are consistently phosphorylated during PKR activation, further stabilizing the homodimerization and resulting in increased catalytic activity (252, 253). Indeed, Thr446 promotes substrate recognition and phosphorylation, as mutating Thr446 was shown to inhibit EIF2α phosphorylation and viral pseudosubstrate binding (252).

Mammalian EIF2 is critical for initiating polypeptide chain synthesis since it promotes the delivery of initiator methionyl transfer RNA (Met-tRNAi) to the 40S ribosome. EIF2α binds Met-tRNAi in a GTP-dependent manner, forming a ternary complex that interacts with subunit 40S. Following Met-tRNAi delivery, EIF5 promotes GTP hydrolysis of EIF2-GTP, triggering the release of EIF2-GDP from the 48S initiation complex. EIF2-GDP must be regenerated to EIF2-GTP by the GTP exchange factor EIF2B, since EIF2-GDP is inactive. When Ser51 on EIF2α is phosphorylated by PKR or any of the other three EIF2α kinases, EIF2 affinity for EIF2B is increased up to 100-fold (254). Consequently, phosphorylated EIF2α competes with EIF2-GDP for binding of EIF2B. This competitive inhibition prevents the regeneration of active EIF2-GTP and as such, initiation of translation is substantially reduced (255). PKR therefore plays a critical role in the antiviral response since it functions

to inhibit global protein translation after sensing viral dsRNA, thus preventing viral replication.

Although RNA is the canonical activator of PKR, PKR can also be activated by cell stress, TLR signaling, and certain cytokines and growth factors (256). There is accumulating evidence to support that PKR is activated by TLR signaling. Cells isolated from PKR-deficient mice were observed to have impaired responses to various TLR ligands and had reduced production of pro-inflammatory cytokines in response to lipopolysaccharide (LPS) challenge (257). Furthermore, PKR interacts with toll/interleukin-1 receptor domain-containing adapter protein (TIRAP) and is phosphorylated in LPS-stimulated wild type (WT) macrophages (258). TIRAP is the adaptor for TLR4 and LPS is a TLR4 ligand, therefore these findings suggest that PKR is involved in TLR4 signaling. Importantly, PKR is also activated in response to CpG motifs present in bacterial DNA, dsRNA, and peptidoglycans (258). CpG engages the TLR9 receptor, suggesting that PKR is activated downstream of TLR9. Interestingly, in addition to being activated directly by dsRNA, PKR can also be indirectly activated by dsRNA through TLR3 signaling (259). Following binding of polyinosinic:polycytidylic acid (poly(I:C)) to the TLR3 receptor, a TAK1-containing complex was observed to translocate to the cytosol and recruit PKR (259). Kinase inactive mutants of TAK1 and PKR inhibited the poly(I:C)-induced TLR-mediated activations of NF-κB. As such, PKR appears to be a downstream component shared by at least three TLRs.

Finally, PKR can be activated by certain growth receptors and cytokines. For example, platelet-derived growth factor triggers PKR phosphorylation, and deletion of PKR impairs the ability of this growth factor to induce transcription of *c-fos* (260). Cytokines that can induce PKR activation include TNFα and IFNγ. In fact, PKR mediates IFNγ-dependent NF-κB

activation, and the antiviral response in PKR knockout mice treated with IFNγ is reduced (261, 262). IFNγ can also activate PKR at the transcriptional level, however type I IFN are stronger transcriptional inducers of PKR compared to IFNγ. Indeed, the best-described transcriptional motif in the PKR promoter is the interferon-stimulated response element (ISRE), which is activated by type I IFN (263). However, chromatin immunoprecipitation sequencing assays have identified many transcription factors that bind to the promoter region of the *EIF2AK2* gene, therefore ISRE is not the only transcriptional inducer of PKR (264).

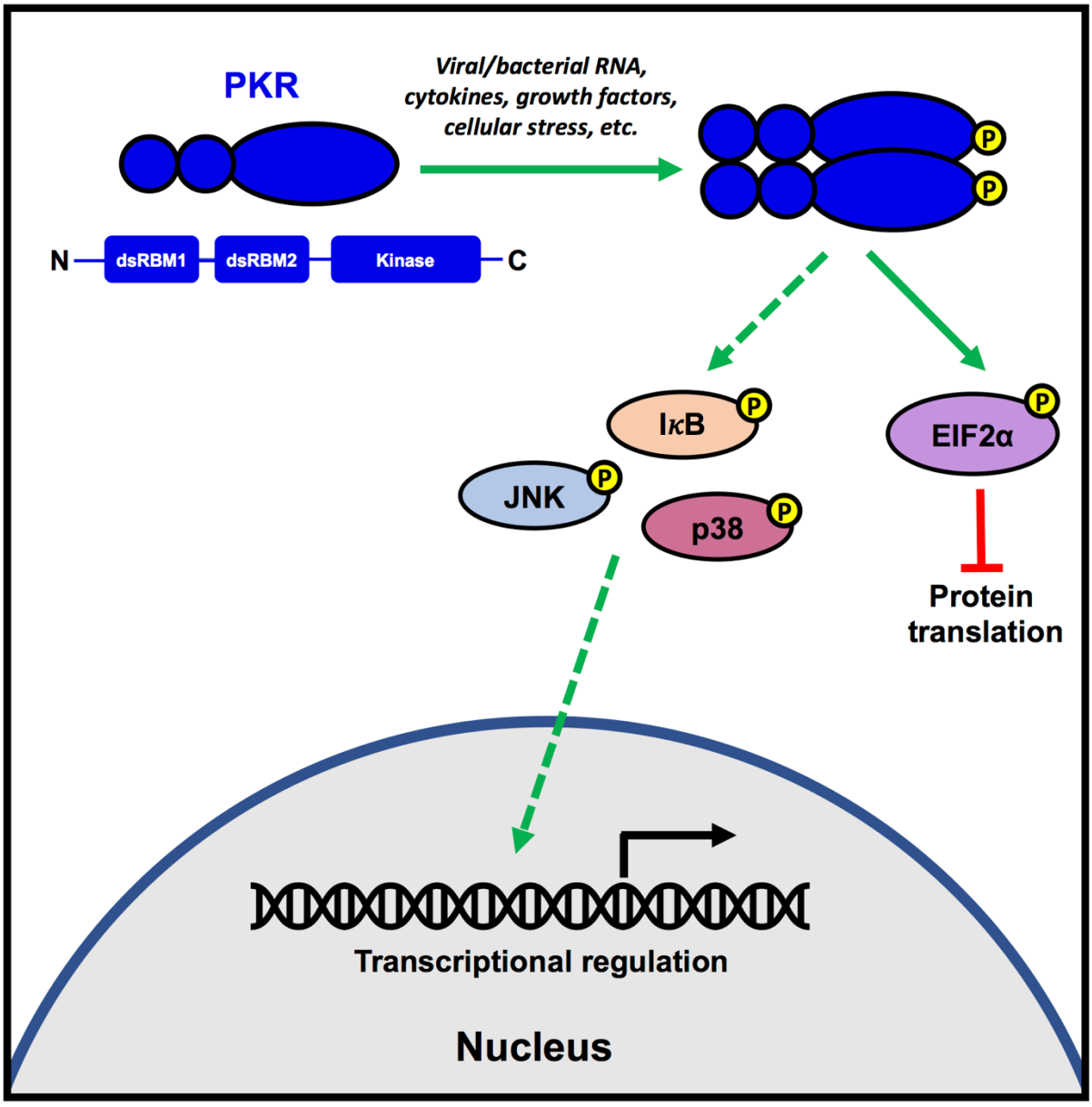
PKR
Viral/bacterial RNA,
cytokines, growth factors,
cellular stress, etc.
P
P
N
dsRBM1
dsRBM2
Kinase
C
IκB
P
JNK
P
p38
P
EIF2α
P
Protein
translation
Transcriptional regulation
Nucleus

Figure 3. Function and mechanism of action of PKR. PKR has a C-terminal kinase domain and an N-terminal dsRNA binding domain that consists of two double-stranded RNA binding motifs (dsRBM1 and dsRBM2). The canonical activator of PKR is viral RNA, however PKR can be activated by a variety of stimuli including bacterial RNA, cytokines, growth factors, and cellular stress. Upon activation, PKR homodimerizes and autophosphorylates at multiple serine and threonine residues. Active PKR phosphorylates the alpha subunit of EIF2 (EIF2α), thus leading to inhibition of protein translation. However, PKR can also regulate many signal transduction pathways through downstream effectors such as mitogen activated protein kinases (MAPKs) JNK and p38. In addition, PKR indirectly activates NF-κB by triggering the phosphorylation of IκB by IκB kinase. The regulation of signal transduction pathways through its downstream effectors allows PKR to influence transcription and cellular processes such as apoptosis and inflammation

1.4.2 Regulation of signal transduction pathways

PKR regulates many signal transduction pathways through downstream effectors such as MAPKs and NF-κB (Figure 3). In doing so, PKR controls cellular processes such as inflammation and apoptosis. MAPKs are serine/threonine kinases that regulate many cellular events. PKR has been observed to activate MAPKs such as JNK and p38. JNK is activated by numerous cell stressors such as ultraviolet or gamma irradiation, toxins, chemotherapeutic agents, heat shock, protein synthesis inhibitors, and pro-inflammatory cytokines. p38 is activated in response to pro-inflammatory cytokines such as IFNγ, TNFα, and IL-1, or in response to cell stress caused by ultraviolet irradiation, osmotic shock, heat shock, and LPS challenge. Both JNK and p38 regulate numerous cell processes such as autophagy, apoptosis, and cell differentiation. JNK is activated by MAPK kinase (MKK)4, whereas p38 is activated by MKK3 or MKK6. Many groups have reported that PKR activates JNK and p38. For example, depletion of PKR by stable knockdown impaired the phosphorylation of JNK and p38 in response to dsRNA or a mutant strain of vaccinia virus (265). Another group observed that PKR expression was required for full activation of JNK and p38 in response to poly(I:C), LPS, IL-1β, and TNFα (257). In that same study, deletion of PKR in mouse embryonic fibroblasts (MEFs) was observed to inhibit MKK4 and MKK3/6 phosphorylation in response to the same stimuli. Interestingly, PKR deletion did not impact p38 or JNK activation in response to stressors that impact cellular components on a global scale, such as ultraviolet radiation, osmotic shock, and heat shock. The PKR-dependent stress stimuli were limited to pro-inflammatory ligands that bind distinct receptors, i.e. PKR as a receptor for dsRNA, CD14 and TLR4 for LPS, and the respective cytokine receptors for IL-1β and TNFα. Thus, it is suggested that PKR mediates activation of p38 and JNK in response to "receptor-mediated"

pro-inflammatory stress stimuli, but not in response to "globally acting" stressors (257). Results from a different study support the observation that PKR activates p38 by acting upstream of MKK6 (266). PKR was observed to phosphorylate MKK6 in response to poly(I:C), an effect that was inhibited by pharmacological inhibition of PKR or expression of a kinase-inactive PKR mutant. Importantly, p38 regulates several transcription factors, such as NF-κB and signal transducer and activator of transcription (STAT)1. As such, PKR can influence these transcriptional pathways through its regulation of p38 activation. There is also some evidence to suggest that PKR mediates extracellular-signal-regulated kinase (ERK) activation. Pharmacological inhibition of PKR in monocytes markedly inhibited the phosphorylation of ERK1/2 in response to BCG infection (267). Furthermore, PKR regulates STAT1 and STAT3 phosphorylation in residues located in ERK consensus sequences, as discussed below (260).

As mentioned in section 1.2.3, NF-κB is crucial in the pro-inflammatory response. NF-κB results in transcription of pro-inflammatory cytokines such as TNFα, IL-1β, and IL-12 (268). There is a cellular inhibitor of NF-κB that prevents its translocation to the nucleus, known as inhibitory κB alpha (IκBα). However, IκB kinase (IKK) phosphorylates IκBα at two serine residues in response to a variety of stimuli, marking IκBα for degradation by the proteasome. This results in the release of IκBα from NF-κB, thus allowing NF-κB to translocate to the nucleus and regulate transcription. PKR is established to indirectly activate NF-κB by activating IKK (269). In PKR null cell-lines, poly(I:C) failed to stimulate IKK activity compared to cells WT for PKR, and NF-κB activation was inhibited (262). Furthermore, coimmunoprecipitation experiments revealed that PKR physically associated with IKK (270). However, whether PKR is merely a structural component in the activation of

IKK remains in debate. Some groups have reported that catalytically inactive PKR mutants can activate IKK efficiently (270), whereas others have shown that complementation of PKR knockout MEFs with WT PKR, but not a catalytically inactive PKR mutant, restores NF-κB activation (271). Thus, the mechanism behind the activation of IKK by PKR remains unknown. Although there are numerous reports that PKR activates NF-κB, there exists some contradictory evidence. For example, one group observed that PKR deletion did not impact NF-κB activation in response to dsRNA or TNFα (272). It has been suggested that there could be cell-specific, PKR-independent mechanisms of NF-κB activation. Consistent with this idea, some NF-κB activity can be triggered in PKR knockout MEFs in response to dsRNA (271). Since TLR3 has been identified as a dsRNA receptor, it is possible that TLR3 recognition of dsRNA can trigger NF-κB activation in a PKR-independent manner (273).

1.4.3 Role during viral infection

PKR is most well-characterized for its role in the antiviral response. The global inhibition of translation triggered upon recognition of dsRNA by PKR prevents the replication of a wide spectrum of viruses. Indeed, PKR is reported to provide host protection from viruses such as vesicular stomatitis virus, lymphocytic choriomeningitis virus, and lethal West Nile virus, to name a few (274–276). However, PKR activation can trigger additional antiviral responses, such as induction of apoptosis. Although the inhibition of protein translation by phosphorylation of EIF2α can lead to apoptosis, PKR can also induce apoptosis independently of EIF2α activation (277). In fact, PKR is reported to induce apoptosis via activation of the FADD/caspase-8/caspase-3 pathway as well as the caspase-9 pathway in an EIF2α-independent manner (278). Interestingly, blocking nuclear translocation of NF-κB by

inhibiting IκBα degradation with proteasome inhibitors or by using a non-phosphorylatable form of IκBα prevented PKR-dependent apoptosis in response to vaccinia virus (279). This effect was independent of EIF2α phosphorylation. As such, it appears as though PKR regulates apoptosis through its effects on NF-κB activation, although further investigation is needed to determine the specific role of NF-κB in this context.

Another antiviral function of PKR is the induction of type I IFN production during viral infection. Numerous studies have found that PKR deficiency impairs IFNβ production upon stimulation with poly(I:C) or viral infection (280). More specifically, PKR is required for IFNβ production in response to viruses detected by the melanoma differentiation-associated gene 5 (MDA5) RNA sensor, such as encephalomyocarditis virus (ECMV) (281). Although IFNβ transcription was highly induced in PKR-deficient cells upon ECMV infection, little or no IFNβ protein was produced, suggesting that PKR impacts the post-transcriptional regulation of IFNβ production (281). Results from the same study revealed that IFNβ transcripts produced in ECMV-infected PKR-deficient cells completely lack a poly(A)tail, indicating that PKR is required for the integrity of IFNβ mRNA and its translation into functional protein. PKR also appears to regulate IFNβ production *in vivo*, since PKR knockout mice infected with ECMV had significantly lower levels of serum IFNβ (281). Type I IFN play an important role during viral defense. Indeed, IFNs exert many antiviral functions such as inhibition of intracellular viral replication and induction of antiviral responses from $CD8^+$ T cells and NK cells.

PKR also plays a role in autophagy activation. An initial study found that EIF2α phosphorylation by the yeast EIF2α kinase GCN2 was essential for starvation-induced autophagy of yeast cells (282). Supplementation of PKR in GCN2-disrupted yeast rescued

autophagy in these cells, indicating a role for PKR in autophagy induction. It is now known that PKR can induce autophagy during viral infection. Indeed, infection of PKR knockout MEFs with a Herpes Simplex Virus-1 (HSV-1) mutant lacking the PKR-inhibiting virulence factor ICP34.5 significantly inhibited colocalization of virions with autophagosomes (283). As such, autophagy activation is another antiviral function of PKR.

1.4.4 Role during non-viral infection

Although PKR was initially discovered as an antiviral protein, there is growing evidence to suggest that PKR plays a role during parasitic and bacterial infection. For example, PKR activation by poly(I:C) resulted in the death of the parasite *Leishmania major*, whereas cells expressing a dominant negative variant of PKR had an increased parasite burden compared to WT cells at 24 hours post-infection (284). In contrast, PKR has been reported to be conducive for *Leishmania amazonesis* infection. Infection with *L. amazonesis* induced the phosphorylation of PKR, and PKR deficiency leads to reduced parasite growth (285). Furthermore, PKR was also observed to enhance IL-10 production, which is permissive for parasitic growth. The stark difference in PKR activity during *L. major* and *L. amazonesis* infection indicates that PKR can be pro- or anti-parasitic depending on the specific parasite. Indeed, PKR was observed to play an anti-parasitic role in response to *Toxoplasma gondii* infection (286). PKR knockout mice exhibited higher parasite load compare to WT mice. Importantly, PKR was required for autophagy induction, LC3 accumulation around the parasite, and lysosomal fusion with vacuole-containing *T. gondii* in macrophages (286). This indicates that PKR not only plays a role in autophagy induction during viral infection, but also during parasitic infection.

There have also been a few reports examining the role of PKR during bacterial infection. As mentioned in section 1.4.1, it is now known that PKR can recognize bacterial RNA in addition to viral RNA, which is indicative of a role for PKR in the antibacterial response. One group observed that macrophage apoptosis in response to *Bacillus anthracis*, *Yersinia pseudotuberculosis,* or *Salmonella* Typhimurium infection required activation via TLR4, and that PKR knockout macrophages did not undergo apoptosis in response to these pathogens (287). These results suggest that PKR plays a role in the antibacterial response of macrophages. However, although PKR was observed to induce macrophage apoptosis during bacterial infection, the overall effect of PKR on bacterial load was not examined. PKR has also been observed to play a role in pyroptosis during bacterial infection, as PKR deficiency inhibited inflammasome activation and the production of IL-1β and IL-18 in response to *Escherichia coli* infection (288).

There is limited knowledge on the role of PKR during mycobacterial infection. A study revealed that PKR phosphorylation is triggered in monocytes infected with BCG, and pharmacological inhibition of PKR suppresses the production of crucial anti-BCG cytokines including TNFα, IL-6, and IL-10 (267). However, once again the effect of PKR on bacterial load was not examined. One group demonstrated that PKR expression and activation is triggered during Mtb infection, and PKR deletion in Mtb-infected macrophages increases the bacterial burden (289). In contrast, another group did not report a difference in CFU in the lungs of infected PKR knockout mice compared to WT mice (290). As such, the role in PKR during Mtb infection remains elusive.

1.4.5 Pharmacological modulators

Accumulation of PKR is correlated with inflammatory and neurodegenerative diseases (291). As such, there is growing interest in evaluating the effects of pharmacological PKR inhibitors. The most widely used pharmacological PKR inhibitor is the imidazole-oxindole C16 (also known as PKRi or Imoxin) (292). C16 targets the ATP-binding site of PKR, thus inhibiting PKR kinase activity and autophosphorylation. 2-aminopurine (2-AP) is a less potent and less specific pharmacological inhibitor of PKR that inhibits phosphorylation of PKR by competing for ATP at the kinase's ATP binding site (293). However, there are no pharmacological inhibitors of PKR that have reached clinical trials.

Due to the role of PKR in apoptosis induction, there is interest in using pharmacological PKR activators for cancer therapy (294). Indeed, bozepinib is a small antitumor agent that has been observed to activate PKR (295). Bozepinib has shown promise in pre-clinical studies as it induces apoptosis in breast and colon cancer cells and has no toxicity at high concentrations in mice (296). Further investigation revealed that PKR is both upregulated and activated by bozepinib, and PKR deletion in MEFs inhibits the ability of the drug to induce apoptosis (295). The mechanism through which bozepinib induces and activates PKR remains unknown. Nitazoxanide (NTZ) is another drug that has been reported to induce the phosphorylation of PKR (297, 298). NTZ is an FDA-approved broad-spectrum antiparasitic and antiviral drug. This drug was originally used to treat cryptosporidiosis infection but has been repurposed for the treatment of viral infections such as hepatitis C. NTZ has been shown to deplete intracellular calcium stores, thereby raising levels of cytosolic calcium. This calcium mobilisation disrupts endoplasmic reticulum/Golgi glycoprotein trafficking and induces endoplasmic reticulum stress, thus resulting in PKR phosphorylation (298). Interestingly, NTZ was observed to exert significant bactericidal activity directly

against both replicating and non-replicating bacteria in 50 different clinical isolates of Mtb (299), and was recently evaluated for treatment of TB in a phase II clinical trial (300). Screening of a compound library identified the synthetic compound BEPP [1*H*-benzimidazole1-ethanol,2,3-dihydro-2-imino-*a*-(phenoxymethyl)-3-(phenylmethyl)-,monohydrochloride] as another PKR activator (301). Treatment of MEFs with BEPP increased PKR and EIF2α phosphorylation in a dose-dependent manner, and expression of dominant-negative PKR revealed that the induction of apoptosis by BEPP is PKR-dependent. However, the mechanism of action of BEPP on PKR activity is unknown. Lastly, a screen of 20,000 small molecules identified 3-(2,3-dihydrobenzo[b][1,4]dioxin-6-yl)-5,7-dihydroxy-4H-chromen-4-one (DHBDC) as a dual activator of PKR and PERK (302). DHBDC was shown to induce the phosphorylation of EIF2α, which was blocked by siRNAs targeting PKR and PERK. The mechanism by which DHBDC activates PKR remains unknown. Both BEPP and DHBDC are commercially available for research use.

1.5 Rationale

Due to the emergence of antibiotic-resistant TB, the development of alternative anti-TB therapeutics is urgently needed. HDT is a promising strategy since it targets the host immune system rather than the bacterium itself, thus circumventing the development of antibiotic-resistance. It has been observed that nearly half of individuals in close contact with highly active TB patients do not produce antibodies against Mtb (303). This suggests that a strong innate immune response can successfully clear Mtb in certain individuals. Since AMs are the first line of defense against inhaled bacteria, the persistence of Mtb is largely determined by the bactericidal capacity of macrophages (304). As such, the ability of certain

individuals to achieve early clearance of Mtb may be due to an enhanced antibacterial response by their macrophages. Targeting host proteins to boost the antibacterial activity of macrophages could therefore be a promising strategy for HDT.

PKR is one such host protein that has been suggested as a prime candidate for HDT against TB infection (220, 289, 305). PKR induces stress-activated apoptosis during viral infection or serum starvation (256), and may play a role in regulating pyroptosis and necroptosis (288, 306). The role of PKR in controlling cell death pathways suggests that it may be a promising target for TB HDT, since the specific mode of cell death that occurs in Mtb-infected macrophages largely influences the progression of infection (304). PKR has also been demonstrated to play a role in autophagy during viral and parasitic infection (283, 286). Autophagy is a relevant defense mechanism in macrophages infected with Mtb, since it can target and degrade cytosolic Mtb after it escapes the phagosome (193). Due to the antibacterial role of autophagy in macrophages, therapeutic activation of autophagy is a promising HDT strategy against TB (220, 221). However, a potential role for PKR in regulating autophagy during bacterial infections has not been studied.

Given that PKR regulates several key macrophage defense mechanisms that are critical for Mtb clearance, PKR could be a promising target for TB HDT. Nevertheless, knowledge of the function of PKR in macrophages during bacterial infection is surprisingly limited. PKR is activated in response to Mtb and BCG infection, and is also reported to enhance production of antibacterial cytokines in response to BCG (267, 289). However, existing reports of the effect of PKR expression on intracellular survival of Mtb are contradicting. While one group reported that PKR deletion in Mtb-infected macrophages increases the bacterial burden (289), another group did not report a difference in CFU in the lungs of infected PKR knockout mice compared to WT mice (290). Furthermore, these reports

are non-comprehensive, as the specific mechanisms regulated by PKR during Mtb infection were not investigated. Since PKR is involved in many different macrophage signalling pathways, the true function of this kinase in the context of TB remains unknown. As such, our goal was to investigate the role of PKR in Mtb infection and assess its suitability as a candidate for TB HDT.

1.6 Hypothesis

We hypothesize that PKR plays a key role in the macrophage antibacterial response to Mtb infection.

1.7 Statement of objectives

1. Examine the effect of PKR overexpression on the antibacterial response of Mtb-infected macrophages
2. Determine the molecular mechanism(s) that underlie the function of PKR during Mtb infection

2. MATERIALS AND METHODS

2.1 Reagents

DHBDC was purchased from Calbiochem (Burlington, MA). Bafilomycin A1 was purchased from Santa Cruz Biotechnology (Dallas, TX). Recombinant human IFNγ and puromycin were purchased from Gibco (Gaithersburg, MD). Rapamycin was purchased from Alfa Aesar (Haverhill, MA).

2.2. Cell culture

THP-1 monocytes (ATCC TIB-202) and primary human monocytes were maintained in Roswell Park Memorial Institute (RPMI) 1640 medium (Gibco). HEK GP-293 cells (Clontech, Mountain View, CA), HEK293T cells (ATCC CRL-3216), and RAW 264.7 cells (ATCC TIB-71) were maintained in Dulbecco's Modified Eagle Medium (DMEM) (Gibco). RPMI 1640 and DMEM medium was supplemented with 2 mM L-glutamine, penicillin-streptomycin (100 I.U./ml penicillin, 100 µg/ml streptomycin), 10 mM HEPES, and 10% heat-inactivated fetal bovine serum purchased from Gibco. Cells were maintained at 37°C in a humidified atmosphere of 5% CO_2. Human peripheral blood mononuclear cells were collected according to approved ethics protocols (Protocol# 2005388-01H) and isolated from buffy coats by the Ficoll-Paque density centrifugation method. Positive selection of monocytes was performed using anti-CD14 coated magnetic particles from StemCell Technologies (Vancouver, BC) according to manufacturer's protocol. Monocytes were then differentiated with 5 ng/ml granulocyte-macrophage colony-stimulating factor (Gibco) for 6 days to obtain

human monocyte-derived macrophages (MDMs). THP-1 monocytes were differentiated with 100 ng/ml phorbol ester 13-phorbol-12-myristate acetate (PMA, Alfa Aesar) for 72 h.

2.3 Maintenance and generation of bacteria

The *M. tuberculosis* H37Rv-derived auxotroph strain mc^26206 was grown in Middlebrook 7H9 medium (BD Biosciences, Franklin Lakes, NJ) supplemented with 0.2% glycerol (Fisher Chemical, Waltham, MA), 0.05% Tween-80 (Acros Organics, Fair Lawn, NJ), 10% OADC (BD Biosciences), 24 μg/ml D-pantothenic acid (Alfa Aesar) and 50 μg/ml L-leucine (Alfa Aesar). Green fluorescent protein (GFP)-expressing *M. tuberculosis* mc^26206 was generated previously (307). *M. tuberculosis* mc^26206 expressing luciferase was generated by transforming the pSMT3 plasmid encoding for firefly luciferase gene. GFP- and luciferase-expressing Mtb were maintained in antibiotic selection with 50 μg/ml hygromycin B (Calbiochem, San Diego, CA). Liquid Mtb cultures were maintained at 37°C with slow shaking (50 rpm). *Salmonella enterica* serovar Typhimurium strain SL1344 and *Listeria monocytogenes* strain 10403s were initially grown in Luria-Bertani broth (Fisher BioReagents, Waltham, MA) at 37°C until reaching the log-phase, as determined by optical density measurement at 600 nm. Bacteria were then frozen in LB medium containing 20% glycerol and stored at -80 in 1 mL aliquots. Concentration of the stocks was determined by assessing CFU. *Escherichia coli* strain NEB Stable (New England Biolabs, Ipswich, MA), was used for plasmid propagation and was routinely grown in Luria-Bertani broth at 37°C.

2.4 Plasmid construction

Plasmid pMSCV-PKR was constructed by inserting the PCR amplified *EIF2AK2* gene (Entrez Gene ID 5610, variant 1) from THP-1 cell-derived cDNA using a custom forward and reverse oligonucleotide pair **(Table 1)** flanked by the XhoI and HpaI restriction sites, respectively, into the multiple cloning site of the overexpression vector pMSCV-puro (Clontech). The parameters for *EIF2AK*2 amplification were 98°C for 30 s, followed by 30 cycles of 98°C for 10 s, 56°C for 15 s, and 72°C for 2 min. The CRISPR/Cas9 knock-out plasmid targeting human PKR was generated by inserting the annealed single guide RNA (sgRNA) oligonucleotide pair **(Table 1)** into a modified LentiCRISPR v2 vector linearized by the restriction enzyme BsmBI. The sgRNA was designed to target the human *EIF2AK2* gene and minimize off-target binding using publicly available online design tools. To optimize the CRISPR-Cas9 system, we performed modifications to the LentiCRISPR v2 vector by creating an A-U base pair flip in the sgRNA stem-loop and by extending the Cas9-binding hairpin structure, as demonstrated by Chen and colleagues (308). LentiCRISPR v2 was a gift from Feng Zhang (Addgene plasmid # 52961 ; http://n2t.net/addgene:52961 ; RRID:Addgene_52961) (309). The resulting plasmids were verified by Sanger sequencing.

Table 1. Primers used for cloning

Target	Primer Type	Forward/ Reverse	Sequence (5'-3')
EIF2AK2	PCR	FW	GCTA**CTCGAG**ATGGCTGGTGATCTTTCAGCAGGTTTC **(XhoI)**
EIF2AK2	PCR	RV	GCTA**GTTAAC**CTAACATGTGTGTCGTTCATTTTTCTCTG **(HpaI)**
EIF2AK2	sgRNA	FW	AGCTGTTGAGATACTTAATA
EIF2AK2	sgRNA	RV	TATTAAGTATCTCAACAGCT

2.5 Transfection

HEK GP-293 or HEK 293T cells were seeded at 50% confluency (100,000 cells/well in a 24-well plate) to produce viral supernatant. 0.4 μg of the retroviral plasmid of interest (empty pMSCV-puro or pMSCV-PKR) was co-transfected with 0.2 μg of the pVSVG envelope plasmid into HEK GP-293 cells to produce retroviral particles. 0.2 μg of the modified LentiCRIPSR plasmid containing sgRNA targeting PKR was co-transfected with 0.1 μg of the pVSVG envelope plasmid and 0.2 μg of the psPAX2 packaging plasmid into HEK 293T cells to produce lentiviral particles. FuGENE (Promega, Madison, WI) was used as the transfection reagent at a ratio of 4:1 (FuGENE:DNA). Culture supernatants were harvested after 48 h by 5 min centrifugation at 350 x g to remove cells and debris. Supernatants were then aliquoted and stored at -80°C.

2.6 Transduction

THP-1 monocytes were seeded (200,000 cells/well in 12-well plates) in a final volume of 300 μl. 700 μl of supernatant containing lentiviral or retroviral particles supplemented with 10 μg/ml diethylaminoethyl-dextran (Sigma-Aldrich, St. Louis, MO) was added to the THP-1 cells. The cells were left for 72 h and then selected using 1 μg/ml puromycin. A western blot was performed to verify knockout or overexpression of PKR protein levels.

2.7 *in vitro* bacterial infection

M. tuberculosis $mc^2$6206 growing in log-phase was quantified by optical density measurement at 600 nm using the conversion of OD 1 = 3 x 10^8 Mtb bacteria per ml. The number of bacteria required for various multiplicity of infections (MOIs) were harvested by 2

min centrifugation at 8,000 x g and resuspended in RPMI 1640 cell culture media without antibiotics. Bacteria were added to the differentiated THP-1 macrophages, primary human MDMs, or RAW 264.7 cells and the plates were kept at 37°C for the duration of the infection. If the infection was to exceed 24 hours, three phosphate buffered saline (PBS) washes were performed after the first 4 h of infection to remove extracellular, non-phagocytosed bacteria and then the infection was continued at 37°C for the desired time. For infections with *Salmonella* Typhimurium and *Listeria monocytogenes*, frozen stocks with pre-determined CFU/ml were thawed and the number of bacteria required for various MOIs were harvested by 5 min centrifugation at 8,000 x g. The bacteria were then resuspended in RPMI 1640 media without antibiotics. The bacteria were added to THP-1 macrophages and the culture plates were centrifuged for 4 min at 400 x g to allow the bacteria to settle to the bottom of the wells. The plates were then incubated at 37°C for 30 min. After 30 min, the extracellular bacteria were removed by performing three PBS washes and the cells were cultured in RPMI medium containing 50 µg/ml gentamicin for 1.5 h. After 1.5 h incubation, cells were washed three times with PBS and cultured in RPMI medium containing 10 µg/ml gentamicin for the remainder of the experiment.

2.8 Resazurin cell viability assay

Serial dilutions of DHBDC, bafilomycin A1, or rapamycin were added to THP-1 macrophages (70,000 cells/well in 96-well plates) and maintained in the medium for the duration of the experiments. The compounds were replenished every second day. At the indicated time points, 30 µL of 0.02% resazurin (Sigma-Aldrich) diluted in PBS was added to the wells. After a 4 h incubation at 37°C, fluorescence was measured using the Synergy™ H1

Hybrid Multi-Mode Reader (BioTek, Winooski, VT) with an excitation wavelength of 560 nm and an emission wavelength of 590 nm. Cell cytotoxicity was assessed by comparing the fluorescence of treated cells to untreated cells.

2.9 Intracellular Mtb survival assay

THP-1 macrophages (70,000 cells/well), human MDMs (50,000 cells/well), or RAW 264.7 cells (50,000 cells/well) in 96-well plates were infected with Mtb-luciferase as described in section 2.7. At the indicated time points, cell culture supernatant was removed from the infected wells and the macrophages were lysed in 50 µl Glo Lysis Buffer (Promega) to measure the amount of viable Mtb in each well. Luciferase activity, proportional to viable bacterial, was determined using the BrightGlo Luciferase Assay System (Promega) according to the manufacturer's protocol. Resultant luminescence was measured with the Synergy^{TM} H1 Hybrid Multi-Mode Microplate Reader (BioTek) using 96-well solid white plates (Corning, Corning, NY) and an integration time of 1 s per well.

2.10 Real-Time Cell Analysis

Macrophage adhesion of THP-1 macrophages (70,000 cells/well) was measured in specialized 96-well plates (E-plate 96) with the xCELLigence Real-time Cell Analyzer (RTCA) SP apparatus (ACEA Biosciences, San Diego, CA). Data was quantified by measuring impedance changes between the sensing electrodes located in the well-bottom, which changes as a function of the adhesion of cells to the surface of the plate. The Cell Index (CI) is a dimensionless value that is representative of these impedance changes. Using this system, macrophage adhesion and therefore viability was monitored in real-time. Plates were

removed after ~72 h of macrophage differentiation for the addition of Mtb for infection. After addition of Mtb, plates were placed back in the RTCA apparatus for kinetic monitoring. The CI at every time point represents the mean of three biological replicates.

2.11 Apoptosis assay

THP-1 macrophages (100,000 cells/well in 24-well plates) were infected with Mtb as described in section 2.7 At the indicated time points, supernatant was collected from the sample wells to preserve detached cells. The wells were washed twice with PBS and 300 µl TrypLE Express Enzyme (Gibco) was added to the wells. The plate was incubated at 37°C for 5 min to allow for detachment of adherent THP-1 macrophages. The floating and harvested cells were combined and washed twice with PBS. Cells were then transferred to 96-well round bottom plates and stained with Annexin V conjugated to FITC (eBioscience, San Diego, CA) according to manufacturer's protocol. Flow cytometric analysis was used to measure apoptotic cells.

2.12 Multiplex cytokine and chemokine analysis

THP-1 macrophages (200,000 cells/well in 24-well plates) were infected with Mtb for 24 h in a final volume of 1 mL. Culture supernatants were harvested and the LEGENDplex™ Human Essential Immune Response bead-based multiplex assay (BioLegend, San Diego, CA) was used according to the manufacturer's protocol to measure expression of the following cytokines: IL-10 (0.77 + 1.18), TGF-β1 (3.10 + 2.92), IL-1β (0.65 + 0.47), TNFα (0.88 + 0.27), IFNγ (0.76 + 0.53), IP-10 (1.28 + 0.48), IL-6 (0.97 + 1.46), IL-8 (1.90 + 0.65), IL-2 (1.81 + 0.93), IL-4 (0.97 + 0.83), IL-17A (2.02 + 0.04), and MCP-1 (1.45 + 0.27). The

minimum detectable concentration (MDC) in pg/ml for each cytokine is reported in brackets as MDC + 2 STDEV. Data analysis was performed using LEGENDplex™ Data Analysis Software Version 7.1 (BioLegend).

2.13 Phagocytosis assay

THP-1 macrophages (100,000 cells/well in 96-well plates) were infected with Mtb-GFP and the plates were kept at room temperature for 20 minutes to synchronize the phagocytosis. The plates were then incubated at 37°C for 4 h and then three PBS washes were performed to remove non-phagocytosed, extracellular bacteria. 100 µl of TrypLE Express Enzyme was added to the wells and the plate was incubated at 37°C for 5 min to allow for detachment of adherent THP-1 macrophages. The cells were then transferred to a 96-well round bottom plate and washed once with PBS. Cells were resuspended in 200 µl PBS with 1% bovine serum albumin (BSA) and phagocytosis levels in macrophages were monitored by flow cytometric analysis of GFP as a marker for internalized Mtb.

2.14 Flow cytometry

Flow cytometric analysis was performed using the CytoFLEX (Beckman Coulter, Indianapolis, IN). Data analysis was performed using CytExpert software (Beckman Coulter) or FlowJo V10 software (BD Life Sciences, Ashland, OR). Flow cytometry was performed to measure apoptosis, cytokine expression, and phagocytosis levels in macrophages.

2.15 Quantitative real-time PCR

Total RNA was isolated from THP-1 macrophages or MDMs (700,000 cells/well in 6-well plates) using the Aurum Total RNA Mini Kit from Bio-Rad (Hercules, CA). 500 ng of total RNA was used in the cDNA synthesis reaction using the iScript Reverse Transcription Supermix (Bio-Rad). 4 µl of synthesized cDNA (out of 10 µl reaction) was used to analyze gene expression of *EIF2AK2* or the reference genes *ACTB* and *GAPDH* by real-time polymerase chain reaction (PCR) on a CFX96 Touch Real-Time PCR Detection System (Bio-Rad) using primers **(Table 2)** in combination with the SsoAdvanced Universal SYBR Green Supermix (Bio-Rad). The custom primers for *EIF2AK2* were designed according to MIQE guidelines. Thermocycling parameters were 95°C for 3 min, followed by 40 cycles of 95°C for 10 s, 60°C for 20 s, and 72°C for 20 s. Gene expression was determined using the ΔΔCq method (310). ΔCq values were obtained by normalizing the Cq values of *EIF2AK2* with the geometric mean of two reference genes (*ACTB* and *GAPDH*). Relative fold expression was estimated as 2^−ΔΔCq when normalizing to uninfected (day 0) macrophages as 1.0.

Table 2. Primers used for qRT-PCR

Target	Forward/ Reverse	Sequence (5'-3')	Source
EIF2AK2	FW	GAAGTGGACCTCTACGCTTTGG	Custom
EIF2AK2	RV	TGATGCCATCCCGTAGGTCTGT	Custom
GAPDH	FW	CAACAGCGACACCCACTCCT	(311, 312)
GAPDH	RV	CACCCTGTTGCTGTAGCCAAA	(311, 312)
ACTB	FW	ATTGCCGACAGGATGCAGAA	(311)
ACTB	RV	GCTGATCCACATCTGCTGGAA	(311)

2.16 Western blot

THP-1 macrophages (1 million cells/well) or MDMs (650,000 cells/well) were washed once with PBS and lysed using RIPA buffer (Sigma-Aldrich) according to manufacturer's

instructions. Protein concentration of the lysates was determined using the RC DC™ Protein Assay Kit (Bio-Rad) according to the manufacturer's protocol. Samples were prepared by adding 4 µl of 4X laemmli buffer (Bio-Rad) supplemented with 10% β-mercaptoethanol to about 20 µg of protein per sample, and RIPA buffer was added up until a final volume of 16 µl was reached. Samples were placed in a heat block set at 95°C for 5 min to denature the proteins. Following a quick centrifugation, samples were separated by SDS-PAGE using handcast 10% polyacrylamide gels (SureCast Gel Handcast System, Invitrogen, Carlsbad, CA) or precast 4 – 15% polyacrylamide gels (Mini-PROTEAN® TGX Gels, Bio-Rad). Electrophoresis was performed at 80 V until the samples travelled through the stacking gel, followed by 100 – 120 V while the samples separated in the resolving gel. Proteins were subsequently transferred to a polyvinylidene diluoride membrane using the Mini Trans-Blot Transfer Cell system (Bio-Rad). Electrotransfer was performed at 100 V for 1 h. Membranes were then blocked for 1 h with 5% skim milk in Tris Buffered Saline Solution containing 0.5% Tween-20 (TBS-T). Primary antibodies **(Table 3)** were diluted in blocking buffer and added to the membranes. Membranes were incubated overnight at 4°C with gentle shaking. The following day, the membranes were washed three times with TBS-T for 10 minutes. Next, the appropriate secondary antibodies **(Table 4)** were diluted in TBS-T and added to the membranes. Membranes were incubated for 1 h with shaking, followed by three washes with TBS-T as described before. Membranes were developed using the Clarity Western Enhanced Chemiluminescence Substrate (Bio-Rad) and detected in an ImageQuant LAS 4000 imaging system (GE Healthcare Life Sciences, Malborough, MA). Densitometry analysis was performed using ImageJ to quantify protein band intensities.

Table 3. Primary antibodies used for western blotting

Name	Dilution	Source	Supplier	Catalog #
PKR	1:1000	Rabbit	Cell Signaling Technology (Danvers, MA)	12297
PKR (phospho T446)	1:1000	Rabbit	ABCAM (Cambridge, MA)	Ab32036
LC3B	1:1000	Rabbit	Cell Signaling Technology	3868
Phospho-SQSTM1/p62 (Ser403)	1:1000	Rabbit	Cell Signaling Technology	39786
SQSTM1	1:750	Mouse	Santa Cruz Biotechnology	sc-28359
GAPDH	1:5000	Mouse	Invitrogen	MA5-15738
Beta tubulin	1:5000	Mouse	Invitrogen	MA5-16308

Table 4. Secondary antibodies used for western blotting

Name	Dilution	Supplier	Catalog #
Goat Anti-Rabbit IgG (H + L)-HRP Conjugate	1:5000	Bio-Rad	1706515
Goat Anti-Mouse IgG (H + L)-HRP Conjugate	1:5000	Bio-Rad	1706516

2.17 Immunofluorescence microscopy

Differentiated THP-1 cells grown on glass coverslips were infected with Mtb-GFP for 4 h and then washed with PBS to remove extracellular bacteria. To label lysosomes, differentiated THP-1 cells were pre-loaded with 5 ng/ml Texas-Red-conjugated dextran (10,000 Molecular Weight, Invitrogen), a non-biodegradable polysaccharide that accumulates in the lysosome, 24 h prior to Mtb infection. At 24 h post-infection, cells were fixed with 4% methanol-free formaldehyde, permeabilized using 0.2% TritonX-100, and then blocked with 1% BSA-PBS. Cells were incubated overnight at 4°C in a humidified chamber with a primary polyclonal rabbit antibody to LC3 (MBL International Corporation, Woburn, MA), followed by incubation with Alexa Fluor 568 goat anti-rabbit secondary antibody (Invitrogen). For cells pre-loaded with Texas-Red-conjugated dextran, Alexa Fluor 647 goat anti-rabbit secondary

antibody (Invitrogen) was used instead. Nuclei were stained with Hoechst 33342 according to manufacturer's protocol (NucBlue™ Live ReadyProbes™ Reagent, Invitrogen). Slides were mounted with FluorSave™ reagent (Calbiochem) and imaged using an Axio Imager M2 microscope with 40X objective (Carl Zeiss AG). Images (z-stacks) were recorded with AxioCam mRm CCD coupled to Zen Blue software and the analyses were performed using Fiji software.

2.18 Statistical analysis

All statistical analyses were performed using GraphPad Prism version 7 (GraphPad Prism Software, San Diego, CA). Error bars depict standard error of the mean (SEM). All data are expressed as the mean ± SEM of three independent biological replicates, except for the qRT-PCR data in Figure 4, which are expressed as the mean ± SEM of three technical replicates. Statistical analysis was performed using unpaired t-tests (Student's t-test) when comparing two independent cell-lines and paired t-tests when comparing within the same cell-line. Values of $p < 0.05$ were considered to be statistically significant, where $*p < 0.05$; $**p < 0.01$; $***p < 0.05$; ns, non-significant. All graphs were made using GraphPad Prism version 7.

3. RESULTS

3.1 The role of PKR in the antibacterial response of macrophages

3.1.1 Infection by *M. tuberculosis* triggers expression and activation of PKR

To investigate whether PKR played a role in the innate immune response to bacterial infections, we measured expression levels of the *EIF2AK2* gene that encodes for PKR following Mtb infection using quantitative real-time polymerase chain reaction (qRT-PCR). Human THP-1 macrophages were infected using the Mtb $mc^2$6206 strain, a derivative of Mtb H37Rv (313) that has been demonstrated to have similar *in vitro* and intra-macrophage replication rates, similar responses to anti-TB drugs, and induces comparable cytokine production relative to the parent strain (40, 314). By day 3 post-infection, qRT-PCR showed a 3-fold increase in the mRNA expression levels of *EIF2AK2* in THP-1 macrophages **(Figure 4A)**. These findings were then confirmed in primary human MDMs, where mRNA expression of *EIF2AK2* at day 3 post-infection was 28-fold higher compared to uninfected macrophages **(Figure 4B)**. To examine whether the increase in PKR expression translated to the protein level, we measured levels of total PKR protein and phosphorylated PKR protein at threonine 446 (p-T446) following Mtb infection over 6 days. Following activation, PKR homodimerizes, which triggers autophosphorylation on multiple serine and threonine sites, including threonine 446 and 451 (253). These two threonine residues are consistently phosphorylated during PKR activation, thus increasing the catalytic activity of PKR and further stabilizing its homodimerization (252, 253). Levels of p-T446 were therefore used as a marker for active PKR. Western blot analysis of cell lysates revealed that total and p-T446 levels of PKR start to increase as early as 24 h post infection **(Figure 5A)**. Total and

phosphorylated levels of PKR increased with the length of infection and stabilized at day 4 post infection, when there was 7- and 17-fold higher total and p-T446 PKR expression, respectively, compared to uninfected macrophages **(Figure 5B)**. These findings were confirmed in primary human MDMs **(Figure 5C)**. By day 6 post-infection, levels of total and p-T446 PKR were 14- and 15-fold higher, respectively, when compared to uninfected macrophages **(Figure 5D)**. Our observations are consistent with findings by Ranjbar and colleagues, as they reported that PKR mRNA and protein levels were increased in THP-1 monocytes following infection with Mtb H37Rv (289). The dramatic increase in PKR expression levels may indicate an innate immune response by macrophages to control bacterial infection.

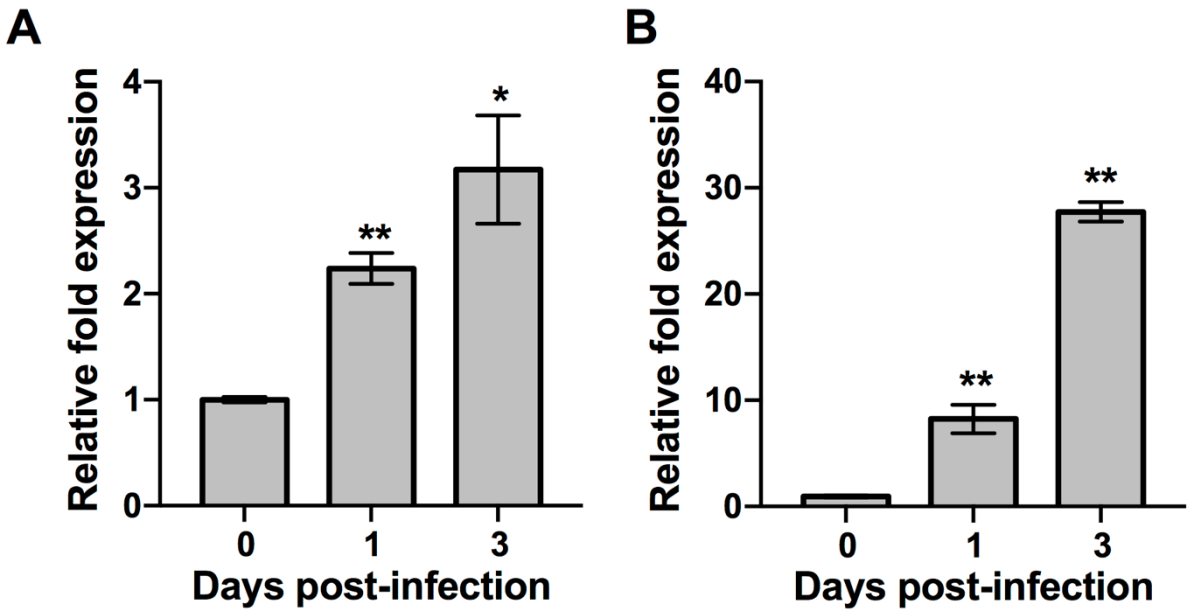
A
Relative fold expression
4
3
2
1
0
**
*
0
1
3
Days post-infection
B
Relative fold expression
40
30
20
10
0
**
**
0
1
3
Days post-infection

Figure 4. *M. tuberculosis* infection upregulates PKR mRNA expression in macrophages. **(A)** THP-1 macrophages or **(B)** primary human MDMs were infected with Mtb at a multiplicity of infection (MOI) of 5 and quantitative real-time PCR was used to measure the relative expression levels of *EIF2AK2* mRNA at 0, 1, and 3 days post-infection. The ΔΔCq method was used for data analysis by normalizing the Cq values of *EIF2AK2* with two reference genes (*ACTB* and *GAPDH*), and relative fold expression was normalized to uninfected (day 0) macrophages as 1.0. Data represent the mean ± SEM of three technical replicates. *$p < 0.05$; **$p < 0.01$ relative to day 0 controls.

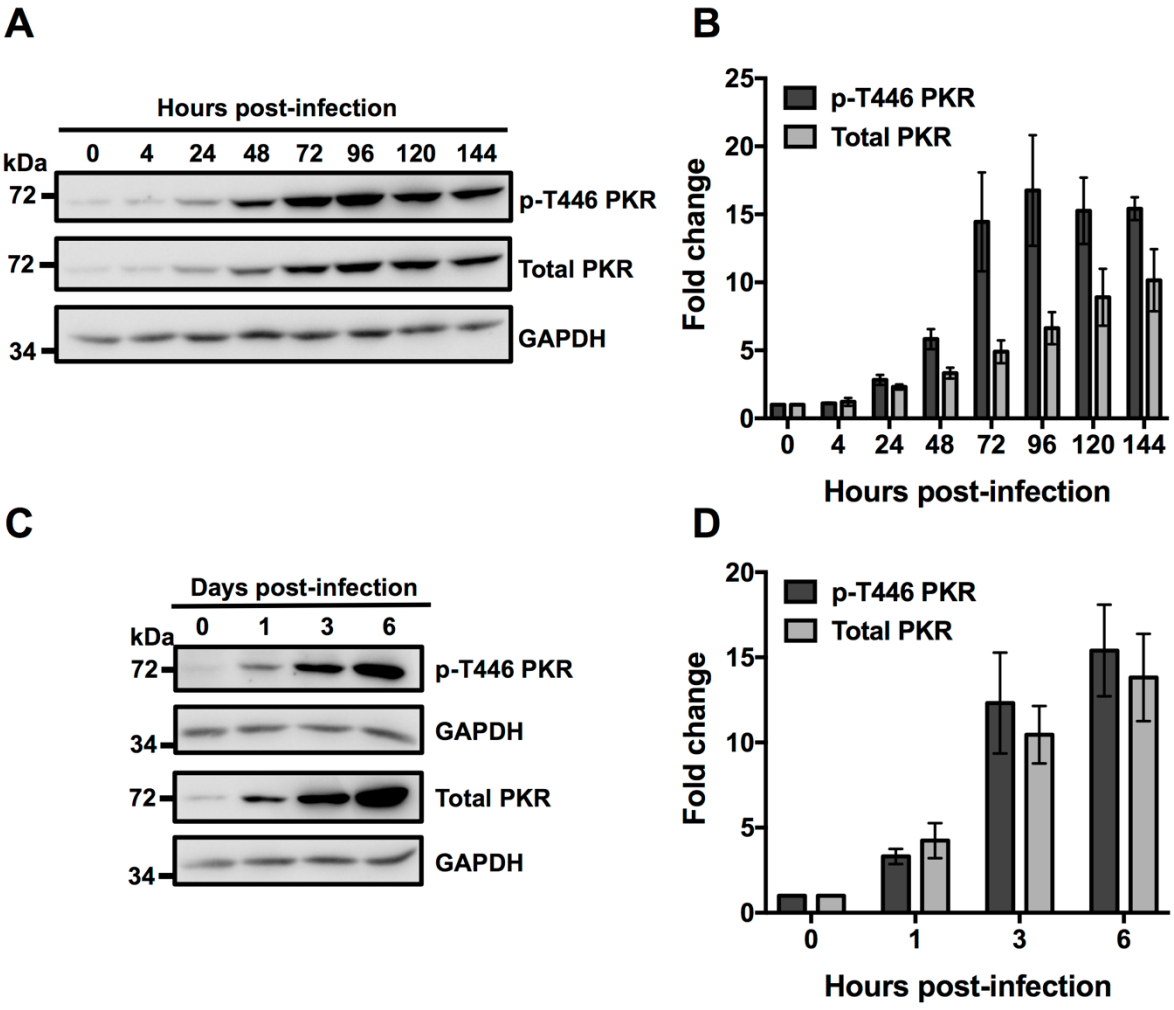
A
Hours post-infection
kDa
0 4 24 48 72 96 120 144
72
p-T446 PKR
72
Total PKR
34
GAPDH
B
p-T446 PKR
Total PKR
Fold change
25
20
15
10
5
0
0 4 24 48 72 96 120 144
Hours post-infection
C
Days post-infection
kDa
0 1 3 6
72
p-T446 PKR
34
GAPDH
72
Total PKR
34
GAPDH
D
p-T446 PKR
Total PKR
Fold change
20
15
10
5
0
0 1 3 6
Hours post-infection

Figure 5. *M. tuberculosis* infection triggers protein expression and activation of PKR in macrophages. (A) THP-1 macrophages were infected with Mtb at an MOI of 5. Cell lysates were prepared at the indicated hours post-infection and total PKR or phosphorylated PKR (p-T446 PKR) protein levels were analyzed by western blotting. **(B)** Densitometry analysis of the blot in (A) was performed by ImageJ to quantify total or p-T446 PKR band intensities as normalized to GAPDH and fold increase of PKR levels is expressed relative to uninfected cells. **(C)** Primary human MDMs were infected as in (A). Cell lysates were prepared at the indicated days post-infection and total PKR or p-T446 PKR protein levels were analyzed by western blotting. **(D)** Densitometry analysis of the blot in (C) was performed by ImageJ to quantify total or p-T446 PKR band intensities as normalized to GAPDH and fold increase of PKR levels is expressed relative to uninfected cells. Error bars represent the mean ± SEM of three independent western blots.

3.1.2 PKR activation and expression is a general response to intracellular bacteria

Since there is limited knowledge on the effect of bacteria on PKR activation, we sought to address whether the increase in PKR expression and phosphorylation observed in Figure 5 was a specific response to Mtb infection. EIF2α, the canonical substrate of PKR, is reported to be phosphorylated during *Listeria monocytogenes, Yersinia pseudotuberculosis*, and *Chlamydia trachomatis* infection, and cells expressing a phosphorylation-defective mutant of EIF2α have increased bacterial burden (315). As such, we predicted that PKR activation is not specific to Mtb challenge since its downstream effector is phosphorylated during infection with other intracellular bacteria. Indeed, western blot analysis of THP-1 cell lysates revealed that infection by *Listeria monocytogenes* and *Salmonella* Typhimurium triggered PKR expression and phosphorylation **(Figure 6)**. This finding indicates that regulation of PKR may be a general response to intracellular bacterial infections.

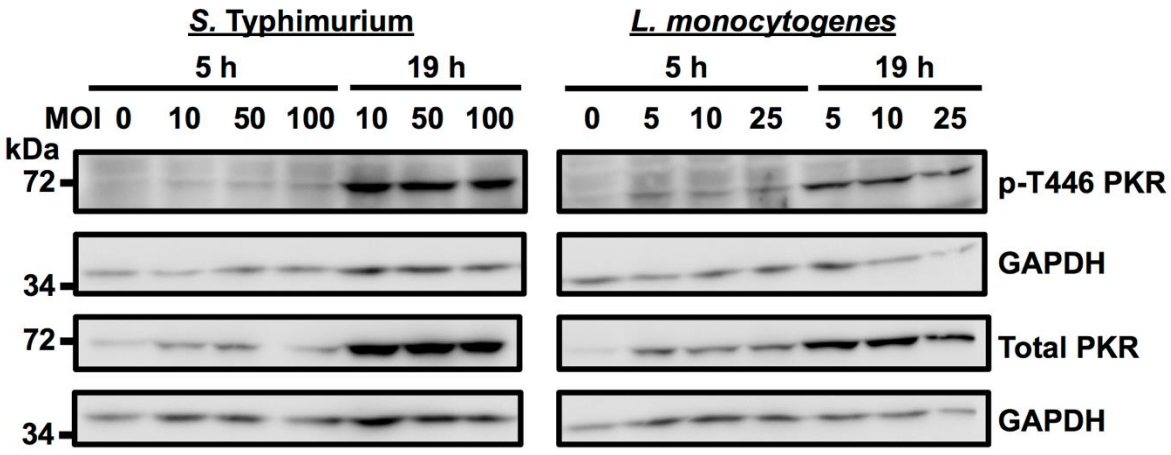
S. Typhimurium
L. monocytogenes
5 h
19 h
5 h
19 h
MOI 0 10 50 100 10 50 100
0 5 10 25 5 10 25
kDa
72
34
72
34
p-T446 PKR
GAPDH
Total PKR
GAPDH

Figure 6. PKR activation and expression is a general response to intracellular bacteria. THP-1 macrophages were infected with *Salmonella* Typhimurium or *Listeria monocytogenes* at the indicated multiplicity of infection (MOI). Cell lysates were prepared at 5 h and 19 h post-infection and total and p-T446 PKR protein levels were analyzed by western blotting.

3.1.3 Deletion of PKR increases the intracellular burden of *M. tuberculosis*

Two previous conflicting studies have examined the effect of PKR deficiency on Mtb survival. While Mundhra and colleagues did not observe an effect of PKR deficiency on Mtb burden in mice (316), Ranjbar et al. reported that PKR knockdown results in increased Mtb survival in macrophages (289). As such, we decided to examine the effect of PKR deletion on the intracellular survival of Mtb in macrophages. We generated PKR knock-out cells (THP-ΔPKR) by transducing THP-1 cells with a lentiviral vector expressing a CRISPR-Cas9 complex targeting exon 2 of the *EIF2AK2* gene. Western blot analysis confirmed that the THP-ΔPKR cells do not express PKR protein **(Figure 7A)**. To measure the viability of intracellular Mtb, we used a well-characterized luciferase reporter system in Mtb (317, 318), which has been demonstrated to correlate strongly with the standard colony unit formation plating method (319). At day 6 post-infection, the bacterial burden of Mtb in THP-ΔPKR macrophages was 84% higher compared to control macrophages **(Figure 7B)**. Our results are consistent with the CFU analysis findings from Ranjbar and colleagues, where at day 4 post-infection the Mtb burden was significantly higher in PKR knockdown THP-1 cells compared to control cells (289). We thus concluded that PKR expression is required to limit Mtb survival in macrophages.

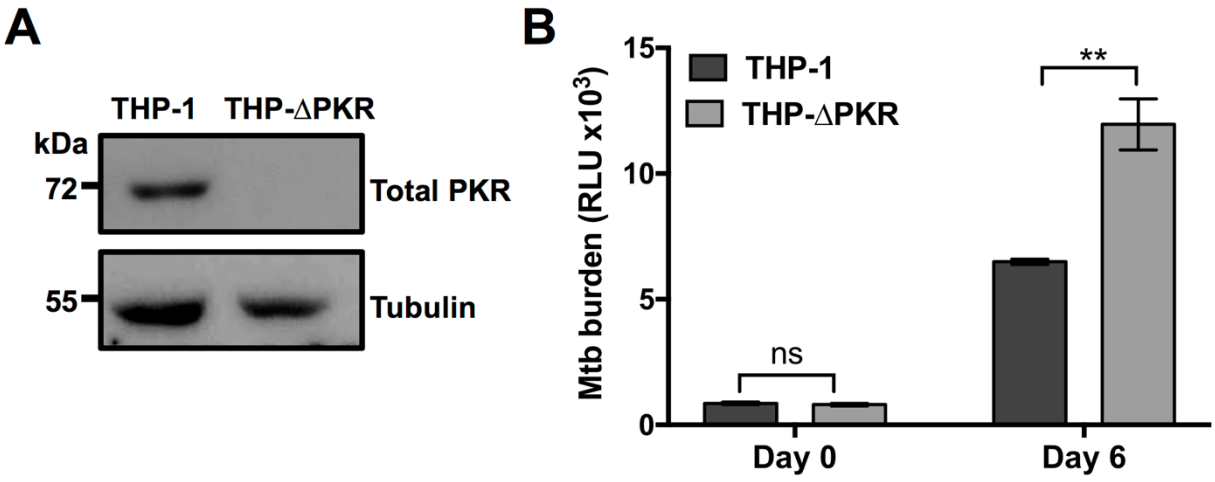
A
THP-1
THP-ΔPKR
kDa
72
Total PKR
55
Tubulin
B
Mtb burden (RLU x10^3)
15
10
5
0
THP-1
THP-ΔPKR
**
ns
Day 0
Day 6

Figure 7. Deletion of PKR increases the intracellular burden of *M. tuberculosis.* (A) THP-1 cells were transduced with a lentiviral vector encoding a single guide RNA targeting *EIF2AK2* to produce PKR knockout (THP-ΔPKR) cells. Cell lysates of THP-1 and THP-ΔPKR cells were prepared and total PKR protein levels were analyzed by western blotting. **(B)** THP-1 and THP-ΔPKR macrophages were infected with Mtb-luciferase at an MOI of 5. Cells were lysed at the indicated time post-infection and viable bacteria were determined by measuring the luminescence signal (RLU, Relative Light Units). Error bars indicate mean ± SEM of three independent biological replicates. $^{**}p < 0.01$.

3.1.4 DHBDC increases *M. tuberculosis* burden and is not a specific activator of PKR

Given our observation that PKR expression and activation is triggered during Mtb infection (Figure 5), and since PKR deletion increased Mtb burden (Figure 7B), we speculated that increased PKR activation in macrophages would improve the antibacterial response. As such, we wanted to assess the feasibility of using pharmacological activation of PKR to limit the intracellular survival of Mtb. DHBDC is a commercially available small molecule compound that activates PKR by an unknown mechanism (302). We first performed a resazurin toxicity assay to determine a non-cytotoxic concentration of DHBDC **(Figure 8A)**. Next, we performed western blot analysis of p-T446 PKR levels in THP-1 cells over the course of DHBDC treatment to determine whether our selected dose of 1 µM was sufficient to induce PKR phosphorylation. We observed that treatment with DHBDC at a concentration of 1 µM induces PKR phosphorylation, but not until at least 72 hours after treatment **(Figure 8B)**. We then treated primary human MDMs with DHBDC and compared the intracellular Mtb burden between DHBDC-treated and mock-treated macrophages. We observed that DHBDC treatment did not reduce the intracellular survival of Mtb in primary human macrophages when compared to mock-treated macrophages **(Figure 9A)**. In fact, DHBDC-treated macrophages showed a 2-fold increase in bacterial burden compared to the mock-treated control macrophages by day 3 post-infection. This trend was also observed in DHBDC-treated THP-1 macrophages **(Figure 9B)** and murine RAW 264.7 macrophages **(Figure 9C)**, with a 2-fold increase in bacterial burden, relative to mock-treated macrophages. We questioned whether the increase in Mtb burden in DHBDC-treated cells was due to PKR activation specifically, or if it was due to off-target effects of the compound. Therefore, we compared the fold change in Mtb burden in DHBDC-treated cells relative to mock-treated cells between THP-1 and THP-ΔPKR macrophages. Consistent with our results in Figure 9A,

Mtb survival was increased in DHBDC-treated THP-1 macrophages compared to the mock-treated macrophages **(Figure 9D)**. Importantly, this increased Mtb burden was also observed in DHBDC-treated THP-ΔPKR macrophages **(Figure 9D)**. Indeed, at day 5 post-infection, the DHBDC-treated PKR knockout cells showed a similar fold increase in bacterial burden as the THP-1 control macrophages **(Figure 9D)**. These data demonstrate that the increase in Mtb burden in macrophages treated with DHBDC is a result of PKR-independent mechanisms, which is consistent with the observation that DHBDC activates both PKR and PERK, in addition to activating downstream effectors of EIF2α phosphorylation (302). Furthermore, the precise molecular mechanism of PKR and PERK activation by DHBDC has yet to be determined (302). Altogether, these results demonstrate that pharmacological activation of PKR with the currently available drug is not successful in reducing Mtb survival in macrophages. However, this is likely due to off-target effects of the drug.

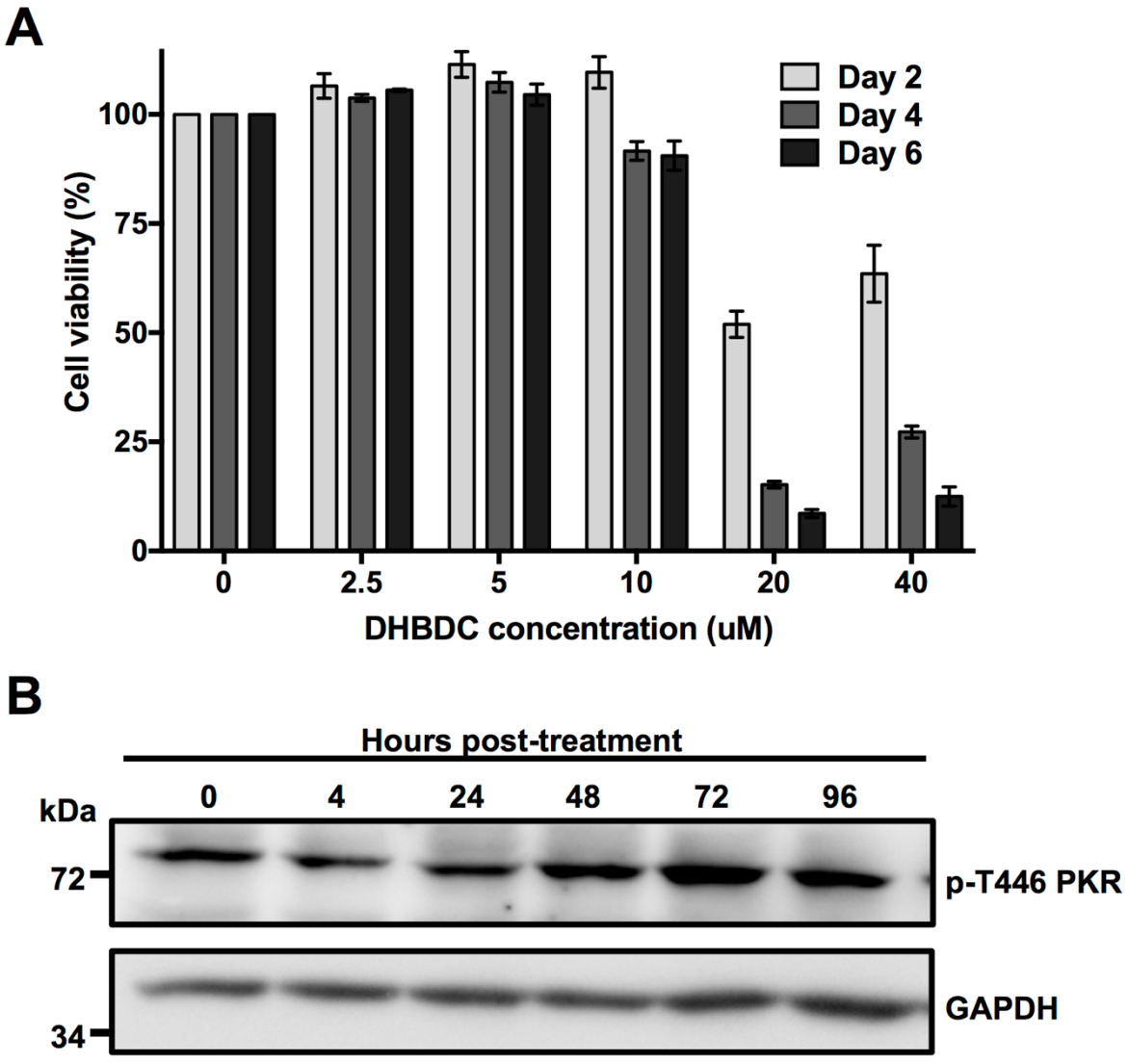
A
Day 2
Day 4
Day 6
Cell viability (%)
100
75
50
25
0
0
2.5
5
10
20
40
DHBDC concentration (uM)
B
Hours post-treatment
kDa
0
4
24
48
72
96
72
p-T446 PKR
34
GAPDH

Figure 8. DHBDC induces PKR phosphorylation at a non-cytotoxic concentration. (A) THP-1 macrophages were treated with DHBDC at the indicated concentrations. At the indicated time points, resazurin was added to the wells and fluorescence was measured following a 4 h incubation. Fluorescence values were normalized to untreated cells as 100% and reported as % cell viability. **(B)** THP-1 macrophages were treated with DHBDC (1 μM). Cell lysates were prepared at the indicated days post-treatment and p-T446 PKR protein levels were analyzed by western blotting. DHBDC was maintained in the medium for the duration of the experiments and replenished every second day. Error bars indicate mean ± SEM of three independent biological replicates.

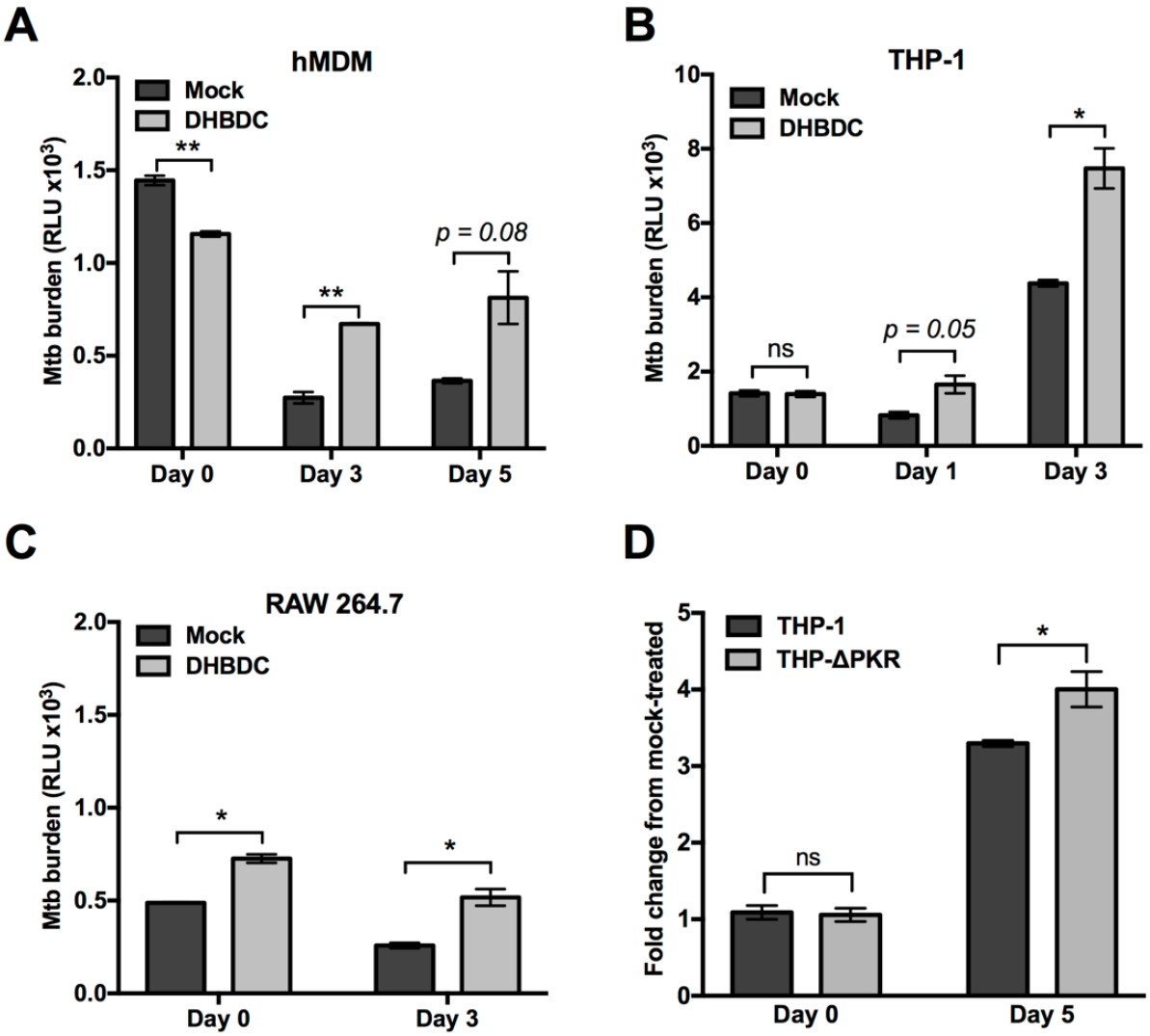
A
hMDM
Mock
DHBDC
Mtb burden (RLU x10³)
2.0
1.5
1.0
0.5
0.0
**
**
p = 0.08
Day 0
Day 3
Day 5
B
THP-1
Mock
DHBDC
Mtb burden (RLU x10³)
10
8
6
4
2
0
ns
p = 0.05
*
Day 0
Day 1
Day 3
C
RAW 264.7
Mock
DHBDC
Mtb burden (RLU x10³)
2.0
1.5
1.0
0.5
0.0
*
*
Day 0
Day 3
D
THP-1
THP-ΔPKR
Fold change from mock-treated
5
4
3
2
1
0
ns
*
Day 0
Day 5

Figure 9. DHBDC increases *M. tuberculosis* burden in a PKR-independent manner.
A) Primary human monocyte-derived macrophages (hMDM), **(B)** THP-1 macrophages, or **(C)** RAW 264.7 macrophages were mock-treated or treated with DHBDC (1 μM) and infected with Mtb-luciferase at an MOI of 5 (A, B) or an MOI of 10 (C). Cells were lysed at the indicated time post-infection and viable bacteria were determined by measuring the luminescence signal (RLU, Relative Light Units). **(D)** THP-1 and THP-ΔPKR macrophages were treated and infected as in (A, B). Cells were lysed at the indicated time post-infection and viable bacteria were determined by measuring RLU. Fold change in RLU of DHBDC-treated cells relative to their respective mock-treated cells is reported as fold change from untreated. DHBDC was maintained in the medium for the duration of the experiments and replenished every second day. Error bars indicate mean ± SEM of three independent biological replicates. *$p < 0.05$; **$p < 0.01$.

3.1.5 Genetic overexpression of PKR results in increased and stable production of active PKR during *M. tuberculosis* infection

Since the pharmacological approach was unsuccessful and limited by the availability of specific PKR activators (Figure 9), we turned to an alternative strategy to genetically overexpress PKR to examine its role in the intracellular survival of Mtb. PKR overexpression cells (THP-PKR) were generated by transducing THP-1 cells with a retroviral expression vector encoding the *EIF2AK2* gene. Western blot analysis confirmed that THP-PKR cells have increased expression of PKR **(Figure 10A)**. Indeed, THP-PKR cells produced 4-fold higher PKR protein levels compared to THP-1 cells transduced with an empty overexpression vector (THP-Ø), which were used as control cells throughout this study **(Figure 10B)**. However, given that PKR expression is already triggered by Mtb infection in WT THP-1 macrophages (Figures 4,5), it was difficult to predict whether there would be a discernible difference in PKR expression between Mtb-infected THP-Ø and THP-PKR macrophages. To evaluate this, we infected THP-Ø and THP-PKR macrophages with Mtb and compared the levels of total PKR expression over the course of infection. Western blot analysis revealed that THP-PKR macrophages produced elevated PKR protein levels before and early after infection with Mtb (4-fold increase at 4 h post-infection), compared to THP-Ø macrophages **(Figure 10 C,D)**. The increased expression of PKR was also sustained at 24 h and 72 h post-infection, when total PKR protein levels remained 2-fold higher in THP-PKR macrophages compared to THP-Ø macrophages **(Figure 10 C,D)**. We next questioned whether the increased level of PKR protein observed in THP-PKR macrophages was also phosphorylated. Since PKR expression and activation stabilizes at day 4 post-infection (Figure 5A), we chose this time point to compare protein levels of p-T446 PKR in THP-Ø and THP-PKR macrophages. Western blot data revealed that at day 4 post-infection, THP-PKR macrophages have 2-fold higher levels

of phosphorylated PKR compared to THP-Ø macrophages **(Figure 10E)**. These data collectively show that the generated THP-PKR cells have higher activation and expression levels of PKR in comparison to control cells during basal conditions as well as during Mtb infection. Thus, the generated THP-PKR macrophages provided a suitable cell-line model to examine whether increased expression of PKR functions to improve the cellular antibacterial response against Mtb infection.

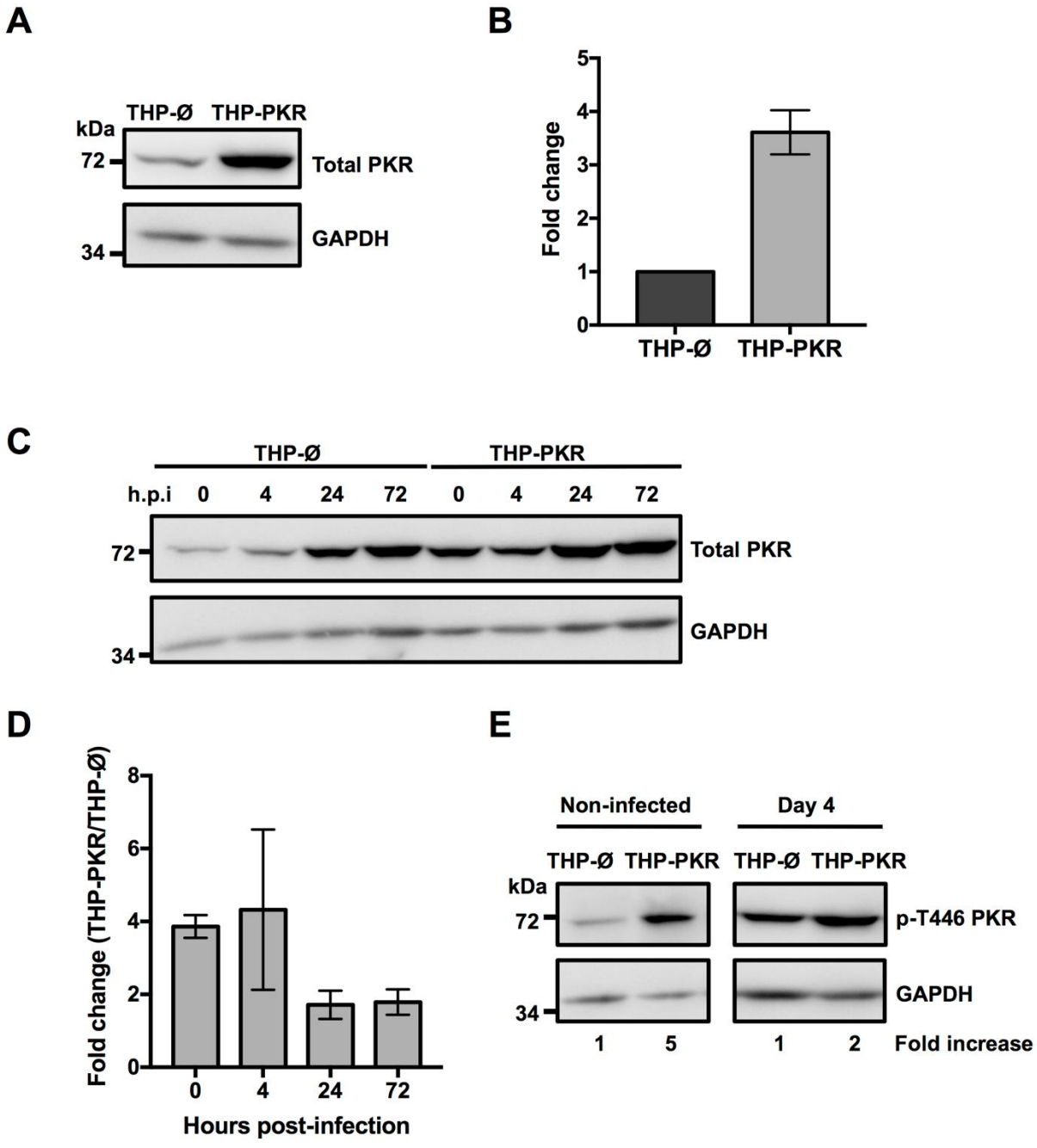
A
THP-Ø
THP-PKR
kDa
72
Total PKR
34
GAPDH
B
Fold change
5
4
3
2
1
0
THP-Ø
THP-PKR
C
THP-Ø
THP-PKR
h.p.i
0
4
24
72
0
4
24
72
72
Total PKR
34
GAPDH
D
Fold change (THP-PKR/THP-Ø)
8
6
4
2
0
0
4
24
72
Hours post-infection
E
Non-infected
Day 4
THP-Ø
THP-PKR
THP-Ø
THP-PKR
kDa
72
p-T446 PKR
34
GAPDH
1
5
1
2
Fold increase

Figure 10. Genetic overexpression of PKR results in increased and stable production of active PKR during *M. tuberculosis* infection. (A) PKR protein levels in cell lysates of control THP-1 wild-type cells transduced with empty vector (THP-Ø) and THP-1 cells transduced with vector overexpressing PKR (THP-PKR) were analyzed by western blotting. **(B)** Densitometry analysis of the blot in (A) was performed using ImageJ to quantify PKR band intensities as normalized to GAPDH and fold increase of total PKR levels in THP-PKR macrophages is expressed relative to THP-Ø macrophages. **(C)** THP-Ø and THP-PKR macrophages were infected with Mtb at an MOI of 5. Cell lysates were prepared at the indicated hours post-infection (h.p.i) and total PKR protein levels were analyzed by western blotting. **(D)** Densitometry analysis of the blot in (C) was performed by ImageJ to quantify PKR band intensities as normalized to GAPDH and fold change of total PKR levels in THP-PKR macrophages relative to THP-Ø macrophages is shown. **(E)** THP-Ø and THP-PKR macrophages were infected as in (C). Cell lysates were prepared at the indicated times post-infection and p-T446 PKR protein levels were analyzed by western blotting. Fold increase of protein expression in THP-PKR macrophages is shown relative to THP-Ø macrophages at the corresponding time points. Error bars represent the mean ± SEM of three independent western blots.

3.1.6 PKR expression alters the immunological profile of macrophages during *M. tuberculosis* infection

To determine whether sustained PKR expression and activation impacts the antibacterial response of macrophages, we first examined the effect of PKR expression on the production of cytokines during Mtb infection. Antibody-based bead multiplex assays were performed to compare cytokine and chemokine production by uninfected and Mtb-infected THP-Ø and THP-PKR macrophages using culture supernatants collected at 24 h post-infection. Consistent with previous reports (161, 307), Mtb infection induced production of IL-6, IL-10, TGF-β1, IL-1β, TNFα, and IP-10 by THP-Ø control macrophages **(Figure 11 A-F)**. Importantly, overexpression of PKR significantly altered production of cytokines that are of relevance to Mtb infection. The most striking observation was that Mtb-infected THP-PKR macrophages produced 15-fold lower levels of IL-6 compared to THP-Ø macrophages **(Figure 11A)**. Mtb is reported to induce production of IL-6 by infected macrophages to inhibit IFNγ-mediated macrophage activation and autophagy (160, 161). Remarkably, Mtb-infected THP-PKR macrophages produced even less IL-6 than uninfected THP-Ø macrophages **(Figure 11A)**. We also observed that THP-PKR macrophages produced decreased levels of IL-10 and TGF-β1 compared to THP-Ø macrophages (**Figure 11 B, C**). IL-10 and TGF-β are reported to be conducive to Mtb survival due to their inhibitory effect on pro-inflammatory cytokine production and T cell activation (167). Furthermore, IL-10 is reported to inhibit autophagy in Mtb-infected macrophages (320). Infected THP-PKR macrophages also produced lower levels of IL-1β and TNFα compared to control macrophages **(Figure 11 D, E)**, two cytokines that are critical for host resistance to Mtb due to their pro-inflammatory effects and their role in activating macrophage cell death (145, 147, 157, 321). Mtb-infected THP-PKR macrophages also produced increased levels of IP-10 **(Figure 11F)**, an IFNγ-

inducible chemokine. IP-10 functions as a chemoattractant for activated T cells and monocytes and has also been positively correlated to autophagy induction (322). Importantly, a role for IP-10 in restricting Mtb growth has been reported (323). Consistent with this, Mtb-infected THP-PKR macrophages also produced higher levels of IFNγ compared to THP-Ø macrophages **(Figure 11G)**. IFNγ is a key cytokine in Mtb immunity due to its critical role in macrophage activation to enhance phagocytosis, apoptosis, autophagy, and the production of reactive nitrogen species (119, 161). Levels of IL-2, MCP-1, IL-4, IL-8, and IL-17A were also measured but their production did not differ significantly between THP-Ø and THP-PKR macrophages **(Figure 11 H-L)**. Collectively, our data show that THP-PKR macrophages produced lower levels of cytokines that are permissive for Mtb infection (IL-6, IL-10, TGF-β1) and increased levels of anti-mycobacterial cytokines (IP-10, IFNγ), which supports our hypothesis that sustained PKR expression could enhance the anti-Mtb response in macrophages.

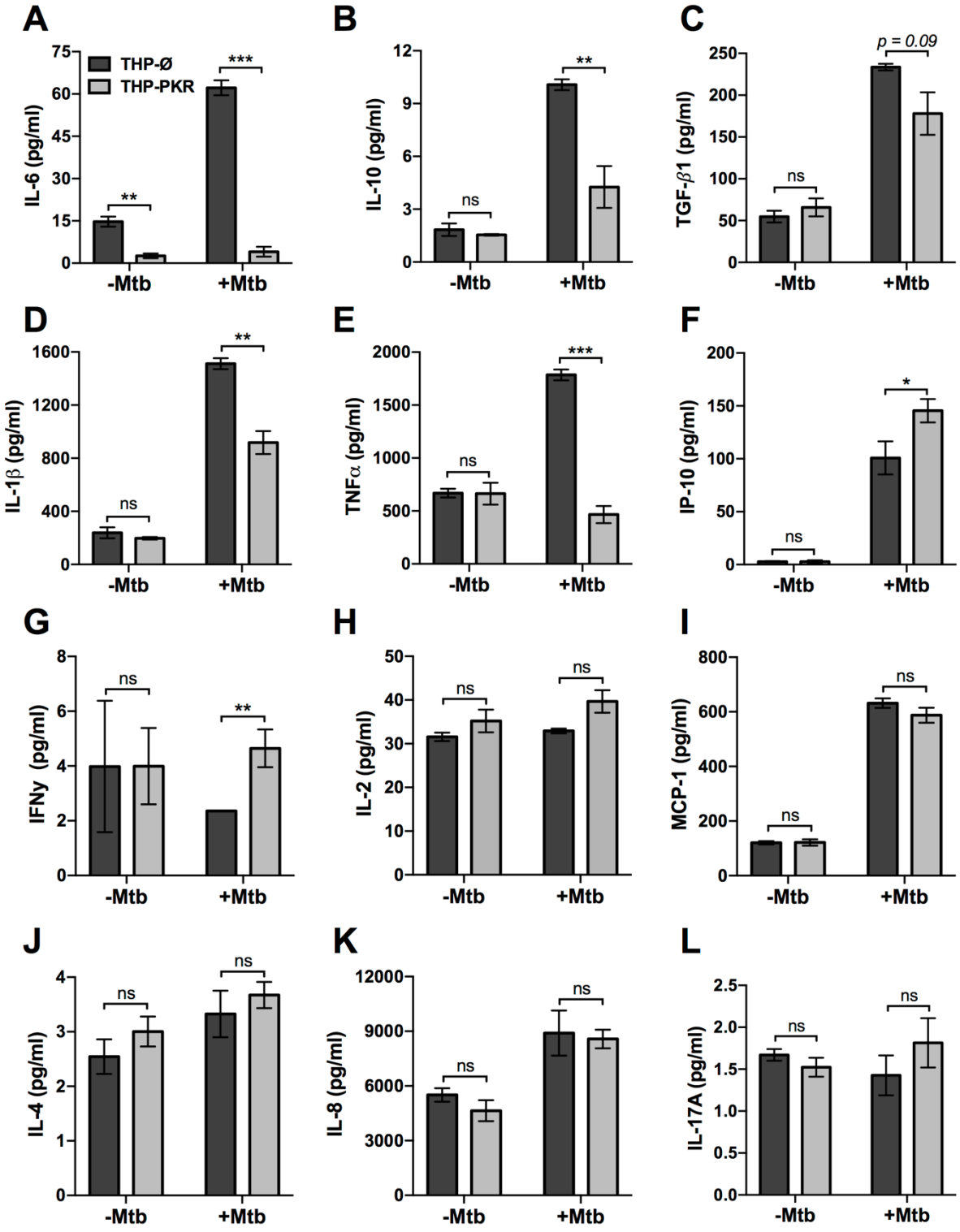
A
THP-Ø
THP-PKR
IL-6 (pg/ml)
75
60
45
30
15
0
**
***
-Mtb
+Mtb
B
IL-10 (pg/ml)
12
9
6
3
0
ns
**
-Mtb
+Mtb
C
TGF-β1 (pg/ml)
250
200
150
100
50
0
p = 0.09
ns
-Mtb
+Mtb
D
IL-1β (pg/ml)
1600
1200
800
400
0
ns
**
-Mtb
+Mtb
E
TNFα (pg/ml)
2000
1500
1000
500
0
ns
***
-Mtb
+Mtb
F
IP-10 (pg/ml)
200
150
100
50
0
ns
*
-Mtb
+Mtb
G
IFNy (pg/ml)
8
6
4
2
0
ns
**
-Mtb
+Mtb
H
IL-2 (pg/ml)
50
40
30
20
10
0
ns
ns
-Mtb
+Mtb
I
MCP-1 (pg/ml)
800
600
400
200
0
ns
ns
-Mtb
+Mtb
J
IL-4 (pg/ml)
4
3
2
1
0
ns
ns
-Mtb
+Mtb
K
IL-8 (pg/ml)
12000
9000
6000
3000
0
ns
ns
-Mtb
+Mtb
L
IL-17A (pg/ml)
2.5
2.0
1.5
1.0
0.5
0.0
ns
ns
-Mtb
+Mtb

Figure 11. PKR expression alters cytokine production by macrophages during *M. tuberculosis* infection. (A-L) THP-Ø and THP-PKR macrophages were infected with Mtb at an MOI of 5 and cell culture supernatant was collected at 24 h post-infection**.** Production of **(A)** IL-6, **(B)** IL-10, **(C)** TGF-β1, **(D)** IL-1β, **(E)** TNFα, **(F)** IP-10, **(G)** IFNγ, **(H)** IL-2, **(I)** MCP-1, **(J)** IL-4, **(K)** IL-8, and **(L)** IL-17A was measured in cell culture supernatant using antibody-based bead multiplex assays. Error bars represent the mean ± SEM of three independent biological replicates. *$p < 0.05$; **$p < 0.01$; ***$p < 0.001$.

3.1.7 Sustained expression of PKR reduces survival of *M. tuberculosis* in macrophages

Since our cytokine profiling data suggested that PKR expression could enhance the antibacterial response of Mtb-infected macrophages, we next sought to determine whether PKR expression functions to limit the intracellular survival of Mtb. Since Mtb-infected THP-PKR macrophages produced higher levels of IFNγ and IFNγ-stimulated genes (IP-10) (Figure 11 F,G), we also wanted to investigate whether PKR functions through an IFNγ-dependent mechanism. We thus performed bacterial survival assays in either mock-treated or IFNγ-treated THP-PKR and THP-Ø macrophages. At day 4 post-infection, the bacterial burden of Mtb in the mock-treated condition was 26% lower in THP-PKR macrophages compared to THP-Ø macrophages **(Figure 12)**. In addition, treatment with IFNγ further reduced the intracellular survival of Mtb in THP-PKR macrophages, resulting in a decrease in bacterial burden of 59% at day 4 post-infection compared to THP-Ø macrophages **(Figure 12)**. Although IFNγ treatment is reported to reduce Mtb burden in mouse macrophages (123), IFNγ treatment did not reduce Mtb survival in the THP-Ø control macrophages **(Figure 12)**. This may be explained by the fact that IFNγ reduces Mtb survival via NO-dependent apoptosis, but PMA-differentiated THP-1 macrophages are reported to have limited NO production (123, 324). Altogether, these findings suggest that the function of PKR to limit the survival of Mtb in macrophages could be enhanced by addition of IFNγ. This finding is consistent with the cytokine data demonstrating that THP-PKR macrophages produced significantly lower levels of IL-6 and IL-10 compared to THP-Ø macrophages (Figure 11 A, B), which antagonize the macrophage activating effects of IFNγ (160, 320, 325).

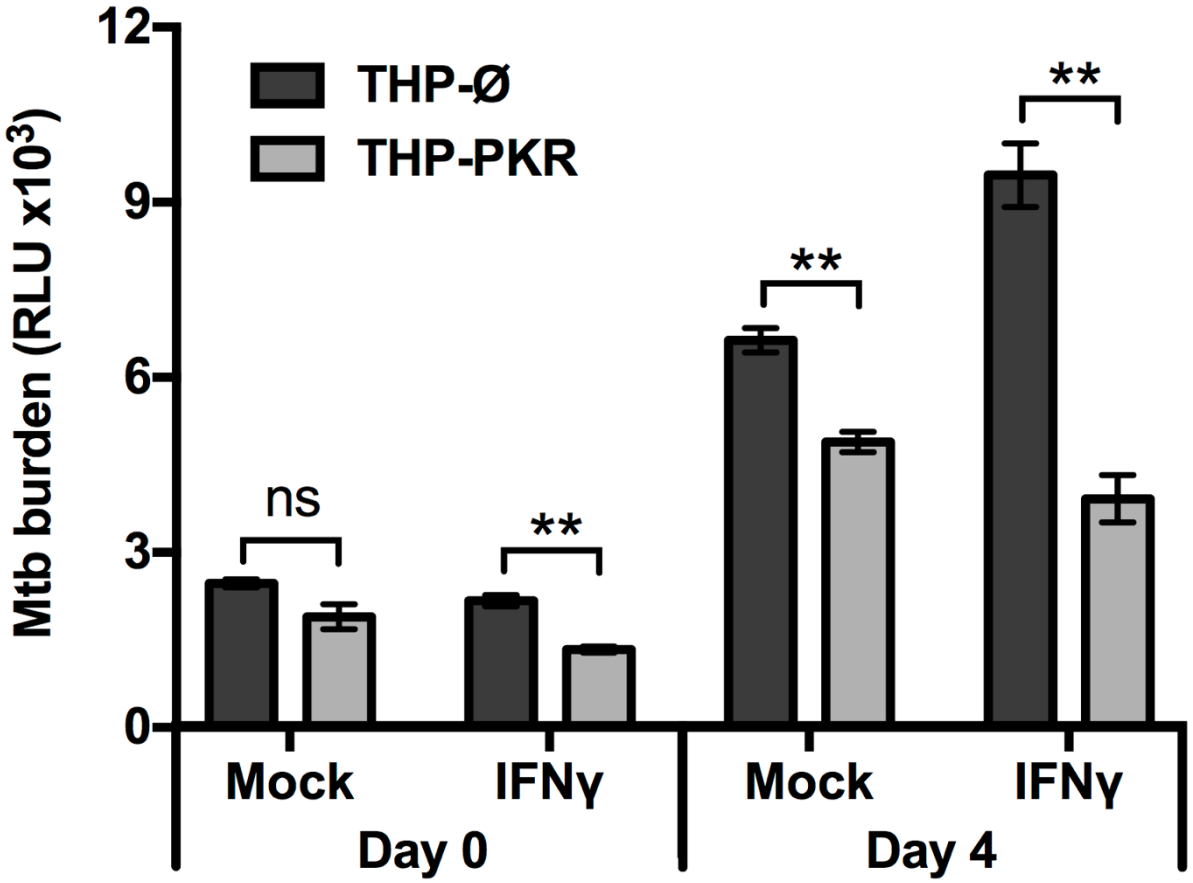
12
9
6
3
0
Mtb burden (RLU x10³)
THP-Ø
THP-PKR
ns
**
**
**
Mock
IFNγ
Mock
IFNγ
Day 0
Day 4

Figure 12. Overexpression of PKR reduces survival of *M. tuberculosis* in macrophages. THP-Ø and THP-PKR macrophages were mock-treated or pre-treated for 24 h with IFNγ (100 ng/ml) as indicated. Macrophages were then infected with Mtb-luciferase at an MOI of 5. IFNγ was maintained in the medium for the duration of the experiment and replenished every second day. Cells were lysed at the indicated time post-infection and viable bacteria were determined by measuring the luminescence signal (RLU, Relative Light Units). Error bars represent mean ± SEM of three independent biological replicates. $^{**}p < 0.01$.

3.2 The molecular mechanism by which PKR controls *M. tuberculosis* survival in macrophages

3.2.1 Inhibition of autophagic flux with bafilomycin A1 blocks the anti-mycobacterial effect of PKR overexpression

Next, we wanted to determine the specific IFNγ-dependent mechanism responsible for the enhanced ability of PKR overexpressing macrophages to kill Mtb. Since IL-6 is reported to inhibit IFNγ-induced autophagy in Mtb-infected macrophages (161), we hypothesized that autophagy could be the mechanism responsible for the reduced Mtb survival in THP-PKR macrophages. This hypothesis is also consistent with our observation that Mtb-infected THP-PKR macrophages produced increased levels of IP-10 (Figure 11F), a chemokine linked to induction of autophagy (322). Furthermore, although the role of PKR in autophagy during bacterial infection has not yet been studied, PKR is reported to induce autophagy during viral (283) and parasitic (286) infections. To investigate whether autophagy is the mechanism responsible for the reduced Mtb survival in THP-PKR macrophages, we examined the impact of bafilomycin A1 treatment on the bacterial burden in Mtb-infected macrophages. Bafilomycin A1 is a vacuolar H^+-ATPase inhibitor that blocks the autophagic flux by inhibiting lysosome acidification (326). After determining a non-cytotoxic concentration of bafilomycin A1 **(Figure 13)**, we measured the intracellular survival of Mtb in mock-treated or bafilomycin A1-treated macrophages. Consistent with our previous bacterial survival assay (Figure 12), mock-treated THP-PKR macrophages showed decreased bacterial burden, with 79% lower intracellular Mtb survival compared to THP-Ø macrophages **(Figure 14)**. The percent decrease in intracellular Mtb survival is higher in Figure 14 than that observed in Figure 12, likely because it was at a later time point during infection (day 6 versus day 4 post-infection). Importantly, treatment with bafilomycin A1 completely inhibited the ability of

THP-PKR macrophages to limit Mtb replication. Indeed, bafilomycin A1-treated THP-PKR macrophages had a 52% increase in bacterial burden compared to THP-Ø macrophages **(Figure 14)** at day 6 post-infection. These data suggest selective autophagy as a potential mechanism responsible for the enhanced ability of THP-PKR macrophages to control intracellular Mtb replication. However, bafilomycin A1 also inhibits acidification of Mtb-containing phagosomes, a molecular pathway distinct from autophagy (122). Therefore, we next sought to examine specific markers of autophagy activation to support this hypothesis.

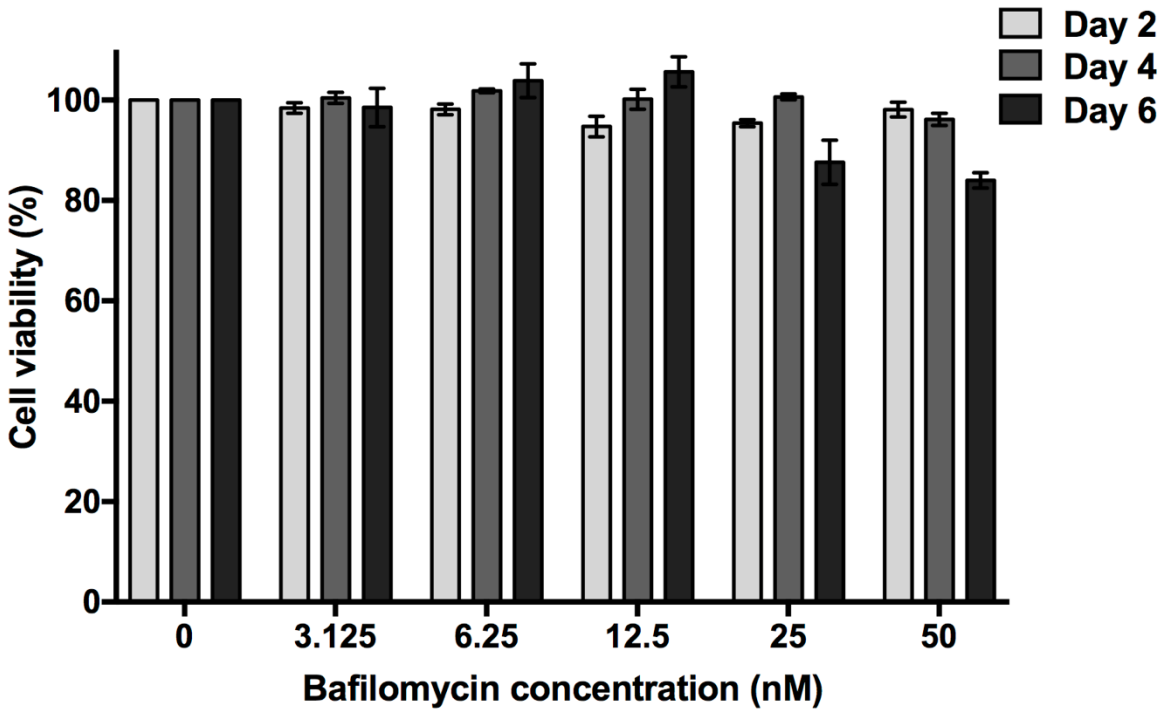
Day 2
Day 4
Day 6
Cell viability (%)
100
80
60
40
20
0
0
3.125
6.25
12.5
25
50
Bafilomycin concentration (nM)

Figure 13. Bafilomycin is non-cytotoxic in THP-1 cells. THP-Ø macrophages were treated with bafilomycin A1 at the indicated concentrations. Bafilomycin A1 was maintained in the medium for the duration of the experiment and replenished every second day. At the indicated time points, resazurin was added to the wells and fluorescence was measured following a 4 h incubation. Fluorescence values were normalized to untreated cells as 100% and reported as % cell viability. Error bars indicate mean ± SEM of three independent biological replicates.

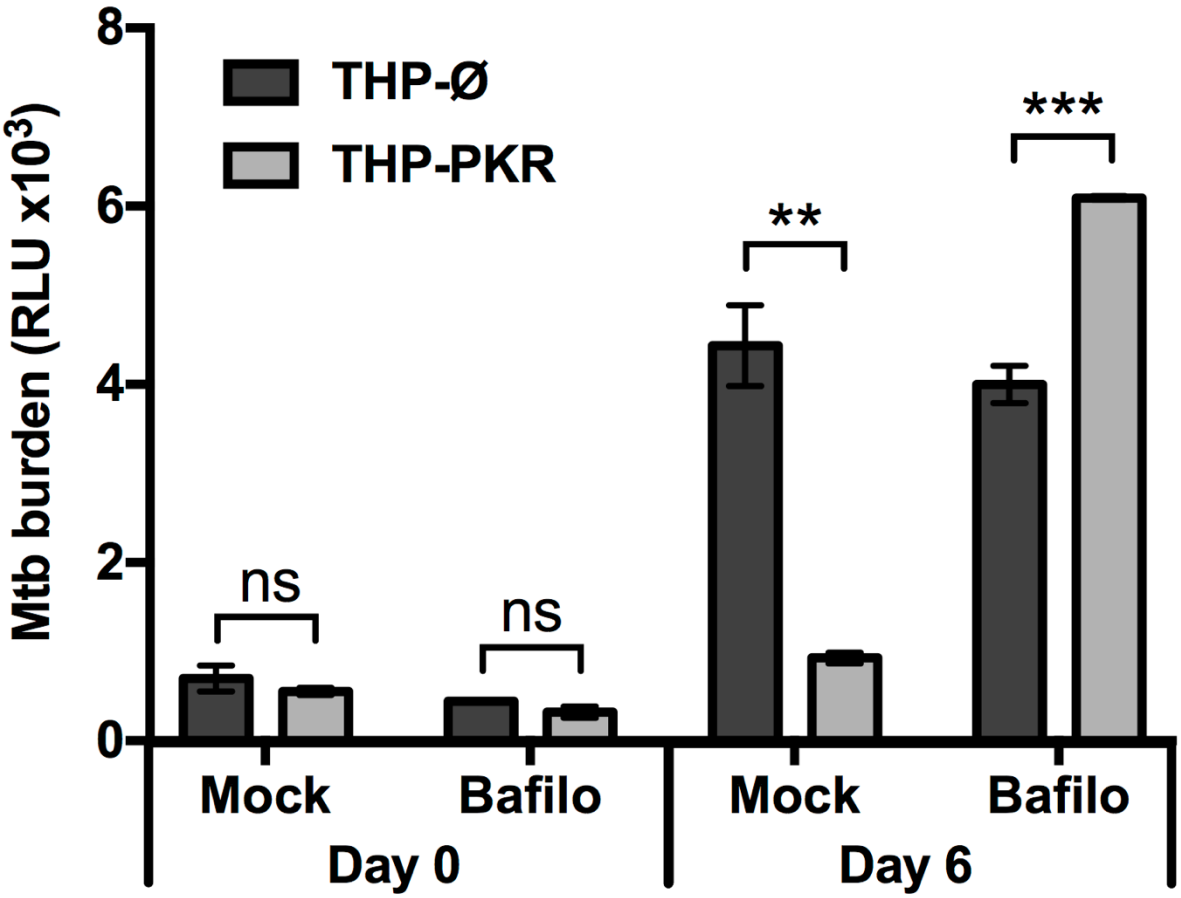
Mtb burden (RLU x10^3)
8
6
4
2
0
THP-Ø
THP-PKR
ns
ns
**
***
Mock
Bafilo
Mock
Bafilo
Day 0
Day 6

Figure 14. Inhibition of autophagic flux blocks the anti-mycobacterial effect of PKR overexpression. THP-Ø and THP-PKR macrophages were mock-treated or pre-treated for 1 h with bafilomycin A1 (12 nM) as indicated. Macrophages were then infected with Mtb-luciferase at an MOI of 5. Bafilomycin A1 was maintained in the medium for the duration of the experiment and replenished every second day. Cells were lysed at the indicated time post-infection and viable bacteria were determined by measuring the luminescence signal (RLU, Relative Light Units). Error bars represent mean ± SEM of three independent biological replicates. $^{**}p < 0.01$; $^{***}p < 0.001$.

3.2.2 PKR expression activates the autophagy pathway in *M. tuberculosis*-infected macrophages

To ascertain that autophagy is indeed the mechanism responsible for reduced Mtb survival in PKR overexpressing macrophages, we examined specific markers of selective autophagy. We compared protein expression levels of p62, phosphorylated p62 (p-S403 p62), and LC3-II in Mtb-infected macrophages treated with bafilomycin A1 **(Figure 15A)**. LC3-II and p62 are well-characterized markers for selective autophagy (327). LC3-II is extensively used to measure autophagic flux, which is the dynamic process of autophagy that takes into account autophagic degradation activity (327). It is necessary to use bafilomycin A1 to block the degradation of autophagy markers when performing western blot experiments to enable a true representation of the autophagic flux (327). An increase in LC3-II expression in bafilomycin A1-treated cells is thus associated with an increase in autophagy. Phosphorylation of serine403 (p-S403) on p62 regulates selective autophagy through the recognition of ubiquitinated bacteria targeted for autophagic degradation (328), and as such, increased levels of p-S403 p62 in bafilomycin A1-treated cells is also an indicator of increased autophagy. Western blot analysis revealed that during Mtb infection, bafilomycin A1-treated THP-PKR macrophages showed 3-fold higher expression levels of LC3-II and 2-fold higher expression of p-S403 p62 compared to THP-Ø macrophages **(Figure 15 A, B)**. Therefore, our western blot data suggest that THP-PKR macrophages have increased autophagy activation compared to control macrophages. However, since western blot analysis of cell lysates only measures bulk autophagy and not selective autophagy, we then used fluorescence microscopy to quantify the specific colocalization between intracellular Mtb and LC3. Immunofluorescence microscopy showed that PKR expression induced LC3 association with Mtb **(Figure 15C)**. A significantly higher percentage of $LC3^{+}$ Mtb autophagosomes was observed in THP-PKR

macrophages (12%) compared to control THP-Ø macrophages (8%) **(Figure 15D)**. Altogether, these data suggest that PKR expression activates selective autophagy.

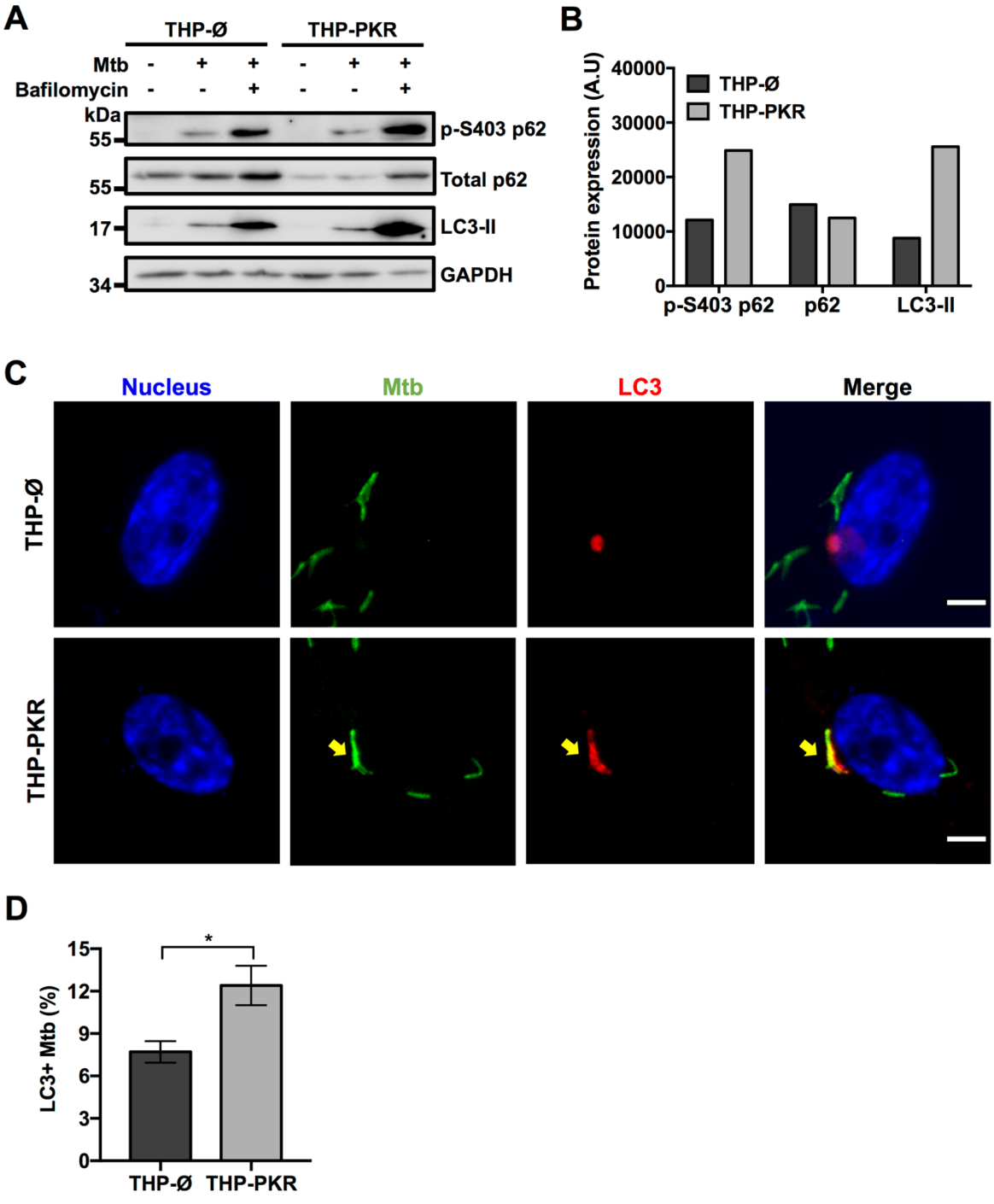
A
THP-Ø
THP-PKR
Mtb - + + - + +
Bafilomycin - - + - - +
kDa
55
p-S403 p62
55
Total p62
17
LC3-II
34
GAPDH
B
Protein expression (A.U)
40000
30000
20000
10000
0
THP-Ø
THP-PKR
p-S403 p62
p62
LC3-II
C
Nucleus
Mtb
LC3
Merge
THP-Ø
THP-PKR
D
LC3+ Mtb (%)
15
12
9
6
3
0
*
THP-Ø
THP-PKR

Figure 15. PKR expression activates the autophagy pathway in *M. tuberculosis*-infected macrophages. (A) THP-Ø and THP-PKR macrophages were pre-treated with bafilomycin A1 (12 nM) for 1 h where indicated and then infected with Mtb at an MOI of 10. Bafilomycin A1 was maintained in the medium for the duration of the experiment. Cell lysates were prepared at 24 h post-infection and phosphorylated p62 (p-S403 p62), total p62, and LC3-II protein levels were analyzed by western blotting. **(B)** Densitometry analysis of the blot in (A) was performed using ImageJ to quantify p-S403 p62, total p62, and LC3-II band intensities in Mtb-infected, bafilomycin A1-treated macrophages as normalized to GAPDH (A.U., arbitrary units). **(C)** THP-Ø and THP-PKR macrophages were infected with Mtb-GFP at an MOI of 10. At 24 h post-infection, cells were fixed, permeabilized, and incubated with an anti-LC3 antibody to visualize autophagosomes. Representative images show nuclei (blue channel), Mtb (green channel), and LC3 (red channel) as detected by fluorescence microscopy. Yellow arrow denotes colocalization between Mtb and LC3. Scale bar, 5 μm. **(D)** Quantification of percent Mtb colocalization with LC3 ($LC3^{+}$Mtb) per total number of intracellular Mtb. A minimum of 20 visual fields, each with 15-30 infected cells, were counted per cell-line. Data represent the mean ± SEM of all the analyzed visual fields. *$p < 0.05$.

3.2.3 PKR expression enhances autophagolysosomal degradation of *M. tuberculosis*

Although THP-PKR macrophages had a higher percentage of $LC3^+$ Mtb autophagosomes, it was important for us to determine the status of the autophagosomes, since Mtb inhibits autophagolysosome formation by blocking autophagosome fusion with lysosomes (213). THP-Ø and THP-PKR macrophages were pre-loaded with dextran, a lysosome marker (329), prior to Mtb infection, and then immunofluorescence microscopy was performed. When specifically counting only Mtb autophagosomes, which are denoted as $LC3^+$ Mtb, we found a higher percentage of lysosome colocalization in THP-PKR macrophages (36%) compared to THP-Ø macrophages (12%) **(Figure 16 A, B)**. This supports our hypothesis that sustained PKR expression enhances the activation of autophagy and promotes increased autophagolysosome fusion. Furthermore, the ability of PKR to increase autophagolysosome fusion explains the reduced bacterial burden observed in THP-PKR macrophages (Figure 12). Importantly, there was no difference in the percentage of lysosome colocalization with LC3-negative Mtb, which are presumed to be located mostly in phagosomes, when comparing THP-PKR and THP-Ø macrophages **(Figure 16B)**. This suggests that the effect of PKR overexpression is specific to the selective autophagy pathway and not the phagosome maturation pathway. Altogether, these findings demonstrate that PKR expression induces selective autophagy in Mtb-infected macrophages, thereby contributing to the reduced intracellular survival of Mtb.

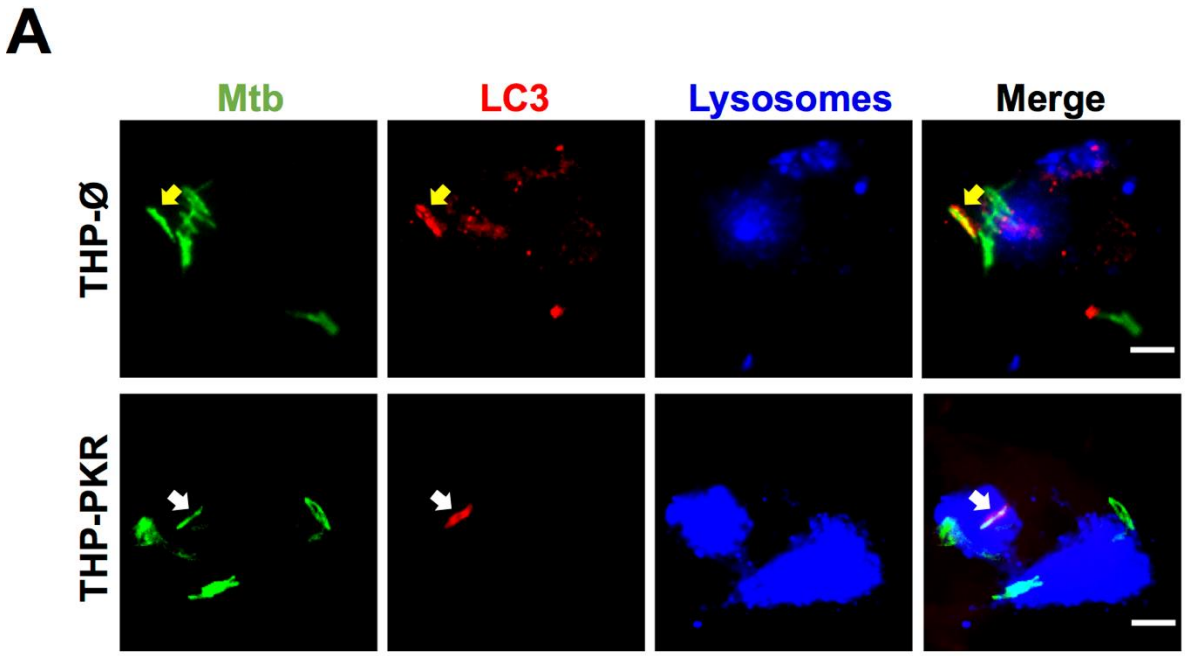
A
Mtb
LC3
Lysosomes
Merge
THP-Ø
THP-PKR

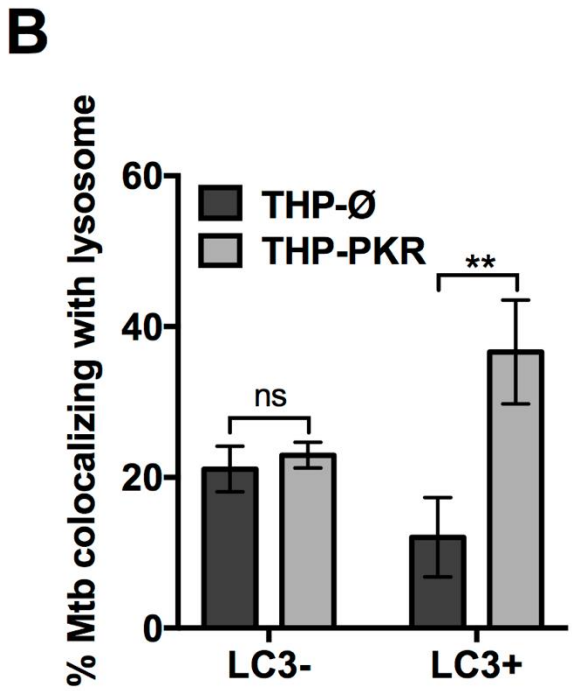
B
% Mtb colocalizing with lysosome
60
40
20
0
THP-Ø
THP-PKR
**
ns
LC3-
LC3+

Figure 16. PKR expression enhances autophagolysosomal degradation of *M. tuberculosis* **(A)** THP-Ø and THP-PKR macrophages were loaded with dextran (lysosome marker) for 24 h and then infected with Mtb-GFP at an MOI of 10. At 24 h post-infection, cells were fixed, permeabilized, and incubated with an anti-LC3 antibody to visualize autophagosomes. Representative images show Mtb (green channel), LC3 (red channel), and lysosomes (blue channel) as detected by fluorescence microscopy. Yellow arrow denotes colocalization between Mtb and LC3, and white arrow denotes colocalization of Mtb with both LC3 and lysosomes. Scale bar, 5 μm. **(B)** Quantification of lysosome colocalization with LC3-negative or LC3-positive Mtb is reported as percentage over the total number of LC3-negative or LC3-positive intracellular Mtb, respectively. A minimum of 20 visual fields, each with 15-30 infected cells, were counted per cell-line. Data represent the mean ± SEM of all the analyzed visual fields. $^{**}p < 0.01$.

3.2.4 Sustained expression of PKR does not alter macrophage cell death pathways

Our data indicate that sustained expression of PKR induces selective autophagy and reduces intracellular survival of Mtb. However, differences in bacterial burden between cell-lines can also be caused by changes in cell death or phagocytosis efficiency. Our cytokine profile revealed that THP-PKR macrophages had altered IL-1β and TNFα production compared to control macrophages (Figure 11 D, E), cytokines that are positively correlated to macrophage cell death (145, 321). Furthermore, although the role of PKR in macrophage apoptosis during bacterial infection is unclear, it has been well-established to activate stress-induced apoptosis during viral infection or serum starvation (256). As such, we sought to rule-out any potential differences in cell death and phagocytosis between the cell-lines as the cause of the reduced bacterial burden in THP-PKR macrophages to further support our hypothesis that autophagy is the mechanism responsible for this effect. We first examined the impact of PKR expression on the apoptosis of Mtb-infected macrophages. At day 1 post-infection, there was no significant difference in apoptosis levels between THP-Ø and THP-PKR macrophages, as measured by Annexin V assays **(Figure 17A)**. At day 3 post-infection, THP-PKR macrophages showed slightly lower levels of apoptosis **(Figure 17A)**. However, uninfected THP-PKR macrophages also showed a minor decrease in baseline apoptosis compared to THP-Ø macrophages (**Figure 17A**). When accounting for this, there was no significant difference in fold-change in apoptosis of infected cells relative to uninfected cells when comparing THP-PKR and THP-Ø macrophages **(Figure 17B)**. These results suggest that PKR expression does not induce apoptosis in Mtb-infected macrophages. However, PKR is also reported to induce other forms of cell death, including pyroptosis (288) and necroptosis (306). To rule-out all types of cell death caused by modulating PKR, we measured overall cell death

using the Real-Time Cell Analysis (RTCA) assay, a method that quantifies the viability of adherent cells over time (330). The RTCA system measures changes in impedance between electrodes at the bottom of E-well plates, which is then translated into a dimensionless value known as the Cell Index (CI). An increase in the CI reflects an increase in macrophage adherence (differentiation), whereas a decrease in the CI reflects the loss of macrophage viability as they detach from the bottom of the well (231). RTCA data revealed that there was no difference in cell death between Mtb-infected THP-Ø and THP-PKR macrophages over the course of infection **(Figure 17C)**. Therefore, we concluded that overexpression of PKR does not affect cell death in Mtb-infected macrophages.

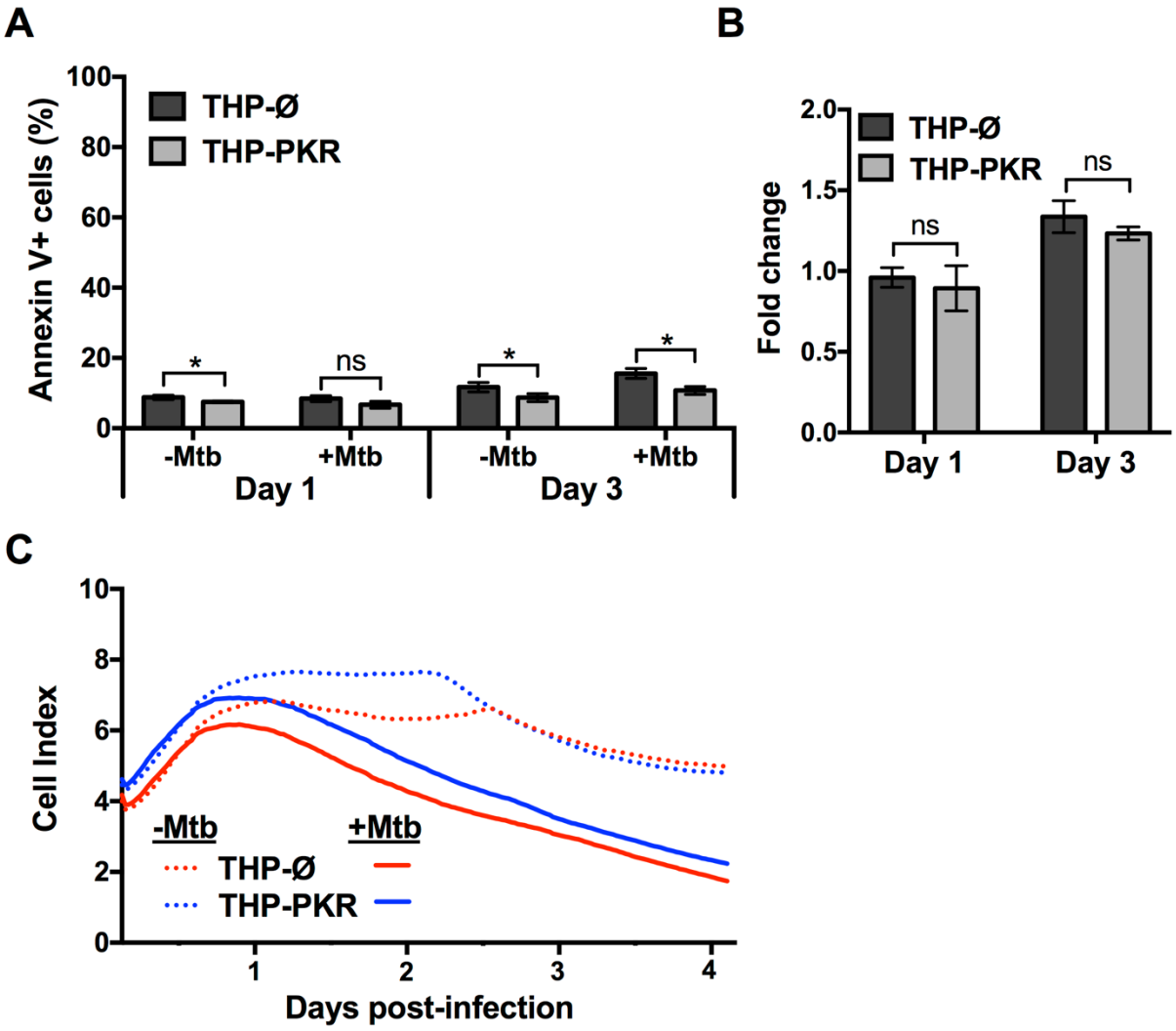
A
Annexin V+ cells (%)
100
80
60
40
20
0
THP-Ø
THP-PKR
*
ns
*
*
-Mtb
+Mtb
-Mtb
+Mtb
Day 1
Day 3
B
Fold change
2.0
1.5
1.0
0.5
0.0
THP-Ø
THP-PKR
ns
ns
Day 1
Day 3
C
Cell Index
10
8
6
4
2
0
-Mtb
+Mtb
THP-Ø
THP-PKR
1
2
3
4
Days post-infection

Figure 17. Sustained expression of PKR does not alter macrophage cell death pathways. **(A, B)** THP-Ø and THP-PKR macrophages were infected with Mtb at an MOI of 5. At the indicated time post-infection, cells were stained with Annexin V and analyzed by flow cytometry to measure **(A)** the percentage of apoptotic cells, and **(B)** the fold change in apoptosis relative to uninfected cells. **(C)** THP-Ø and THP-PKR macrophages were infected with Mtb at an MOI of 5 and changes in cell adherence were monitored by RTCA as indicated by the Cell Index. Cell Index (viability) was measured continuously for 96 h post-infection. Error bars indicate mean ± SEM of three independent biological replicates. *$p < 0.05$.

3.2.5 Sustained expression of PKR does not alter the phagocytic ability of macrophages

We also wanted to ensure that the reduced bacterial burden observed in THP-PKR macrophages was not due to an altered ability to phagocytose Mtb. We infected THP-Ø and THP-PKR macrophages with Mtb expressing GFP for 4 h to allow for bacterial uptake. After 4 h, extensive washes were performed to remove extracellular bacteria and the macrophages were analyzed by flow cytometry to compare the level of phagocytosis using GFP as a marker for internalized Mtb. We observed no significant differences in the percentage of GFP-positive cells or in the numbers of Mtb per macrophage between the two cell-lines **(Figure 18)**. Therefore, we concluded that the reduced Mtb burden in THP-PKR macrophages is not due to an impact of PKR expression on the phagocytic ability of macrophages. These data indicate that the reduced Mtb survival in THP-PKR macrophages is not due to an effect of PKR expression phagocytosis, further supporting our hypothesis that autophagy is the predominant mechanism responsible for this effect.

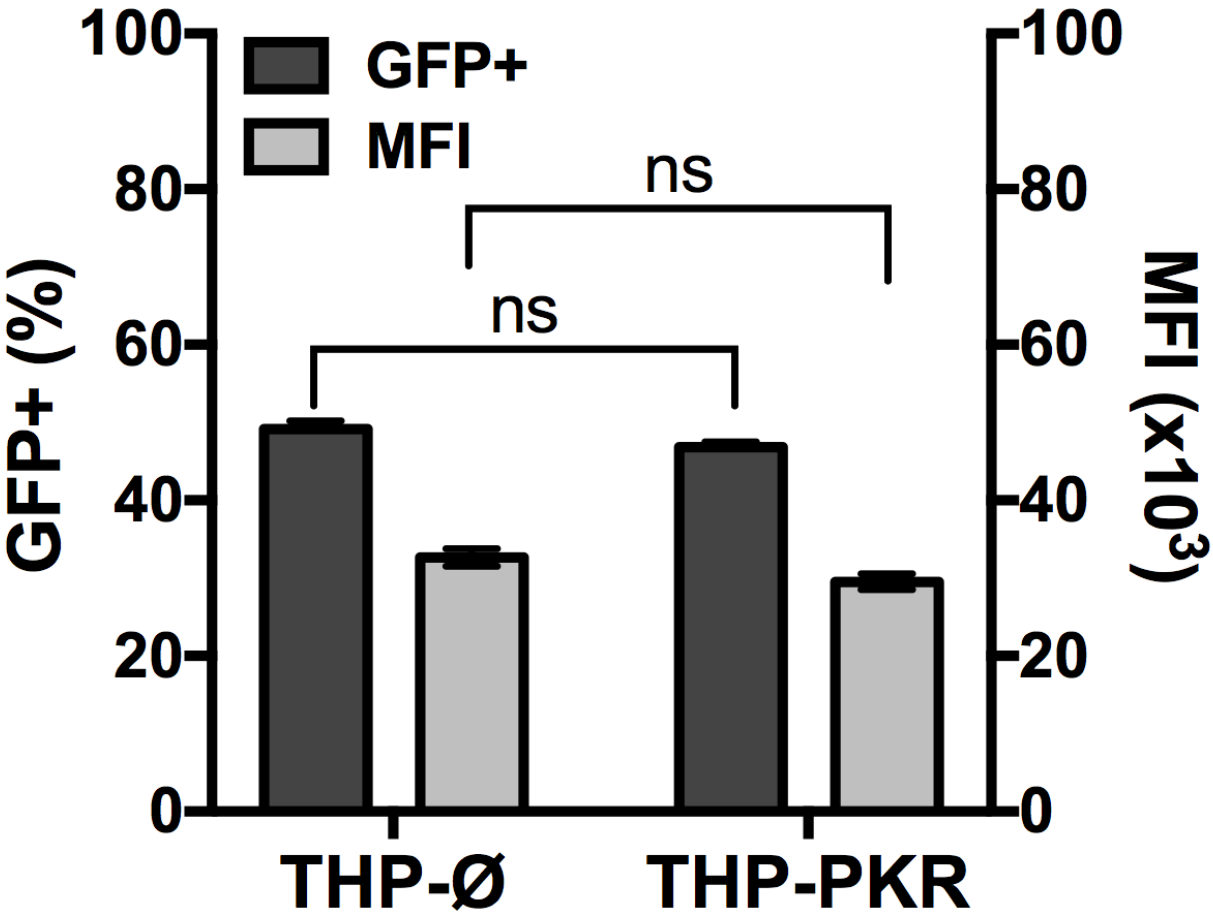
GFP+
MFI
ns
ns
100
80
60
40
20
0
GFP+ (%)
MFI (x10³)
THP-Ø
THP-PKR

Figure 18. Sustained expression of PKR does not alter the phagocytic ability of macrophages. THP-Ø and THP-PKR macrophages were infected with Mtb-GFP at an MOI of 10. At 4 h post-infection, PBS washes were performed to remove the extracellular bacteria and the macrophages were analyzed by flow cytometry to quantify the level of phagocytosis using GFP as a marker for internalized Mtb. (MFI, mean fluorescence intensity). Error bars indicate mean ± SEM of three independent biological replicates.

3.2.6 Pharmacological induction of autophagy potentiates the anti-mycobacterial effect of PKR overexpression

Since we observed that genetic upregulation of PKR can limit Mtb survival in macrophages by inducing selective autophagy, we wanted to determine whether pharmacological activation of autophagy in PKR overexpression macrophages could enhance this effect. Rapamycin, an mTOR inhibitor (244), was used to pharmacologically activate autophagy. After selecting 50 nM as a non-cytotoxic dose of rapamycin **(Figure 19A)**, a western blot was performed to verify that this concentration of rapamycin was enough to induce LC3-II expression **(Figure 19 B, C)**. We then measured the intracellular survival of Mtb in mock-treated or rapamycin-treated THP-Ø and THP-PKR macrophages **(Figure 20)**. Interestingly, while mock-treated THP-PKR macrophages did not show a decrease in Mtb survival compared to THP-Ø macrophages at day 2 post-infection, rapamycin-treated THP-PKR macrophages showed a 45% reduction in Mtb burden relative to similarly treated THP-Ø macrophages **(Figure 20)**. This result showed that rapamycin treatment accelerated and enhanced the effect of PKR overexpression on reducing Mtb burden. At day 4 post-infection, the percent decrease in Mtb burden relative to THP-Ø macrophages remained larger in rapamycin-treated THP-PKR macrophages (66%) than mock-treated THP-PKR macrophages (59%) **(Figure 20)**. This proof-of-concept experiment supports our hypothesis that PKR functions to decrease Mtb survival through a mechanism dependent on activation of autophagy. Importantly, these findings also suggest that induction of PKR activation/expression in combination with autophagy activation could be a promising strategy for HDT against TB.

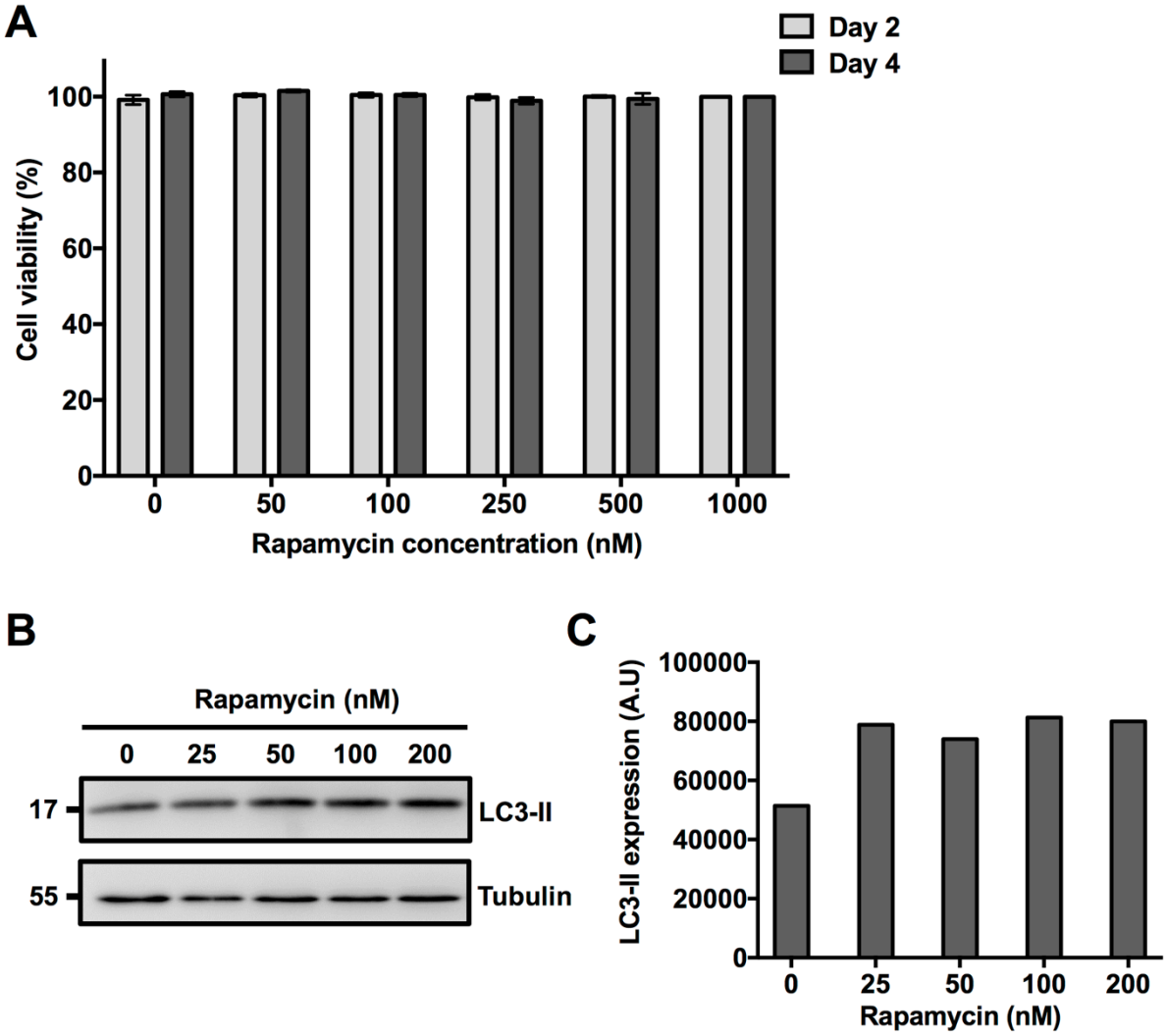
A
Day 2
Day 4
Cell viability (%)
100
80
60
40
20
0
0
50
100
250
500
1000
Rapamycin concentration (nM)
B
Rapamycin (nM)
0
25
50
100
200
17
LC3-II
55
Tubulin
C
LC3-II expression (A.U)
100000
80000
60000
40000
20000
0
0
25
50
100
200
Rapamycin (nM)

Figure 19. Rapamycin induces LC3-II expression at a non-cytotoxic concentration. (A) THP-1 macrophages were treated with rapamycin at the indicated concentrations. Rapamycin was maintained in the medium for the duration of the experiment and replenished every second day. At the indicated time points, resazurin was added to the wells and fluorescence was measured following a 4 h incubation. Fluorescence values were normalized to untreated cells as 100% and reported as % cell viability. **(B)** THP-1 macrophages were treated with rapamycin at the indicated concentrations. Cell lysates were prepared at 24 h post-treatment and LC3-II protein levels were analyzed by Western blotting. **(C)** Densitometry analysis of the blot in (B) was performed by ImageJ to quantify LC3-II band intensities in rapamycin-treated macrophages as normalized to tubulin (A.U., arbitrary units). Data in (A) represent the mean ± SEM of three independent biological replicates.

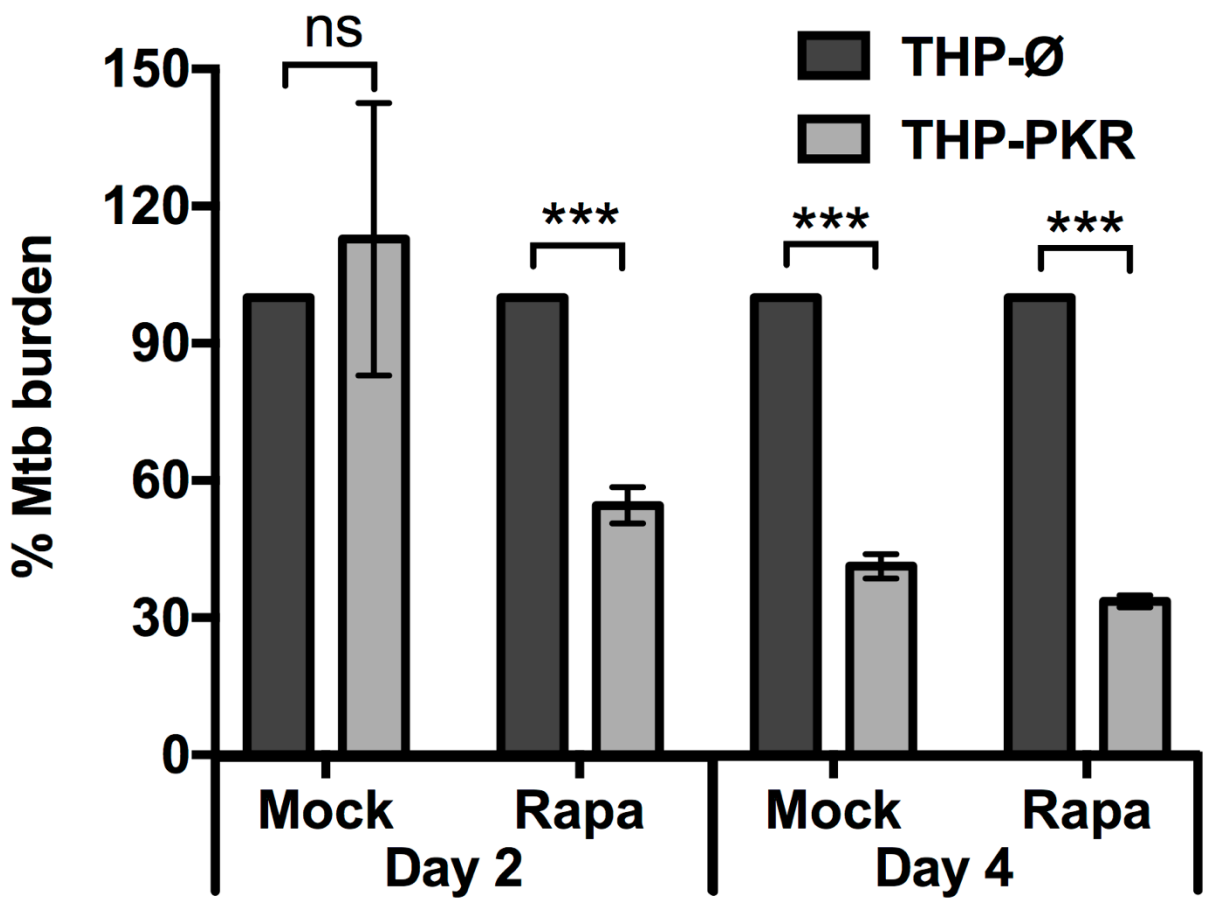
ns
***
***
***
THP-Ø
THP-PKR
% Mtb burden
150
120
90
60
30
0
Mock
Rapa
Mock
Rapa
Day 2
Day 4

Figure 20. Pharmacological activation of autophagy enhances the anti-mycobacterial effect of PKR overexpression. THP-1 macrophages were mock-treated or pre-treated with rapamycin (50 nM) for 1 h and then infected with Mtb-luciferase at an MOI of 5. Rapamycin was maintained in the medium for the duration of the experiment and replenished every second day. Infected macrophages were lysed at the indicated time post-infection and viable bacteria were determined by measuring the luminescence signal (RLU, Relative Light Units). RLU signals were normalized to THP-Ø as 100% and reported as % Mtb burden. Error bars indicate mean ± SEM of three independent biological replicates. ***$p < 0.001$.

4. DISCUSSION

4.1 Modulation of host proteins to alter intracellular *M. tuberculosis* survival

A screen of differentially expressed genes in macrophages led Wu and colleagues to explore PKR as a potential target for HDT against TB (305). However, this group investigated the effects of PKR deletion rather than activation, since PKR deletion leaves mice in good health and shows limited or no phenotype upon challenge with certain viruses (274). While Wu and colleagues initially reported that PKR deficiency in mice decreases Mtb burden in the lungs (305), there was a discrepancy between the genetic backgrounds of the mutant and control mice used in the study (290). Indeed, a follow-up study by Mundhra and colleagues using mutant and control mice from the same genetic background revealed that PKR deficiency has no effect on Mtb burden (290, 316). In contrast, Ranjbar and colleagues recently reported that PKR knockdown in THP-1 cells increases intracellular survival of Mtb (289). The discrepancy in findings could be due to a difference in experimental systems used, as Mundhra and colleagues used an *in vivo* mouse model whereas Ranjbar and colleagues tested human THP-1 cells *in vitro*. The discrepancy could also be due to a difference in the method of PKR perturbation used in the studies. While Ranjbar and colleagues used a CRISPR guide RNA targeting the PKR promoter, the follow-up study by Mundhra and colleagues used mice with a deletion in the catalytic domain of PKR. Importantly, it has been shown that the catalytic domain of PKR is not required for NF-κB activation. Indeed, PKR binds IKK to indirectly activate NF-κB, and a catalytically inactive PKR mutant is still capable of exerting this effect (270). In contrast, dsRNA-dependent NF-κB signalling is diminished in MEFs with

an N-terminal truncation in PKR (262). NF-κB plays an important role in regulating inflammation and has been shown to control Mtb load in granulomas (331). As such, it is possible that PKR knockdown inhibited NF-κB signalling and led to increased Mtb burden in the study by Ranjbar and colleagues, whereas NF-κB activation was not impaired in mice lacking PKR catalytic activity and therefore there was no effect on Mtb burden observed by Mundhra and colleagues. It is also possible that the lack of effect of PKR deficiency observed by Mundhra and colleagues was due to a redundant role of PKR. There are four EIF2α kinases, and the catalytic domain of PKR is shared among all four of these kinases. Indeed, one group showed that EIF2α is still phosphorylated after PKR deletion, albeit to a lesser extent, suggesting that one or more of the other known EIF2α kinases may compensate for the loss of PKR (272).

We successfully reproduced the results reported by Ranjbar and colleagues by observing that Mtb burden is increased in PKR knockout macrophages compared to control cells (Figure 7B) (289). Therefore, we speculated that that PKR expression and activation could instead produce a pro-host effect to reduce Mtb burden. Pharmacological activation or genetic overexpression of PKR has been shown to be well-tolerated in mice (296, 332), and PKR is reported to play a role in the innate immune response to viral and parasitic infection (283, 286). As such, we decided it was worthwhile to investigate PKR overexpression as a strategy for TB HDT. Importantly, our findings show that macrophages overexpressing PKR have significantly lower Mtb burden compared to control cells, suggesting that PKR is indeed a promising target for novel TB therapeutics (Figure 12). This finding is consistent with a report that EIF2α, the main substrate of PKR, is phosphorylated during infection with the intracellular bacteria *Listeria monocytogenes*, *Yersinia pseudotuberculosis*, and *Chlamydia*

trachomatis, and that cells expressing a non-phosphorylatable mutant of EIF2α have increased bacterial burden (315).

Previous reports support our conclusion that modulation of host proteins is a promising strategy for HDT against TB. Indeed, a chemical screen identified 133 host-targeting small molecules that restrict intracellular Mtb growth in macrophages (241). Among these, 15 were kinase activators or inhibitors. Importantly, there are approved pharmacological kinase inhibitors that offer the potential to be repurposed for TB treatment. For example, imatinib, an Abelson tyrosine kinase inhibitor used for cancer therapy, was observed to reduce bacterial load and associated pathology in Mtb-infected mice (333). In the same study, imatinib was able to reduce the bacterial burden of antibiotic-resistant mycobacteria and worked synergistically with RIF treatment to lower Mtb burden. As such, imatinib underlines the promising potential of modulating host proteins as a strategy for TB HDT. Host phosphatase inhibition has also been explored in the context of TB HDT. Schaaf and colleagues demonstrated that Mtb induces the expression of host phosphatase PPM1A to inhibit macrophage apoptosis (231). Importantly, knockdown of PPM1A increased apoptosis of Mtb-infected macrophages, thus suggesting that pharmacological inhibition of PPM1A could be a promising strategy for TB HDT (231). Lastly, although inhibition of host kinases (such as tyrosine kinases) is a more common therapeutic strategy, pharmacological activation of host kinases is starting to gain research interest. For example, the antidiabetic drug metformin and the anticonvulsant drug carbamazepine have both been shown to reduce intracellular Mtb survival by activating the autophagy-inducing kinase AMPK (240, 246). These studies with AMPK activators exemplify the promising potential of pharmacologically activating kinases as an anti-TB therapy and reinforces our conclusion that PKR is a feasible target for TB HDT.

4.2 Alteration of cytokine production by PKR in response to mycobacterial infection

Our data showing an antibacterial effect for PKR is consistent with a previous report that PKR is required for the production of anti-mycobacterial cytokines in response to BCG infection (267). While Cheung and colleagues observed that PKR inhibition by a pharmacological compound or by the transfection of a transdominant negative PKR mutant decreases production of IL-6, IL-10, and TNFα during BCG infection (267), we report that PKR overexpression decreases the production of these cytokines during Mtb infection (Figure 11 A,B,E). This discrepancy in findings is likely due to the strain of mycobacteria used, since Mtb is capable of escaping into the macrophage cytosol to trigger the cytosolic surveillance pathway and the induction of autophagy (193) whereas BCG is known to be incapable of escaping the phagosome (186). In addition, Cheung and colleagues used macrophage precursors, human $CD14^+$ blood monocytes, and promonocytic U937 cells, whereas we used primary human MDMs and differentiated THP-1 macrophages. Cheung and colleagues suggest that the effect of PKR on anti-BCG cytokine production is due to downstream activation of NF-κB, since pharmacological inhibition of NF-κB lowered the production of IL-6, IL-10, and TNFα in response to BCG infection, and treatment with the PKR inhibitor 2-AP prevented NF-κB activation (267). However, 2-AP inhibits the catalytic activity of PKR, and as discussed in section 4.1, NF-κB activation by PKR can occur regardless of its catalytic activity. Furthermore, 2-AP has been shown to inhibit other kinases (334). Taken together, these findings suggest that the effect of 2-AP treatment on NF-κB inhibition observed by Cheung and colleagues may be due to PKR-independent effects of the compound. Further investigation is required to identify the mechanisms responsible for the impact of PKR on anti-mycobacterial cytokine production.

Our observation that Mtb-infected macrophages overexpressing PKR have reduced IL-1β (Figure 11D) and TNFα (Figure 11E) production was also unexpected since these cytokines are reported to assist in Mtb clearance (145, 147, 157, 321), yet PKR overexpressing macrophages had reduced bacterial burden despite lower production of these cytokines. However, Mtb-infected PKR overexpressing macrophages also produced lower amounts of IL-10 (Figure 11B) and TGF-β1 (Figure 11C), two anti-inflammatory cytokines that function to counteract the effects of TNFα and IL-1β (167). As such, it is possible that PKR overexpressing macrophages require a lower threshold of TNFα and IL-1β to prevent hyper-inflammation. Consistent with our findings, PKR has been previously suggested to inhibit IL-1β production. Yim and colleagues observed that primary macrophages from PKR knockout mice had increased IL-1β production following inflammasome activation by LPS and nigericin treatment (335). Since PKR induces the production of type I IFN in response to certain viruses (281), and type I IFN have been observed to downregulate IL-1β mRNA expression in Mtb-infected macrophages (336), it is possible that our PKR overexpression macrophages had reduced IL-1β production as a result of increased type I IFN production.

4.3 The impact of PKR on macrophage cell death regulation

Our findings suggest that PKR does not regulate macrophage apoptosis during Mtb infection (Figure 17 A,B). This finding is inconsistent with previous reports that PKR induces apoptosis during viral infection (337) and is required for macrophage apoptosis following TLR4 activation by *Salmonella* Typhimurium, *Yersinia pseudotuberculosis*, and *Bacillus anthracis* infection (287). However, a crucial aspect of Mtb virulence is to inhibit macrophage apoptosis. Indeed, while PKR has been reported to play a role in TNFα-induced apoptosis

(338, 339), virulent Mtb strains release soluble TNFα receptor-2, which forms a complex with the inactive cytokine to inhibit TNFα-induced apoptosis (340). Furthermore, PKR mediates apoptosis in a FADD-dependent manner (278, 341), but macrophages collected from pulmonary TB patients by bronchoalveolar lavage showed decreased FADD expression (342). In addition, MAPK p38, NF-κB, and p53 are downstream effectors of PKR that may play a role in PKR-induced apoptosis (265, 279, 339), however Mtb secretes protein-tyrosine phosphatase PtpB to inhibit these effectors (343). Indeed, PtpB has been observed to simultaneously block NF-κB and p38 signal pathways and inhibit p53 expression (343). Altogether, these findings indicate that Mtb inhibits many pro-apoptotic effectors utilized by PKR to induce apoptosis. Since Mtb is effective at inhibiting macrophage apoptosis, our finding that PKR overexpression did not impact apoptosis of Mtb-infected macrophages was not surprising.

Our RTCA data did not reveal differences in general cell death between THP-PKR and THP-Ø macrophages (Figure 17C), which suggests that PKR does not induce pyroptosis or necroptosis. Whether PKR plays a role in inflammasome activation and subsequent pyroptosis induction is still in debate. Four studies have assessed the role of PKR in inflammasome activation, and there is disagreement between the findings from each study. Lu et al. and Hett et al. both reported that PKR promotes inflammasome activation (288, 344), whereas He et and colleagues reported that PKR is dispensable for inflammasome activation (345). Most recently, Yim and colleagues concluded that PKR represses inflammasome activity (335). There are many factors that could explain the discrepancy between these reports, such as variation in the cell models used. For example, He et al. reported that PKR did not impact inflammasome activity in murine bone marrow-derived macrophages, but these

cells require cytokine supplementation for survival *in vitro* and were demonstrated by Yim and colleagues to have diminished PKR-dependent responses (335). In contrast, Yim and colleagues used primary mouse peritoneal macrophages which are differentiated *in vivo* and do not require manipulation following isolation (335). Another point of variance between the studies is the murine strains that were used. Although Hett et al. and Lu et al. observed increased inflammasome activity by PKR, these groups used mice that were variable on the 129v background. Importantly, the 129 mouse strain has attenuated inflammasome activity due to reduced caspase-11 expression (346). Caspase-11 expression is induced by the CCAAT-enhancer protein homologous protein, and EIF2α phosphorylation controls expression of this protein (347). As such, it is unsurprising that PKR activity could rescue the impaired inflammasome activity in the 129 strain by restoring caspase-11 expression. Overall, the role of PKR in inflammasome activation and pyroptosis remains unclear. Our results suggest that PKR does not impact pyroptosis, which aligns most closely to the report from He and colleagues. Future studies should examine the effect of PKR modulation on inflammasome activity during Mtb infection to determine whether PKR plays a role in Mtb-induced pyroptosis.

There is one report that PKR is required for IFNγ-induced necroptosis (306). However, this form of necroptosis occurred in an artificial system comprising MEFs with a genetic deletion of FADD or expressing a phosphomimetic FADD mutant. PKR is reported to induce apoptosis in a FADD-dependent manner (278, 341), therefore it is questionable whether this PKR-dependent form of necroptosis would occur under normal conditions without artificial inactivation or deletion of FADD. Furthermore, stimulation with exogenous IFNγ was required for this form of PKR-dependent necroptosis to occur (306). We observed that both

uninfected and Mtb-infected THP-1 macrophages produced low concentrations of IFNγ (Figure 11G), therefore it is unsurprising that PKR did not induce necroptosis in our system. The role of PKR in necroptosis during bacterial infection has not yet been studied, therefore further investigation is required to determine whether this kinase is involved in Mtb-induced necroptosis.

4.4 Activation of cytosolic nucleic acid sensors by mycobacteria

Our findings demonstrate that PKR expression and activation is induced during Mtb infection (Figures 4, 5). These findings are consistent with previous reports that Mtb activates cytosolic nucleic acid sensors. Multiple groups have shown that the DNA sensor cGAS recognizes Mtb DNA, thus triggering the STING pathway and type I IFN production (193, 348, 349). However, it has also been observed that cGAS or STING knockout mice have comparable lung bacterial burden and inflammation compared to WT mice, suggesting that other sensors may compensate during inhibition of the DNA sensing pathway (193, 349, 350).

More recently, it was reported that cytosolic Mtb RNA induces IFNβ production through the activation of retinoid acid-inducible gene I (RIG-I), an RNA sensor (351). This discovery indicated that Mtb nucleic acids are recognized by both DNA and RNA sensors. It has also been shown that the RNA sensor MDA-5 contributes to IFNβ production and bacterial control in Mtb-infection macrophages (250). However, RIG-I recognizes specific Mtb mRNAs that are not recognized by MDA-5 (351). This indicates that distinct Mtb products are recognized by different cytosolic RNA sensors and that MDA-5 and RIG-I have nonredundant roles during Mtb infection. Although PKR signals independently from the MDA-5 and RIG-I pathway, PKR has been reported to be activated by bacterial RNA (Chai

et al, 2020). As such, Ranjbar and colleagues investigated the effect of Mtb infection on PKR activation. Importantly, this group observed that PKR expression and activation is induced in macrophages during Mtb infection (289). Therefore, our findings in Figures 4 and 5 are consistent with those of Ranjbar and colleagues.

Although we and others have observed that PKR expression and activation is triggered by Mtb infection, the upstream effectors responsible for PKR induction remain unknown. Since PKR is an RNA sensor, it is reasonable to speculate that PKR is directly activated by cytosolic Mtb RNA. However, there is evidence that PKR can be activated by the DNA-sensing pathway. Indeed, Hu et al. recently reported that exogenous DNA recognition by cGAS triggers PKR activation (352). The cGAS/STING/TBK-1 axis leads to activation of IRF-3, which induces transcription of IFNβ (353). IFNβ triggers assembly and nuclear translocation of the transcription factor interferon-stimulated gene factor 3 (ISGF3), which regulates the PKR promoter (354). It is therefore possible that the DNA-sensing pathway indirectly induces PKR by triggering IFNβ production and downstream ISGF3 activation. Overall, PKR may be activated by both cytosolic Mtb RNA and DNA. It is important to note however that BCG has been observed to trigger PKR phosphorylation (267). Importantly, BCG lacks ESX-1 and is incapable of perforating the phagosome (185, 186, 355), suggesting that PKR can be activated in the absence of cytosolic mycobacterial DNA or RNA. Since Mtb glycoliproteins, lipoproteins, and glycolipids are reported to be ligands for TLR4 and TLR2 (356, 357), Ranjbar and colleagues suggest that TLR recognition of Mtb is responsible for PKR induction during Mtb infection (289). Similar to the cGAS/STING/TBK-1 pathway, TLR2 and TLR4 signaling can trigger IRF-3 activation and the production of type I IFN (356). Taken together, we speculate that PKR can be activated by a variety of pathways during Mtb

infection, including cytosolic RNA- and DNA-sensing pathways and TLR signalling **(Figure 21)**.

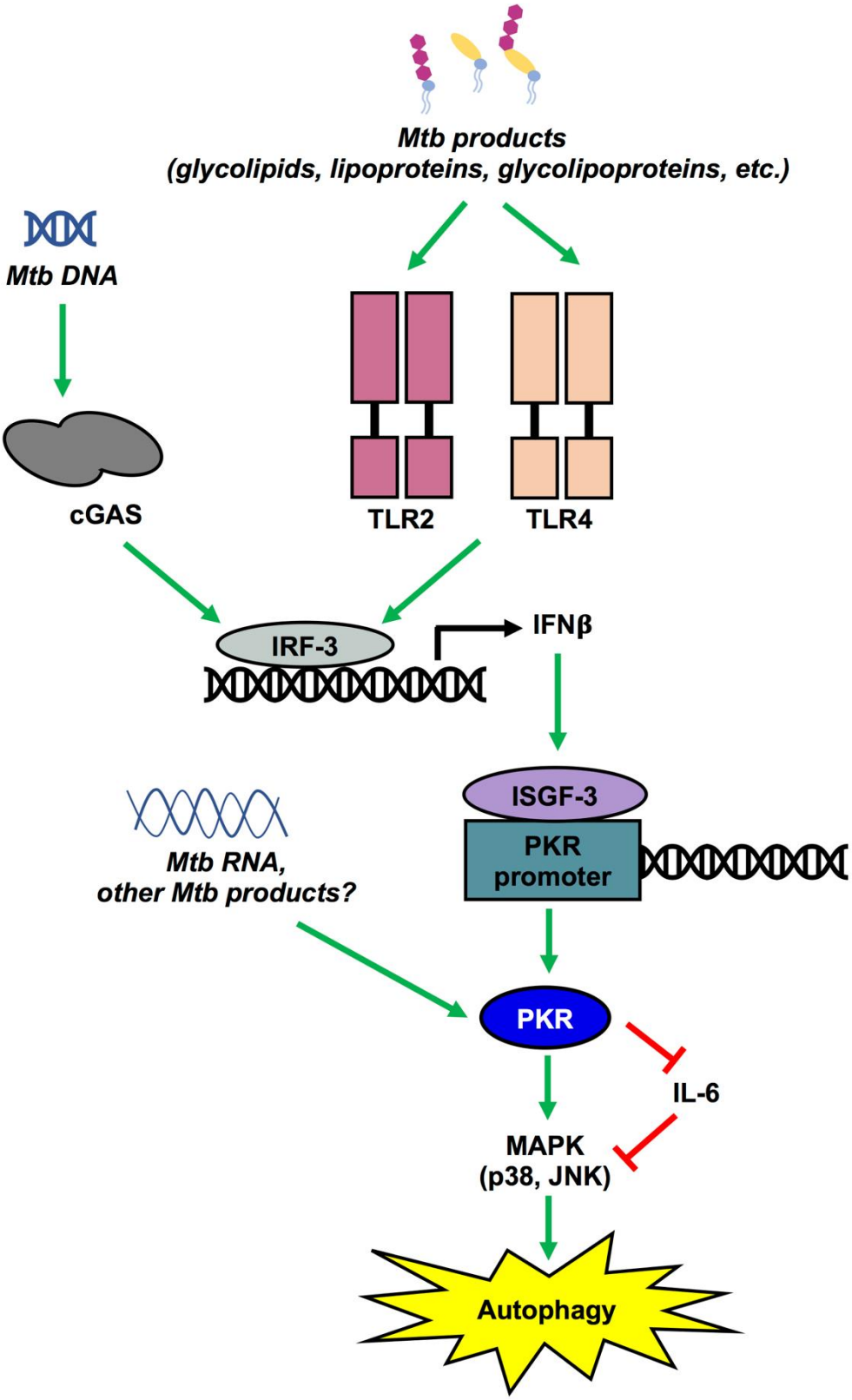
Mtb products
(glycolipids, lipoproteins, glycolipoproteins, etc.)
Mtb DNA
cGAS
TLR2
TLR4
IRF-3
IFNβ
ISGF-3
PKR
promoter
Mtb RNA,
other Mtb products?
PKR
IL-6
MAPK
(p38, JNK)
Autophagy

Figure 21. Proposed model of PKR activation and downstream autophagy induction during Mtb infection. Mtb glycoproteins, lipoproteins, and glycolipoproteins are ligands for macrophage PRRs such as TLR2 and TLR4. TLR2 and TLR4 signaling leads to activation of IRF-3. Cytosolic Mtb DNA is recognized by the DNA sensor cGAS, which also triggers IRF-3 activation via the STING pathway. IRF-3 drives the transcription of IFNβ, which triggers the assembly and nuclear translocation of the transcription factor ISGF3. ISGF3 then regulates the PKR promoter to induce transcription of PKR. Cytosolic Mtb RNA and other Mtb products may also interact directly with PKR to trigger its activation. PKR may indirectly activate autophagy by inhibiting the production of IL-6, a cytokine that hinders macrophage autophagy activation by preventing MAPK p38 and JNK phosphorylation. Alternatively, PKR expression may induce autophagy by activating MAPK p38 and JNK.

4.5 The role of PKR during selective autophagy

PKR has been demonstrated to play a role in bulk autophagy activation during starvation or in response to chemical autophagy inducers (282, 358). However, knowledge of the role of PKR during selective autophagy of pathogens is limited. Our data suggest a new role for PKR in the regulation of selective autophagy in response to intracellular bacterial infection. Western blot analysis of autophagy markers and immunofluorescence microscopy analysis of LC3 and lysosome colocalization with Mtb reveal that PKR expression induces selective autophagy of Mtb (Figures 15, 16). Inhibition of autophagy also reversed the effects of PKR overexpression on intracellular Mtb survival (Figure 14). These findings are consistent with previous reports that PKR induces LC3-associated autophagy of *Toxoplasma gondii* (286) and is required for autophagic degradation of HSV-1 (283).

Given the key role that IFNγ plays in induction of macrophage autophagy (122), and considering that IL-6 inhibits IFNγ-induced autophagy (161), we speculate that the increased activation of autophagy observed in PKR overexpressing macrophages is due, at least in part, to decreased production of IL-6 and increased production of IP-10 and IFNγ by these cells. Consistent with this, we observed that addition of IFNγ enhanced the ability of THP-PKR macrophages to limit the intracellular survival of Mtb (Figure 12). IFNγ activates autophagy in Mtb-infected macrophages by inducing phosphorylation of MAPK p38 and JNK, whereas IL-6 inhibits phosphorylation of these kinases to block IFNγ-induced autophagy (161). The dependence of IFNγ-induced autophagy on p38 activation has also been shown in *Listeria monocytogenes*- and *Salmonella* Typhimurium-infected macrophages (359). Although the specific mechanisms by which p38 and JNK activate autophagy during bacterial infection have not yet been elucidated, these two proteins are reported to induce autophagy during

starvation through indirect effects on beclin-1. p38 plays a critical role during starvation-induced autophagy by activating MK2 and MK3, which then phosphorylate beclin-1 (209). It is not understood why beclin-1 must be phosphorylated, but it was shown that this phosphorylation is critical for starvation-induced autophagy since the expression of a non-phosphorylatable mutant of beclin-1 severely inhibited this process (209). JNK activates autophagy during starvation by phosphorylating Bcl-2, triggering its dissociation from beclin-1 (208). Bcl-2 is a negative regulator of autophagy that binds to beclin-1 to prevent it from interacting with ATG14 in the class III PI3K complex during the phagophore formation stage of autophagy (360). Interestingly, PKR is reported to activate JNK and p38 in response to viral infection (265) and bacterial endotoxin challenge (361). As such, it is possible that the induction of autophagy in PKR overexpressing macrophages is dependent on a mechanism involving JNK and p38 activation, whether by a direct effect of PKR on MAPK activation and/or an indirect effect from decreased IL-6 production by PKR overexpressing macrophages (Figure 21). Future studies will identify the specific downstream effectors regulated by PKR to activate selective autophagy in Mtb-infected macrophages.

4.6 Activation of selective autophagy as a host-directed therapy strategy

Activation of macrophage autophagy is frequently explored as an HDT strategy for TB, since this process serves as an antibacterial response that can assist in the clearance of Mtb (122, 123, 215, 217). In fact, current TB antibiotics PYZ and INH activate autophagy in Mtb-infected macrophages, and inhibition of autophagy reduces the effectiveness of these drugs (218). Importantly, pharmacological activation of autophagy is a feasible treatment strategy, since many existing small molecule drugs have been shown to induce autophagy

during Mtb infection and offer the potential for being repurposed for anti-TB therapy. Carbamazepine, rapamycin, and NTZ are examples of such drugs. Carbamazepine is an anti-convulsant drug that was shown to induce autophagy via AMPK activation (246). This drug was observed to reduce Mtb burden and lung pathology in mice infected with MDR-TB and also induced autophagic killing of Mtb in primary human macrophages (246). While rapamycin is used as an immunosuppressant to prevent organ rejection following transplantation, this drug is known to activate autophagy by inhibiting mTOR (244). Due to its role in autophagy activation, rapamycin has been suggested as a candidate for TB HDT (243). Indeed, inhalable particles containing rapamycin are being investigated as a means to enhance autophagy in AMs during Mtb infection (362). Furthermore, our results demonstrated that rapamycin treatment accelerated and enhanced the decrease in Mtb burden observed in PKR overexpressing macrophages relative to control cells (Figure 20). However, the poor solubility, long intracellular half-life, and immunosuppressive effects of rapamycin decreases its appeal for use as a TB therapeutic (243). More promisingly, NTZ has an excellent clinical safety record when used as an anti-parasitic agent (363, 364) and has been shown to induce autophagosome formation and inhibit mTOR signaling in Mtb-infected macrophages (365). Importantly, multiple groups have reported that NTZ reduces intracellular survival of Mtb in macrophages (289, 365). Although approved drugs such as carbamazepine, rapamycin, and NTZ have been shown to be successful in limiting Mtb survival, these repurposed drugs have multiple effects in the host. As such, it is difficult to discern whether the effects are solely due to autophagy activation. TB HDT is lacking novel host targets and new drugs that can specifically target the autophagy pathway. Importantly, our findings unveil PKR as a novel host target that activates autophagy and reduces Mtb survival in macrophages.

It is also important to determine whether these repurposed drugs have direct antibacterial activity. Indeed, NTZ has been shown to directly kill Mtb (366), which raises the question of whether NTZ inhibits Mtb replication in macrophages solely by targeting the bacteria themselves or through its effects on autophagy induction. Therapeutics that have direct bactericidal activity are accompanied with increased risk of drug resistance, whereas HDTs that solely function to boost the host response can circumvent the development of drug-resistant bacteria. In the case of NTZ, a concentration of 10 μM was shown to completely inhibit mTOR signaling and strongly stimulate autophagy, whereas this concentration was less effective at directly inhibiting Mtb growth in liquid culture (365). Furthermore, this concentration of NTZ inhibited the replication of Mtb in THP-1 cells more strongly than it inhibited Mtb directly. As such, it was suggested that concentrations of NTZ that directly kill Mtb would also activate autophagy, and that the autophagy-activating effects of NTZ contribute more than its direct antibacterial activity to the inhibition of Mtb growth (365). Importantly, NTZ has been observed to limit the growth of both replicating and non-replicating Mtb, suggesting it can evade the emergence of NTZ-resistant Mtb (366).

4.7 Feasibility of using pharmacological PKR activators for host-directed therapy

Altogether, our findings suggest that PKR is a promising target for HDT against TB. Importantly, pharmacological activation of PKR is well-tolerated in mice (296), suggesting that pharmacological activation of PKR would be a safe treatment strategy in humans. As such, we sought to assess the feasibility of using pharmacological PKR activators as a TB HDT. We examined the effect of DHBDC, a small molecule PKR activator, on the Mtb burden in primary human macrophages. Although DHBDC treatment did not reduce the Mtb burden

(Figure 9 A-C), our studies using PKR knockout macrophages demonstrated that DHBDC has off-target effects (Figure 9D). This is consistent with a previous finding that DHBDC activates PERK in addition to PKR (302). To our knowledge, this is the first report of a direct effect of DHBDC on PKR phosphorylation, as a previous study used activation of EIF2α as a downstream marker for PKR activation (302). Although DHBDC did not reduce intracellular Mtb survival, PKR still offers a feasible target for HDT. Indeed, it has been demonstrated that PKR can be activated by other small molecules, such as BEPP and heparin (301, 367). Endogenous heparin is located in secretory granules within mast cells and is not present in the cytosol, therefore it is not likely to activate PKR *in vivo* (367). However, the ability of heparin to induce PKR phosphorylation *in vitro* demonstrates the ability of molecules as small as 2 kDa to activate PKR, thus providing incentive to search for novel small molecule PKR activators (367). Future work will investigate the effects of more specific pharmacological PKR activators on Mtb burden both *in vitro* and in mouse models.

There are also existing drugs that offer the potential for being repurposed as PKR activators, including bozepinib and NTZ. Bozepinib is an anti-tumour agent that is particularly promising for use as a pharmacological PKR activator since it not only induces phosphorylation of PKR but also increases expression levels (295). This suggests that bozepinib would mimic our model closely since THP-PKR cells had both increased expression and phosphorylation of PKR compared to control cells (Figure 10). Importantly, bozepinib is non-toxic at high concentrations in the mouse model, suggesting this PKR activator could be safe for use in humans (296). Unfortunately, this compound is not available commercially, which is why we could not test it in this study. Interestingly, in addition to its autophagy-inducing effects, NTZ has been shown to trigger PKR activation (297, 298).

However, two groups have reported contrary findings that NTZ does not induce PKR phosphorylation (289, 368). It is important to note that both groups used a concentration of 10 μM NTZ, which was previously shown to be inadequate in triggering PKR phosphorylation. Indeed, while treatment of cells with 10 μM NTZ had little or no effect on PKR activation, 25 μM NTZ resulted in phosphorylation of both PKR and EIF2α (298). Overall, NTZ has been shown to induce autophagy, trigger PKR phosphorylation, and reduce Mtb burden in macrophages (289, 298, 365). As such, NTZ exemplifies the feasibility and promising potential of pharmacologically activating PKR and/or autophagy as a strategy for TB HDT.

4.8 Conclusion

There is an urgent need for the development of novel TB therapeutics due to the emergence of antibiotic-resistant Mtb strains. Autophagy induction in Mtb-infected macrophages is a promising HDT strategy, however currently approved drugs that can be repurposed as autophagy activators have many targets in the host. Identification of novel autophagy-inducing drugs with a specific host target would be extremely beneficial in the field of TB HDT. Since PKR has been suggested as a potential target for host-directed therapy against TB infection (220, 289, 305), we investigated the role of PKR in the antibacterial response of Mtb-infected macrophages. The work presented in this thesis provides evidence to support that PKR is a promising target for HDT **(Figure 22)**. We show that PKR expression and activation is triggered by Mtb infection (Figures 4 and 5), and that PKR enhances the immunological profile of Mtb-infected macrophages by stimulating or inhibiting the production of autophagy-regulating proteins IL-6, IL-10, and IP-10 (Figure 11 A, B, F). Importantly, we show that PKR expression limits the intracellular survival of Mtb in

macrophages through a mechanism dependent on the activation of selective autophagy (Figures 12-16). PKR is a feasible target for TB HDT since there are existing pharmacological PKR activators with good safety profiles *in vivo*, and there is also the potential for identifying novel small molecules that can activate this kinase. As such, future work will focus on assessing the efficacy of specific PKR activators both *in vitro* and in the mouse model. Furthermore, it will be beneficial to characterize the upstream events that induce PKR activation/expression during Mtb infection and identify the downstream effectors regulated by PKR to activate selective autophagy.

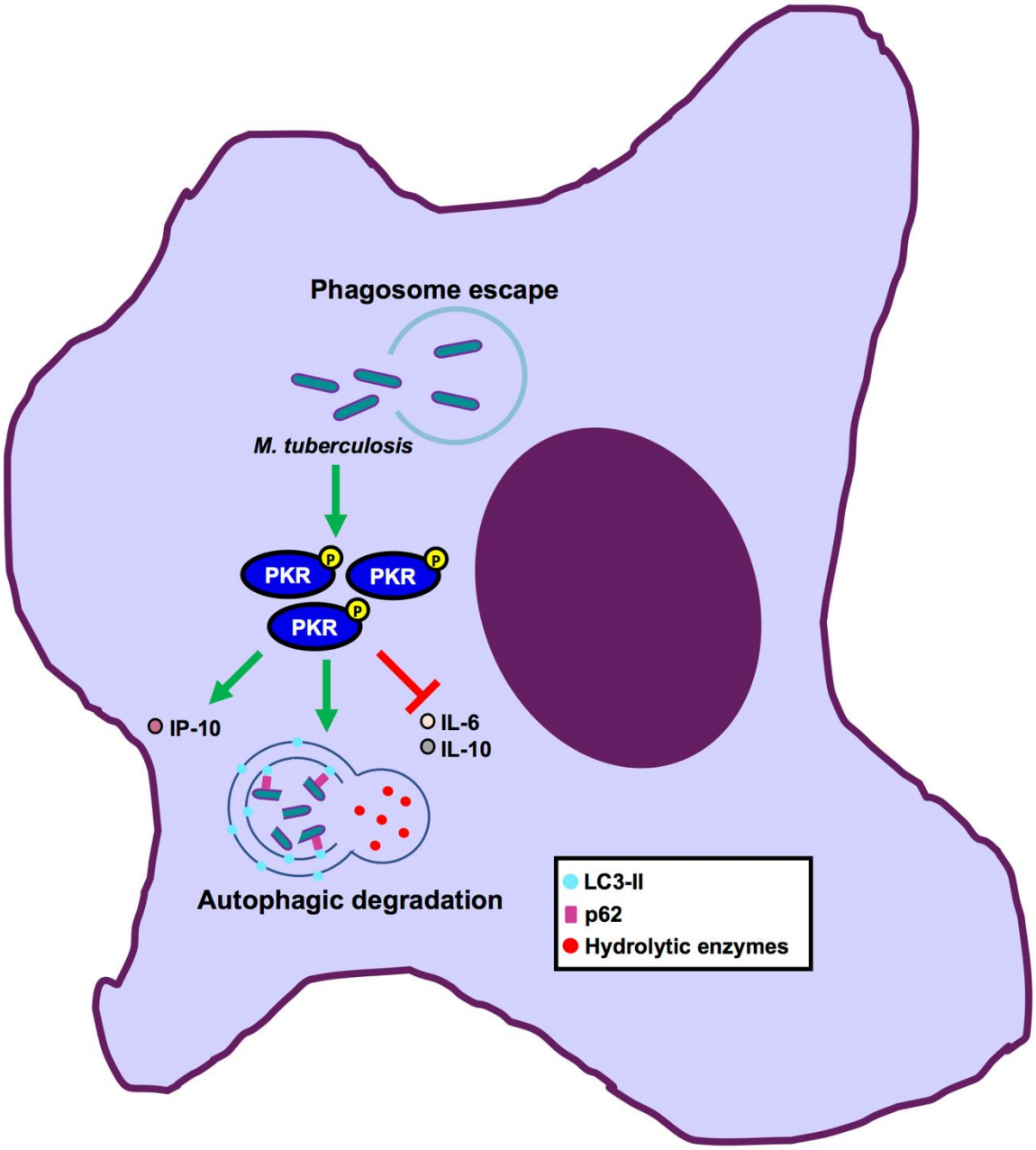
Phagosome escape
M. tuberculosis
PKR
PKR
PKR
IP-10
IL-6
IL-10
Autophagic degradation
LC3-II
p62
Hydrolytic enzymes

Figure 22. Model depicting the role of PKR in the antibacterial response of *M. tuberculosis*-infected macrophages. Mtb infection triggers phosphorylation and expression of PKR. PKR expression increases macrophage production of the autophagy-inducing protein IP-10 and decreases production of autophagy-inhibiting cytokines IL-6 and IL-10. PKR expression also activates selective autophagy targeting cytosolic Mtb, as indicated by increased p-S403 p62 and LC3-II expression and Mtb colocalization with autophagolysosomes. The bacteria are degraded in the autophagolysosomes, resulting in reduced intracellular survival of Mtb.

5. REFERENCES

1. Spigelman, M., H. D. Donoghue, Z. Abdeen, S. Ereqat, I. Sarie, C. L. Greenblatt, I. Pap, I. Szikossy, I. Hershkovitz, G. K. Bar-Gal, and C. Matheson. 2015. Evolutionary changes in the genome of Mycobacterium tuberculosis and the human genome from 9000 years BP until modern times. *Tuberculosis* 95: S145–S149.

2. Gutierrez, M. C., S. Brisse, R. Brosch, M. Fabre, B. Omaïs, M. Marmiesse, P. Supply, and V. Vincent. 2005. Ancient origin and gene mosaicism of the progenitor of Mycobacterium tuberculosis. *PLoS Pathog.* 1: e5.

3. Barberis, I., N. L. Bragazzi, L. Galluzzo, and M. Martini. 2017. The history of tuberculosis: From the first historical records to the isolation of Koch's bacillus. *J. Prev. Med. Hyg.* 58: E9–E12.

4. Schatz, A., E. Bugle, and S. A. Waksman. 1944. Streptomycin, a substance exhibiting antibiotic activity against gram-positive and gram-negative bacteria. *Exp. Biol. Med.* 55: 66–69.

5. Daniel, T. M. 2006. The history of tuberculosis. *Respir. Med.* 100: 1862–1870.

6. WHO. 2020. Global tuberculosis report 2019. *WHO*.

7. Narasimhan, P., J. Wood, C. R. Macintyre, and D. Mathai. 2013. Risk factors for tuberculosis. *Pulm. Med.* 2013: 11.

8. Vachon, J., V. Gallant, and W. Siu. 2018. Tuberculosis in Canada, 2016. *Canada Commun. Dis. Rep.* 44: 75–81.

9. Patterson, M., S. Finn, and K. Barker. 2018. Addressing tuberculosis among Inuit in Canada. *Canada Commun. Dis. Rep.* 44: 82–85.

10. Koch, R. 1882. Die ätiologie der tuberkulose. *Berliner Klin. Wochenschrift* 19: 221–230.

11. Wayne, L. G. 1974. The genus Mycobacterium. *Int. J. Syst. Bacteriol.* 24: 308–308.

12. Cook, G. M., M. Berney, S. Gebhard, M. Heinemann, R. A. Cox, O. Danilchanka, and M. Niederweis. 2009. Physiology of mycobacteria. *Adv. Microb. Physiol.* 55: 81.

13. Dartois, V. 2014. The path of anti-tuberculosis drugs: from blood to lesions to mycobacterial cells. *Nat. Rev. Microbiol.* 12: 159–167.

14. Augenstreich, J., and V. Briken. 2020. Host cell targets of released lipid and secreted protein effectors of Mycobacterium tuberculosis. *Front. Cell. Infect. Microbiol.* 10: 595029.

15. Brennan, P. J. 2003. Structure, function, and biogenesis of the cell wall of

Mycobacterium tuberculosis. *Tuberculosis*. 83: 91–97.

16. Pfyffer, G. E., and F. Palicova. 2011. Mycobacterium: General Characteristics, Laboratory Detection, and Staining Procedures. In *Manual of Clinical Microbiology*, 10th ed. J. Versalovic, K. Carroll, G. Funke, J. Jorgensen, M. Landry, and D. Warnock, eds. American Society of Microbiology Press, Washington, DC. p. 472–502.

17. Long, R., and K. Schwartzman. 2014. *Canadian Tuberculosis Standards Chapter 2: Pathogenesis and Transmission of Tuberculosis*, 7th ed. Public Health Agency of Canada, Ottawa, ON. p. 7–63.

18. Farhat, M., C. Greenaway, M. Pai, and D. Menzies. 2006. False-positive tuberculin skin tests: what is the absolute effect of BCG and non-tuberculous mycobacteria? *Int. J. Tuberc. Lung Dis.* 10: 1192–1204.

19. Pym, A. S., P. Brodin, R. Brosch, M. Huerre, and S. T. Cole. 2002. Loss of RD1 contributed to the attenuation of the live tuberculosis vaccines Mycobacterium bovis BCG and Mycobacterium microti. *Mol. Microbiol.* 46: 709–717.

20. Andersen, P., M. E. Munk, J. M. Pollock, and T. M. Doherty. 2000. Specific immune-based diagnosis of tuberculosis. *Lancet* 356: 1099–1104.

21. World Health Organization. 2010. Tuberculosis diagnostics automated DNA test. *WHO.*

22. Lawn, S. D., and M. P. Nicol. 2011. Xpert® MTB/RIF assay: development, evaluation and implementation of a new rapid molecular diagnostic for tuberculosis and rifampicin resistance. *Future Microbiol.* 6: 1067–1082.

23. Roy, A., M. Eisenhut, R. J. Harris, L. C. Rodrigues, S. Sridhar, S. Habermann, L. Snell, P. Mangtani, I. Adetifa, A. Lalvani, and I. Abubakar. 2014. Effect of BCG vaccination against Mycobacterium tuberculosis infection in children: systematic review and meta-analysis. *BMJ* 349: g4643.

24. Mangtani, P., I. Abubakar, C. Ariti, R. Beynon, L. Pimpin, P. E. M. Fine, L. C. Rodrigues, P. G. Smith, M. Lipman, P. F. Whiting, and J. A. Sterne. 2014. Protection by BCG vaccine against tuberculosis: a systematic review of randomized controlled trials. *Clin. Infect. Dis.* 58: 470–480.

25. Trunz, B. B., P. Fine, and C. Dye. 2006. Effect of BCG vaccination on childhood tuberculous meningitis and miliary tuberculosis worldwide: a meta-analysis and assessment of cost-effectiveness. *Lancet* 367: 1173–1180.

26. Dodd, P. J., C. M. Yuen, C. Sismanidis, J. A. Seddon, and H. E. Jenkins. 2017. The global burden of tuberculosis mortality in children: a mathematical modelling study. *Lancet Glob. Heal.* 5: e898–e906.

27. Stanford, J. L., M. J. Shield, and G. A. W. Rook. 1981. How environmental

mycobacteria may predetermine the protective efficacy of BCG. *Tubercle* 62: 55–62.

28. Li, X. X., and X. N. Zhou. 2013. Co-infection of tuberculosis and parasitic diseases in humans: a systematic review. *Parasites and Vectors* 6: 79.

29. Zhang, L., H. W. Ru, F. Z. Chen, C. Y. Jin, R. F. Sun, X. Y. Fan, M. Guo, J. T. Mai, W. X. Xu, Q. X. Lin, and J. Liu. 2016. Variable virulence and efficacy of BCG vaccine strains in mice and correlation with genome polymorphisms. *Mol. Ther.* 24: 398–405.

30. Aguirre-Blanco, A. M., P. T. Lukey, J. M. Cliff, and H. M. Dockrell. 2007. Strain-dependent variation in Mycobacterium bovis BCG-induced human T-cell activation and gamma interferon production in vitro. *Infect. Immun.* 75: 3197–3201.

31. Moliva, J. I., J. Turner, and J. B. Torrelles. 2017. Immune responses to bacillus Calmette-Guérin vaccination: why do they fail to protect against Mycobacterium tuberculosis? *Front. Immunol.* 8: 407.

32. Tuberculosis Vaccine Initiative. 2020. Pipeline of vaccines. *TBVI.*

33. Banerjee, A., E. Dubnau, A. Quemard, V. Balasubramanian, K. S. Um, T. Wilson, D. Collins, G. De Lisle, and W. R. Jacobs. 1994. inhA, a gene encoding a target for isoniazid and ethionamide in Mycobacterium tuberculosis. *Science* 263: 227–230.

34. Dessen, A., A. Quémard, J. S. Blanchard, W. R. Jacobs, and J. C. Sacchettini. 1995. Crystal structure and function of the isoniazid target of Mycobacterium tuberculosis. *Science* 267: 1638–1641.

35. Campbell, E. A., N. Korzheva, A. Mustaev, K. Murakami, S. Nair, A. Goldfarb, and S. A. Darst. 2001. Structural mechanism for rifampicin inhibition of bacterial RNA polymerase. *Cell* 104: 901–912.

36. Goude, R., A. G. Amin, D. Chatterjee, and T. Parish. 2009. The arabinosyltransferase EmbC is inhibited by ethambutol in Mycobacterium tuberculosis. *Antimicrob. Agents Chemother.* 53: 4138–4146.

37. Zhang, Y., M. M. Wade, A. Scorpio, H. Zhang, and Z. Sun. 2003. Mode of action of pyrazinamide: disruption of Mycobacterium tuberculosis membrane transport and energetics by pyrazinoic acid. *J. Antimicrob. Chemother.* 52: 790–795.

38. Ramachandran, G., and S. Swaminathan. 2015. Safety and tolerability profile of second-line anti-tuberculosis medications. *Drug Saf.* 38: 253–269.

39. Kjellsson, M. C., L. E. Via, A. Goh, D. Weiner, K. M. Low, S. Kern, G. Pillai, C. E. Barry, and V. Dartois. 2012. Pharmacokinetic evaluation of the penetration of antituberculosis agents in rabbit pulmonary lesions. *Antimicrob. Agents Chemother.* 56: 446–457.

40. Schaaf, K., V. Hayley, A. Speer, F. Wolschendorf, M. Niederweis, O. Kutsch, and J. Sun. 2016. A macrophage infection model to predict drug efficacy against Mycobacterium tuberculosis. *Assay Drug Dev. Technol.* 14: 345–354.

41. Batt, S. M., D. E. Minnikin, and G. S. Besra. 2020. The thick waxy coat of mycobacteria, a protective layer against antibiotics and the host's immune system. *Biochem. J.* 447: 1983–2006.

42. Viveiros, M., M. Martins, L. Rodrigues, D. Machado, I. Couto, J. Ainsa, and L. Amaral. 2012. Inhibitors of mycobacterial efflux pumps as potential boosters for anti-tubercular drugs. *Expert Rev. Anti. Infect. Ther.* 10: 983–998.

43. Park, H. D., K. M. Guinn, M. I. Harrell, R. Liao, M. I. Voskuil, M. Tompa, G. K. Schoolnik, and D. R. Sherman. 2003. Rv3133c/dosR is a transcription factor that mediates the hypoxic response of Mycobacterium tuberculosis. *Mol. Microbiol.* 48: 833–843.

44. Voskuil, M. I., D. Schnappinger, K. C. Visconti, M. I. Harrell, G. M. Dolganov, D. R. Sherman, and G. K. Schoolnik. 2003. Inhibition of respiration by nitric oxide induces a Mycobacterium tuberculosis dormancy program. *J. Exp. Med.* 198: 705–713.

45. Shiloh, M. U., P. Manzanillo, and J. S. Cox. 2008. Mycobacterium tuberculosis senses host-derived carbon monoxide during macrophage infection. *Cell Host Microbe* 3: 323–330.

46. Gengenbacher, M., and S. H. E. Kaufmann. 2012. Mycobacterium tuberculosis: success through dormancy. *FEMS Microbiol. Rev.* 36: 514–532.

47. Tavanaee Sani, A., H. Ashna, A. Kaffash, A. Khaledi, and K. Ghazvini. 2018. Mutations of rpob gene associated with rifampin resistance among Mycobacterium tuberculosis isolated in Tuberculosis Regional Reference Laboratory in northeast of Iran during 2015-2016. *Ethiop. J. Health Sci.* 28: 299–304.

48. Hazbón, M. H., M. Brimacombe, M. B. Del Valle, M. Cavatore, M. I. Guerrero, M. Varma-Basil, H. Billman-Jacobe, C. Lavender, J. Fyfe, L. García-García, C. I. León, M. Bose, F. Chaves, M. Murray, K. D. Eisenach, J. Sifuentes-Osornio, M. D. Cave, A. P. De León, and D. Alland. 2006. Population genetics study of isoniazid resistance mutations and evolution of multidrug-resistant Mycobacterium tuberculosis. *Antimicrob. Agents Chemother.* 50: 2640–2649.

49. Tweed, C. D., R. Dawson, D. A. Burger, A. Conradie, A. M. Crook, C. M. Mendel, F. Conradie, A. H. Diacon, N. E. Ntinginya, D. E. Everitt, F. Haraka, M. Li, C. H. van Niekerk, A. Okwera, M. S. Rassool, K. Reither, M. A. Sebe, S. Staples, E. Variava, and M. Spigelman. 2019. Bedaquiline, moxifloxacin, pretomanid, and pyrazinamide during the first 8 weeks of treatment of patients with drug-susceptible or drug-resistant pulmonary tuberculosis: a multicentre, open-label, partially randomised, phase 2b trial. *Lancet Respir. Med.* 7: 1048–1058.

50. Conradie, F., A. H. Diacon, N. Ngubane, P. Howell, D. Everitt, A. M. Crook, C. M.

Mendel, E. Egizi, J. Moreira, J. Timm, T. D. McHugh, G. H. Wills, A. Bateson, R. Hunt, C. Van Niekerk, M. Li, M. Olugbosi, and M. Spigelman. 2020. Treatment of highly drug-resistant pulmonary tuberculosis. *N. Engl. J. Med.* 382: 893–902.

51. Nguyen, T. V. A., R. M. Anthony, A. L. Bañuls, D. H. Vu, and J. W. C. Alffenaar. 2018. Bedaquiline resistance: its emergence, mechanism, and prevention. *Clin. Infect. Dis.* 66: 1625–1630.

52. Chun, R. F., J. S. Adams, and M. Hewison. 2011. Immunomodulation by vitamin D: implications for TB. *Expert Rev. Clin. Pharmacol.* 4: 583–591.

53. Young, C., G. Walzl, and N. Du Plessis. 2020. Therapeutic host-directed strategies to improve outcome in tuberculosis. *Mucosal Immunol.* 13: 190–204.

54. Liu, P. T., S. Stenger, D. H. Tang, and R. L. Modlin. 2007. Cutting edge: vitamin D-mediated human antimicrobial activity against Mycobacterium tuberculosis is dependent on the induction of cathelicidin. *J. Immunol.* 179: 2060–2063.

55. Fabri, M., S. Stenger, D. M. Shin, J. M. Yuk, P. T. Liu, S. Realegeno, H. M. Lee, S. R. Krutzik, M. Schenk, P. A. Sieling, R. Teles, D. Montoya, S. S. Iyer, H. Bruns, D. M. Lewinsohn, B. W. Hollis, M. Hewison, J. S. Adams, A. Steinmeyer, U. Zügel, G. Cheng, E. K. Jo, B. R. Bloom, and R. L. Modlin. 2011. Vitamin D is required for IFN-γ-mediated antimicrobial activity of human macrophages. *Sci. Transl. Med.* 3: 104ra102.

56. Yuk, J. M., D. M. Shin, H. M. Lee, C. S. Yang, H. S. Jin, K. K. Kim, Z. W. Lee, S. H. Lee, J. M. Kim, and E. K. Jo. 2009. Vitamin D3 induces autophagy in human monocytes/macrophages via cathelicidin. *Cell Host Microbe* 6: 231–243.

57. Salahuddin, N., F. Ali, Z. Hasan, N. Rao, M. Aqeel, and F. Mahmood. 2013. Vitamin D accelerates clinical recovery from tuberculosis: results of the SUCCINCT Study [Supplementary cholecalciferol in recovery from tuberculosis]. A randomized, placebo-controlled, clinical trial of vitamin D supplementation in patients with pulmonary tuberculosis'. *BMC Infect. Dis.* 13: 22.

58. Tukvadze, N., E. Sanikidze, M. Kipiani, G. Hebbar, K. A. Easley, N. Shenvi, R. R. Kempker, J. K. Frediani, V. Mirtskhulava, J. A. Alvarez, N. Lomtadze, L. Vashakidze, L. Hao, C. Del Rio, V. Tangpricha, H. M. Blumberg, and T. R. Ziegler. 2015. High-dose vitamin D3 in adults with pulmonary tuberculosis: a double-blind randomized controlled trial. *Am. J. Clin. Nutr.* 102: 1059–1069.

59. Wejse, C., V. F. Gomes, P. Rabna, P. Gustafson, P. Aaby, I. M. Lisse, P. L. Andersen, H. Glerup, and M. Sodemann. 2009. Vitamin D as supplementary treatment for tuberculosis: a double-blind, randomized, placebo-controlled trial. *Am. J. Respir. Crit. Care Med.* 179: 843–850.

60. Ehlers, S., and U. E. Schaible. 2012. The granuloma in tuberculosis: dynamics of a host-pathogen collusion. *Front. Immunol.* 3: 411.

61. Chakravarty, S. D., G. Zhu, M. C. Tsai, V. P. Mohan, S. Marino, D. E. Kirschner, L. Huang, J. A. Flynn, and J. Chan. 2008. Tumor necrosis factor blockade in chronic murine tuberculosis enhances granulomatous inflammation and disorganizes granulomas in the lungs. *Infect. Immun.* 76: 916–926.

62. Bourigault, M.-L., R. Vacher, S. Rose, M. L. Olleros, J.-P. Janssens, V. F. Quesniaux, and I. Garcia. 2013. Tumor necrosis factor neutralization combined with chemotherapy enhances Mycobacterium tuberculosis clearance and reduces lung pathology. *Am. J. Clin. Exp. Immunol.* 2: 124–34.

63. Wallis, R. S., P. Kyambadde, J. L. Johnson, L. Horter, R. Kittle, M. Pohle, C. Ducar, M. Millard, H. Mayanja-Kizza, C. Whalen, and A. Okwera. 2004. A study of the safety, immunology, virology, and microbiology of adjunctive etanercept in HIV-1-associated tuberculosis. *AIDS* 18: 257–264.

64. Maitra, A., S. D. S. Bates, M. Shaik, Di. Evangelopoulos, I. Abubakar, T. D. McHugh, M. Lipman, and S. Bhakta. 2016. Repurposing drugs for treatment of tuberculosis: a role for non-steroidal anti-inflammatory drugs. *Br. Med. Bull.* 118: 138–148.

65. Mai, N. T., N. Dobbs, N. H. Phu, R. A. Colas, L. T. Thao, N. T. Thuong, H. D. Nghia, N. H. Hanh, N. T. Hang, A. D. Heemskerk, J. N. Day, L. Ly, D. DA Thu, L. Merson, E. Kestelyn, M. Wolbers, R. Geskus, D. Summers, N. V. Chau, J. Dalli, and G. E. Thwaites. 2018. A randomised double blind placebo controlled phase 2 trial of adjunctive aspirin for tuberculous meningitis in HIV-uninfected adults. *Elife* 7: e33478.

66. Bruns, H., F. Stegelmann, M. Fabri, K. Döhner, G. van Zandbergen, M. Wagner, M. Skinner, R. L. Modlin, and S. Stenger. 2012. Abelson tyrosine kinase controls phagosomal acidification required for killing of Mycobacterium tuberculosis in human macrophages. *J. Immunol.* 189: 4069–4078.

67. Hawn, T. R., A. I. Matheson, S. N. Maley, and O. Vandal. 2013. Host-directed therapeutics for tuberculosis: can we harness the host? *Microbiol. Mol. Biol. Rev.* 77: 608–627.

68. Stancu, C., and A. Sima. 2001. Statins: mechanism of action and effects. *J. Cell. Mol. Med.* 5: 378–387.

69. Parihar, S. P., R. Guler, R. Khutlang, D. M. Lang, R. Hurdayal, M. M. Mhlanga, H. Suzuki, A. D. Marais, and F. Brombacher. 2014. Statin therapy reduces the Mycobacterium tuberculosis burden in human macrophages and in mice by enhancing autophagy and phagosome maturation. *J. Infect. Dis.* 209: 754–763.

70. Lobato, L. S., P. S. Rosa, J. Da Silva Ferreira, A. Da Silva Neumann, M. G. Da Silva, D. C. Nascimento, C. T. Soares, S. C. B. Pedrini, D. S. L. De Oliveira, C. P. Monteiro, G. M. B. Pereira, M. Ribeiro-Alves, M. A. Hacker, M. O. Moraes, M. C. V. Pessolani, R. S. Duarte, and F. A. Lara. 2014. Statins increase rifampin Mycobactericidal effect. *Antimicrob. Agents Chemother.* 58: 5766–5774.

71. Skerry, C., M. L. Pinn, N. Bruiners, R. Pine, M. L. Gennaro, and P. C. Karakousis. 2014. Simvastatin increases the in vivo activity of the first-line tuberculosis regimen. *J. Antimicrob. Chemother.* 69: 2453–2457.

72. Li, Y., Y. Wang, and X. Liu. 2012. The role of airway epithelial cells in response to mycobacteria infection. *Clin. Dev. Immunol.* 2012: 791392

73. Lin, Y., M. Zhang, and P. F. Barnes. 1998. Chemokine production by a human alveolar epithelial cell line in response to Mycobacterium tuberculosis. *Infect. Immun.* 66: 1121–1126.

74. Harriff, M. J., M. E. Cansler, K. G. Toren, E. T. Canfield, S. Kwak, M. C. Gold, and D. M. Lewinsohn. 2014. Human lung epithelial cells contain Mycobacterium tuberculosis in a late endosomal vacuole and are efficiently recognized by CD8+ T Cells. *PLoS One* 9: e97515.

75. Schlesinger, L. S. 1993. Macrophage phagocytosis of virulent but not attenuated strains of Mycobacterium tuberculosis is mediated by mannose receptors in addition to complement receptors. *J. Immunol.* 150: 2920–2930.

76. Astarie-Dequeker, C., E. N. N'Diaye, V. Le Cabec, M. G. Rittig, J. Prandi, and I. Maridonneau-Parini. 1999. The mannose receptor mediates uptake of pathogenic and nonpathogenic mycobacteria and bypasses bactericidal responses in human macrophages. *Infect. Immun.* 67: 469–477.

77. Kang, P. B., A. K. Azad, J. B. Torrelles, T. M. Kaufman, A. Beharka, E. Tibesar, L. E. DesJardin, and L. S. Schlesinger. 2005. The human macrophage mannose receptor directs Mycobacterium tuberculosis lipoarabinomannan-mediated phagosome biogenesis. *J. Exp. Med.* 202: 987–999.

78. Schlesinger, L., J. Torrelles, A. Azad, L. Henning, and T. Carlson. 2008. Role of c-type lectins in mycobacterial infections. *Curr. Drug Targets* 9: 102–112.

79. Armstrong, J. A., and P. D'Arcy Hart. 1975. Phagosome lysosome interactions in cultured macrophages infected with virulent tubercle bacilli. Reversal of the usual nonfusion pattern and observations on bacterial survival. *J. Exp. Med.* 142: 1–16.

80. Schlesinger, L. S., C. G. Bellinger-Kawahara, N. R. Payne, and M. A. Horwitz. 1990. Phagocytosis of Mycobacterium tuberculosis is mediated by human monocyte complement receptors and complement component C3. *J. Immunol.* 144: 2771–2780.

81. Ferguson, J. S., J. J. Weis, J. L. Martin, and L. S. Schlesinger. 2004. Complement protein C3 binding to Mycobacterium tuberculosis is initiated by the classical pathway in human bronchoalveolar lavage fluid. *Infect. Immun.* 72: 2564–2573.

82. Rooyakkers, A. W. J., and R. W. Stokes. 2005. Absence of complement receptor 3 results in reduced binding and ingestion of Mycobacterium tuberculosis but has no

significant effect on the induction of reactive oxygen and nitrogen intermediates or on the survival of the bacteria in resident and interferon-gamma activated macrophages. *Microb. Pathog.* 39: 57–67.

83. Zaffran, Y., L. Zhang, and J. J. Ellner. 1998. Role of CR4 in Mycobacterium tuberculosis-human macrophages binding and signal transduction in the absence of serum. *Infect. Immun.* 66: 4541–4544.

84. Hirsch, C. S., J. J. Ellner, D. G. Russell, and E. A. Rich. 1994. Complement receptor-mediated uptake and tumor necrosis factor-alpha-mediated growth inhibition of Mycobacterium tuberculosis by human alveolar macrophages. *J. Immunol.* 152: 743–753.

85. Schlesinger, L. S., A. K. Azad, J. B. Torrelles, E. Roberts, I. Vergne, and V. Deretic. 2017. Determinants of phagocytosis, phagosome biogenesis and autophagy for Mycobacterium tuberculosis. In *Handbook of Tuberculosis.* S. Kaufmann, E. Rubin, W. Britton, and P. van Helden, eds. Wiley-VCH Verlag GmbH & Co. KGaA, Weinheim, Germany. p. 1–22.

86. Sia, J. K., M. Georgieva, and J. Rengarajan. 2015. Innate immune defenses in human tuberculosis: an overview of the interactions between Mycobacterium tuberculosis and innate immune cells. *J. Immunol. Res.* 2015: 747543.

87. Wewers, M. D., S. I. Rennard, A. J. Hance, P. B. Bitterman, and R. G. Crystal. 1984. Normal human alveolar macrophages obtained by bronchoalveolar lavage have a limited capacity to release interleukin-1. *J. Clin. Invest.* 74: 2208–2218.

88. Lambrecht, B. N. 2006. Alveolar macrophage in the driver's seat. *Immunity* 24: 366–368.

89. Roth, M. D., and S. H. Golub. 1993. Human pulmonary macrophages utilize prostaglandins and transforming growth factor β_1 to suppress lymphocyte activation. *J. Leukoc. Biol.* 53: 366–371.

90. Guirado, E., L. S. Schlesinger, and G. Kaplan. 2013. Macrophages in tuberculosis: friend or foe. *Semin. Immunopathol.* 35: 563–583.

91. Cohen, S. B., B. H. Gern, J. L. Delahaye, K. N. Adams, C. R. Plumlee, J. K. Winkler, D. R. Sherman, M. Y. Gerner, and K. B. Urdahl. 2018. Alveolar macrophages provide an early Mycobacterium tuberculosis niche and initiate dissemination. *Cell Host Microbe* 24: 439-446.

92. Sadek, M. I., E. Sada, Z. Toossi, S. K. Schwander, and E. A. Rich. 1998. Chemokines induced by infection of mononuclear phagocytes with mycobacteria and present in lung alveoli during active pulmonary tuberculosis. *Am. J. Respir. Cell Mol. Biol.* 19: 513–521.

93. Eum, S. Y., J. H. Kong, M. S. Hong, Y. J. Lee, J. H. Kim, S. H. Hwang, S. N. Cho, L. E. Via, and C. E. Barry. 2010. Neutrophils are the predominant infected phagocytic cells in the

airways of patients with active pulmonary TB. *Chest* 137: 122–128.

94. Martineau, A. R., S. M. Newton, K. A. Wilkinson, B. Kampmann, B. M. Hall, N. Nawroly, G. E. Packe, R. N. Davidson, C. J. Griffiths, and R. J. Wilkinson. 2007. Neutrophil-mediated innate immune resistance to mycobacteria. *J. Clin. Invest.* 117: 1988–1994.

95. Ong, C. W. M., P. T. Elkington, S. Brilha, C. Ugarte-Gil, M. T. Tome-Esteban, L. B. Tezera, P. J. Pabisiak, R. C. Moores, T. Sathyamoorthy, V. Patel, R. H. Gilman, J. C. Porter, and J. S. Friedland. 2015. Neutrophil-derived MMP-8 drives AMPK-dependent matrix destruction in human pulmonary tuberculosis. *PLoS Pathog.* 11: e1004917.

96. Elkington, P. T. G., and J. S. Friedland. 2006. Matrix metalloproteinases in destructive pulmonary pathology. *Thorax* 61: 259–266.

97. Esin, S., C. Counoupas, A. Aulicino, F. L. Brancatisano, G. Maisetta, D. Bottai, M. Di Luca, W. Florio, M. Campa, and G. Batoni. 2013. Interaction of Mycobacterium tuberculosis cell wall components with the human natural killer cell receptors NKp44 and toll-like receptor 2. *Scand. J. Immunol.* 77: 460–469.

98. Liu, C. H., H. Liu, and B. Ge. 2017. Innate immunity in tuberculosis: host defense vs pathogen evasion. *Cell. Mol. Immunol.* 14: 963–975.

99. Vankayalapati, R., B. Wizel, S. E. Weis, H. Safi, D. L. Lakey, O. Mandelboim, B. Samten, A. Porgador, and P. F. Barnes. 2002. The NKp46 receptor contributes to NK cell lysis of mononuclear phagocytes infected with an intracellular bacterium. *J. Immunol.* 168: 3451–3457.

100. Carson, W. E., M. E. Ross, R. A. Baiocchi, M. J. Marien, N. Boiani, K. Grabstein, and M. A. Caligiuri. 1995. Endogenous production of interleukin 15 by activated human monocytes is critical for optimal production of interferon-γ by natural killer cells in vitro. *J. Clin. Invest.* 96: 2578–2582.

101. Dhiman, R., M. Indramohan, P. F. Barnes, R. C. Nayak, P. Paidipally, L. V. M. Rao, and R. Vankayalapati. 2009. IL-22 produced by human NK cells inhibits growth of Mycobacterium tuberculosis by enhancing phagolysosomal fusion. *J. Immunol.* 183: 6639–6645.

102. Serbina, N. V., and E. G. Pamer. 2006. Monocyte emigration from bone marrow during bacterial infection requires signals mediated by chemokine receptor CCR2. *Nat. Immunol.* 7: 311–317.

103. Sköld, M., and S. M. Behar. 2008. Tuberculosis triggers a tissue-dependent program of differentiation and acquisition of effector functions by circulating monocytes. *J. Immunol.* 181: 6349–6360.

104. Mayer-Barber, K. D., B. B. Andrade, D. L. Barber, S. Hieny, C. G. Feng, P. Caspar, S.

Oland, S. Gordon, and A. Sher. 2011. Innate and adaptive interferons suppress IL-1α and IL-1β production by distinct pulmonary myeloid subsets during Mycobacterium tuberculosis infection. *Immunity* 35: 1023–1034.

105. Cambier, C. J., S. M. O'Leary, M. P. O'Sullivan, J. Keane, and L. Ramakrishnan. 2017. Phenolic glycolipid facilitates mycobacterial escape from microbicidal tissue-resident macrophages. *Immunity* 47: 552-565.

106. Wolf, A. J., L. Desvignes, B. Linas, N. Banaiee, T. Tamura, K. Takatsu, and J. D. Ernst. 2008. Initiation of the adaptive immune response to Mycobacterium tuberculosis depends on antigen production in the local lymph node, not the lungs. *J. Exp. Med.* 205: 105–115.

107. Balboa, L., M. M. Romero, N. Yokobori, P. Schierloh, L. Geffner, J. I. Basile, R. M. Musella, E. Abbate, S. De La Barrera, M. C. Sasiain, and M. Alemán. 2010. Mycobacterium tuberculosis impairs dendritic cell response by altering CD1b, DC-SIGN and MR profile. *Immunol. Cell Biol.* 88: 716–726.

108. Wolf, A. J., B. Linas, G. J. Trevejo-Nuñez, E. Kincaid, T. Tamura, K. Takatsu, and J. D. Ernst. 2007. Mycobacterium tuberculosis infects dendritic cells with high frequency and impairs their function in vivo. *J. Immunol.* 179: 2509–2519.

109. Tallieux, L., O. Schwartz, J. L. Herrmann, E. Pivert, M. Jackson, A. Amara, L. Legres, D. Dreher, L. P. Nicod, J. C. Gluckman, P. H. Lagrange, B. Gicquel, and O. Neyrolles. 2003. DC-SIGN is the major Mycobacterium tuberculosis receptor on human dendritic cells. *J. Exp. Med.* 197: 121–127.

110. Monin, L., and S. A. Khader. 2014. Chemokines in tuberculosis: The good, the bad and the ugly. *Semin. Immunol.* 26: 552–558.

111. Olmos, S., S. Stukes, and J. D. Ernst. 2010. Ectopic activation of Mycobacterium tuberculosis-specific CD4 + T cells in lungs of CCR7 − / − mice. *J. Immunol.* 184: 895–901.

112. Samstein, M., H. A. Schreiber, I. M. Leiner, B. Sušac, M. S. Glickman, and E. G. Pamer. 2013. Essential yet limited role for CCR2+ inflammatory monocytes during Mycobacterium tuberculosis-specific T cell priming. *Elife* 2: e01086.

113. Srivastava, S., and J. D. Ernst. 2014. Cell-to-cell transfer of M. tuberculosis antigens optimizes CD4 T cell priming. *Cell Host Microbe* 15: 741–752.

114. Barber-Mayer, K. D., and D. L. Barber. 2015. Innate and adaptive cellular immune responses to Mycobacterium tuberculosis infection. *Cold Spring Harb. Perspect. Med.* 5: a018424.

115. Walker, N. F., G. Meintjes, and R. J. Wilkinson. 2013. HIV-1 and the immune response to TB. *Future Virol.* 8: 57–80.

116. Kursar, M., K. Bonhagen, A. Köhler, T. Kamradt, S. H. E. Kaufmann, and H.-W. Mittrücker. 2002. Organ-specific CD4 + T cell response during Listeria monocytogenes infection. *J. Immunol.* 168: 6382–6387.

117. Winslow, G. M., A. Cooper, W. Reiley, M. Chatterjee, and D. L. Woodland. 2008. Early T-cell responses in tuberculosis immunity. *Immunol. Rev.* 225: 284–299.

118. Sia, J. K., and J. Rengarajan. 2019. Immunology of Mycobacterium tuberculosis infections. *Microbiol. Spectr.* 7: 10.1128.

119. Flynn, J. A. L., J. Chan, K. J. Triebold, D. K. Dalton, T. A. Stewart, and B. R. Bloom. 1993. An essential role for interferon γ in resistance to Mycobacterium tuberculosis infection. *J. Exp. Med.* 178: 2249–2254.

120. Jung, J. Y., R. Madan-Lala, M. Georgieva, J. Rengarajan, C. D. Sohaskey, F. C. Bange, and C. M. Robinson. 2013. The intracellular environment of human macrophages that produce nitric oxide promotes growth of mycobacteria. *Infect. Immun.* 81: 3198–3209.

121. Newport, M. J., C. M. Huxley, S. Huston, C. M. Hawrylowicz, B. A. Oostra, R. Williamson, and M. Levin. 1996. A mutation in the interferon-γ –receptor gene and susceptibility to mycobacterial infection. *N. Engl. J. Med.* 335: 1941–1949.

122. Gutierrez, M. G., S. S. Master, S. B. Singh, G. A. Taylor, M. I. Colombo, and V. Deretic. 2004. Autophagy is a defense mechanism inhibiting BCG and Mycobacterium tuberculosis survival in infected macrophages. *Cell* 119: 753–766.

123. Herbst, S., U. E. Schaible, and B. E. Schneider. 2011. Interferon gamma activated macrophages kill mycobacteria by nitric oxide induced apoptosis. *PLoS One* 6: e19105.

124. Chamie, G., A. Luetkemeyer, M. Walusimbi-Nanteza, A. Okwera, C. C. Whalen, R. D. Mugerwa, D. V. Havlir, and E. D. Charlebois. 2010. Significant variation in presentation of pulmonary tuberculosis across a high resolution of CD4 strata. *Int. J. Tuberc. Lung Dis.* 14: 1295–1302.

125. Rodrigo, T., J. Caylà, P. García de Olalla, H. Galdós-Tangüis, J. Jansà, P. Miranda, and T. Brugal. 1997. Characteristics of tuberculosis patients who generate secondary cases. *Int. J. Tuberc. Lung Dis.* 1: 352–357.

126. Ramachandra, L., E. Noss, W. H. Boom, and C. V. Harding. 2001. Processing of Mycobacterium tuberculosis antigen 85B involves intraphagosomal formation of peptide-major histocompatibility complex II complexes and is inhibited by live bacilli that decrease phagosome maturation. *J. Exp. Med.* 194: 1421–1432.

127. Stenger, S., R. J. Mazzaccaro, K. Uyemura, S. Cho, P. F. Barnes, J. P. Rosat, A. Sette, M. B. Brenner, S. A. Porcelli, B. R. Bloom, and R. L. Modlin. 1997. Differential effects of cytolytic T cell subsets on intracellular infection. *Science* 276: 1684–1687.

128. Lyashchenko, K., R. Colangeli, M. Houde, H. Al Jahdali, D. Menzies, and M. L. Gennaro. 1998. Heterogeneous antibody responses in tuberculosis. *Infect. Immun.* 66: 3936–3940.

129. Achkar, J. M., J. Chan, and A. Casadevall. 2015. B cells and antibodies in the defense against Mycobacterium tuberculosis infection. *Immunol. Rev.* 264: 167–181.

130. Maglione, P. J., J. Xu, and J. Chan. 2007. B cells moderate inflammatory progression and enhance bacterial containment upon pulmonary challenge with Mycobacterium tuberculosis. *J. Immunol.* 178: 7222–7234.

131. Bénard, A., I. Sakwa, P. Schierloh, A. Colom, I. Mercier, L. Tailleux, L. Jouneau, P. Boudinot, T. Al-Saati, R. Lang, J. Rehwinkel, A. G. Loxton, S. H. E. Kaufmann, V. Anton-Leberre, A. O'Garra, M. Del Carmen Sasiain, B. Gicquel, S. Fillatreau, O. Neyrolles, and D. Hudrisier. 2018. B cells producing type I IFN modulate macrophage polarization in tuberculosis. *Am. J. Respir. Crit. Care Med.* 197: 801–813.

132. Saunders, B. M., and A. M. Cooper. 2000. Restraining mycobacteria: role of granulomas in mycobacterial infections. *Immunol. Cell Biol.* 78: 334–341.

133. Kaneko, H., H. Yamada, S. Mizuno, T. Udagawa, Y. Kazumi, K. Sekikawa, and I. Sugawara. 1999. Role of tumor necrosis factor-α in Mycobacterium-induced granuloma formation in tumor necrosis factor-α-deficient mice. *Lab. Investig.* 79: 379–386.

134. Cooper, A. M., A. D. Roberts, E. R. Rhoades, J. E. Callahan, D. M. Getzy, and I. M. Orme. 1995. The role of interleukin-12 in acquired immunity to Mycobacterium tuberculosis infection. *Immunology* 84: 423–32.

135. Flynn, J. L., H. P. Gideon, J. T. Mattila, and P. ling Lin. 2015. Immunology studies in non-human primate models of tuberculosis. *Immunol. Rev.* 264: 60–73.

136. Gideon, H. P., and J. L. Flynn. 2011. Latent tuberculosis: what the host "sees"? *Immunol. Res.* 50: 202–212.

137. Lin, P. L., S. Pawar, A. Myers, A. Pegu, C. Fuhrman, T. A. Reinhart, S. V. Capuano, E. Klein, and J. A. L. Flynn. 2006. Early events in Mycobacterium tuberculosis infection in cynomolgus macaques. *Infect. Immun.* 74: 3790–3803.

138. Lin, P. L., M. Rodgers, L. Smith, M. Bigbee, A. Myers, C. Bigbee, I. Chiosea, S. V. Capuano, C. Fuhrman, E. Klein, and J. A. L. Flynn. 2009. Quantitative comparison of active and latent tuberculosis in the cynomolgus macaque model. *Infect. Immun.* 77: 4631–4642.

139. Lin, P. L., C. B. Ford, M. T. Coleman, A. J. Myers, R. Gawande, T. Ioerger, J. Sacchettini, S. M. Fortune, and J. L. Flynn. 2014. Sterilization of granulomas is common in active and latent tuberculosis despite within-host variability in bacterial killing. *Nat. Med.* 20: 75–79.

140. Driver, E. R., G. J. Ryan, D. R. Hoff, S. M. Irwin, R. J. Basaraba, I. Kramnik, and A. J. Lenaerts. 2012. Evaluation of a mouse model of necrotic granuloma formation using C3HeB/FeJ mice for testing of drugs against Mycobacterium tuberculosis. *Antimicrob. Agents Chemother.* 56: 3181–3195.

141. Basu, J., D. M. Shin, and E. K. Jo. 2012. Mycobacterial signaling through toll-like receptors. *Front. Cell. Infect. Microbiol.* 2: 145.

142. Wu, S., X. Liu, L. Chen, Y. Wang, M. Zhang, M. Wang, and J. Q. He. 2020. Polymorphisms of TLR2, TLR4 and TOLLIP and tuberculosis in two independent studies. *Biosci. Rep.* 40: 20193141.

143. Fremond, C. M. C., D. M. M. Nicolle, D. S. Torres, and V. F. J. Quesniaux. 2003. Control of Mycobacterium bovis BCG infection with increased inflammation in TLR4-deficient mice. *Microbes Infect.* 5: 1070–1081.

144. Kawai, T., and S. Akira. 2010. The role of pattern-recognition receptors in innate immunity: update on toll-like receptors. *Nat. Immunol.* 11: 373–384.

145. Keane, J., M. K. Balcewicz-Sablinska, H. G. Remold, G. L. Chupp, B. B. Meek, M. J. Fenton, and H. Kornfeld. 1997. Infection by Mycobacterium tuberculosis promotes human alveolar macrophage apoptosis. *Infect. Immun.* 65: 298–304.

146. Parameswaran, N., and S. Patial. 2010. Tumor necrosis factor-α signaling in macrophages. *Crit. Rev. Eukaryot. Gene Expr.* 20: 87–103.

147. Flynn, J. A. L., M. M. Goldstein, J. Chan, K. J. Triebold, K. Pfeffer, C. J. Lowenstein, R. Schrelber, T. W. Mak, and B. R. Bloom. 1995. Tumor necrosis factor-α is required in the protective immune response against mycobacterium tuberculosis in mice. *Immunity* 2: 561–572.

148. Keane, J., S. Gershon, R. P. Wise, E. Mirabile-Levens, J. Kasznica, W. D. Schwieterman, J. N. Siegel, and M. M. Braun. 2001. Tuberculosis associated with infliximab, a tumor necrosis factor α-neutralizing agent. *N. Engl. J. Med.* 345: 1098–1104.

149. Abu Shaikha, S., K. Mansour, and H. Riad. 2012. Reactivation of tuberculosis in three cases of psoriasis after initiation of anti-TNF therapy. *Case Rep. Dermatol.* 4: 41–46.

150. Cooper, A. M., J. Magram, J. Ferrante, and I. M. Orme. 1997. Interleukin 12 (IL-12) is crucial to the development of protective immunity in mice intravenously infected with Mycobacterium tuberculosis. *J. Exp. Med.* 186: 39–45.

151. Pompei, L., S. Jang, B. Zamlynny, S. Ravikumar, A. McBride, S. P. Hickman, and P. Salgame. 2007. Disparity in IL-12 release in dendritic cells and macrophages in response to Mycobacterium tuberculosis is due to use of distinct TLRs. *J. Immunol.* 178: 5192–5199.

152. Giacomini, E., E. Iona, L. Ferroni, M. Miettinen, L. Fattorini, G. Orefici, I. Julkunen,

and E. M. Coccia. 2001. Infection of human macrophages and dendritic cells with Mycobacterium tuberculosis induces a differential cytokine gene expression that modulates T cell response. *J. Immunol.* 166: 7033–7041.

153. Sugawara, I., H. Yamada, H. Kaneko, S. Mizuno, K. Takeda, and S. Akira. 1999. Role of interleukin-18 (IL-18) in mycobacterial infection in IL-18- gene-disrupted mice. *Infect. Immun.* 67: 2585–2589.

154. Schneider, B. E., D. Korbel, K. Hagens, M. Koch, B. Raupach, J. Enders, S. H. E. Kaufmann, H. W. Mittrücker, and U. E. Schaible. 2010. A role for IL-18 in protective immunity against Mycobacterium tuberculosis. *Eur. J. Immunol.* 40: 396–405.

155. Kinjo, Y., K. Kawakami, K. Uezu, S. Yara, K. Miyagi, Y. Koguchi, T. Hoshino, M. Okamoto, Y. Kawase, K. Yokota, K. Yoshino, K. Takeda, S. Akira, and A. Saito. 2002. Contribution of IL-18 to Th1 response and host defense against infection by Mycobacterium tuberculosis: a comparative study with IL-12p40. *J. Immunol.* 169: 323–329.

156. Sologuren, I., S. Boisson-Dupuis, J. Pestano, Q. B. Vincent, L. Fernández-Pérez, A. Chapgier, M. Cárdenes, J. Feinberg, M. I. García-Laorden, C. Picard, E. Santiago, X. Kong, L. Jannière, E. Colino, E. Herrera-Ramos, A. Francés, C. Navarrete, S. Blanche, E. Faria, P. Remiszewski, A. Cordeiro, A. Freeman, S. Holland, K. Abarca, M. Valerón-Lemaur, J. Gonçalo-Marques, L. Silveira, J. M. García-Castellano, J. Caminero, J. L. Pérez-Arellano, J. L. A. Bustamante, L. Abel, J. L. Casanova, and C. Rodríguez-Gallego. 2011. Partial recessive IFN-γR1 deficiency: genetic, immunological and clinical features of 14 patients from 11 kindreds. *Hum. Mol. Genet.* 20: 1509–1523.

157. Mayer-Barber, K. D., D. L. Barber, K. Shenderov, S. D. White, M. S. Wilson, A. Cheever, D. Kugler, S. Hieny, P. Caspar, G. Núñez, D. Schlueter, R. A. Flavell, F. S. Sutterwala, and A. Sher. 2010. Cutting edge: caspase-1 independent IL-1β production is critical for host resistance to Mycobacterium tuberculosis and does not require TLR signaling in vivo. *J. Immunol.* 184: 3326–3330.

158. Domingo-Gonzalez, R., O. Prince, A. Cooper, and S. A. Khader. 2016. Cytokines and chemokines in Mycobacterium tuberculosis infection. *Microbiol. Spectr.* 4.

159. Ladel, C. H., C. Blum, A. Dreher, K. Reifenberg, M. Kopf, and S. H. E. Kaufmann. 1997. Lethal tuberculosis in interleukin-6-deficient mutant mice. *Infect. Immun.* 65: 4843–4849.

160. Nagabhushanam, V., A. Solache, L.-M. Ting, C. J. Escaron, J. Y. Zhang, and J. D. Ernst. 2003. Innate inhibition of adaptive immunity: Mycobacterium tuberculosis-induced IL-6 inhibits macrophage responses to IFNγ. *J. Immunol.* 171: 4750–4757.

161. Dutta, R. K., M. Kathania, M. Raje, and S. Majumdar. 2012. IL-6 inhibits IFN-γ induced autophagy in Mycobacterium tuberculosis H37Rv infected macrophages. *Int. J. Biochem. Cell Biol.* 44: 942–954.

162. Fiorentino, D. F., A. Zlotnik, P. Vieira, T. R. Mosmann, M. Howard, K. W. Moore, and A. O'Garra. 1991. IL-10 acts on the antigen-presenting cell to inhibit cytokine production by Th1 cells. *J. Immunol.* 146.

163. Redford, P. S., P. J. Murray, and A. O'Garra. 2011. The role of IL-10 in immune regulation during M. tuberculosis infection. *Mucosal Immunol.* 4: 261–270.

164. Duan, L., M. Yi, J. Chen, S. Li, and W. Chen. 2016. Mycobacterium tuberculosis EIS gene inhibits macrophage autophagy through up-regulation of IL-10 by increasing the acetylation of histone H3. *Biochem. Biophys. Res. Commun.* 473: 1229–1234.

165. O'Leary, S., M. P. O'Sullivan, and J. Keane. 2011. IL-10 blocks phagosome maturation in Mycobacterium tuberculosis-infected human macrophages. *Am. J. Respir. Cell Mol. Biol.* 45: 172–180.

166. Hirsch, C. S., J. J. Ellner, R. Blinkhorn, and Z. Toossi. 1997. In vitro restoration of T cell responses in tuberculosis and augmentation of monocyte effector function against Mycobacterium tuberculosis by natural inhibitors of transforming growth factor β. *Proc. Natl. Acad. Sci. U. S. A.* 94: 3926–3931.

167. Othieno, C., C. S. Hirsch, B. D. Hamilton, K. Wilkinson, J. J. Ellner, and Z. Toossi. 1999. Interaction of Mycobacterium tuberculosis-induced transforming growth factor β1 and interleukin-10. *Infect. Immun.* 67: 5730–5735.

168. Mindell, J. A. 2012. Lysosomal acidification mechanisms. *Annu. Rev. Physiol.* 74: 69–86.

169. Yates, R. M., A. Hermetter, and D. G. Russell. 2005. The kinetics of phagosome maturation as a function of phagosome/lysosome fusion and acquisition of hydrolytic activity. *Traffic* 6: 413–420.

170. Nunes, P., N. Demaurex, and M. C. Dinauer. 2013. Regulation of the NADPH oxidase and associated ion fluxes during phagocytosis. *Traffic* 14: 1118–1131.

171. Köster, S., S. Upadhyay, P. Chandra, K. Papavinasasundaram, G. Yang, A. Hassan, S. J. Grigsby, E. Mittal, H. S. Park, V. Jones, F. F. Hsu, M. Jackson, C. M. Sassetti, and J. A. Philips. 2017. Mycobacterium tuberculosis is protected from NADPH oxidase and LC3-associated phagocytosis by the LCP protein CpsA. *Proc. Natl. Acad. Sci. U. S. A.* 114: E8711–E8720.

172. Sun, J., V. Singh, A. Lau, R. W. Stokes, A. Obregón-Henao, I. M. Orme, D. Wong, Y. Av-Gay, and Z. Hmama. 2013. Mycobacterium tuberculosis nucleoside diphosphate kinase inactivates small GTPases leading to evasion of innate immunity. *PLoS Pathog.* 9: e1003499.

173. Piddington, D. L., F. C. Fang, T. Laessig, A. M. Cooper, I. M. Orme, and N. A. Buchmeier. 2001. Cu,Zn superoxide dismutase of Mycobacterium tuberculosis contributes

to survival in activated macrophages that are generating an oxidative burst. *Infect. Immun.* 69: 4980–4987.

174. Ng, V. H., J. S. Cox, A. O. Sousa, J. D. MacMicking, and J. D. McKinney. 2004. Role of KatG catalase-peroxidase in mycobacterial pathogenisis: countering the phagocyte oxidative burst. *Mol. Microbiol.* 52: 1291–1302.

175. Deffert, C., J. Cachat, and K. H. Krause. 2014. Phagocyte NADPH oxidase, chronic granulomatous disease and mycobacterial infections. *Cell. Microbiol.* 16: 1168–1178.

176. Fratti, R. A., J. Chua, I. Vergne, and V. Deretic. 2003. Mycobacterium tuberculosis glycosylated phosphatidylinositol causes phagosome maturation arrest. *Proc. Natl. Acad. Sci. U. S. A.* 100: 5437–5442.

177. Vergne, I., J. Chua, H. H. Lee, M. Lucas, J. Belisle, and V. Deretic. 2005. Mechanism of phagolysosome biogenesis block by viable Mycobacterium tuberculosis. *Proc. Natl. Acad. Sci. U. S. A.* 102: 4033–4038.

178. Sun, J., X. Wang, A. Lau, T.-Y. A. Liao, C. Bucci, and Z. Hmama. 2010. Mycobacterial nucleoside diphosphate kinase blocks phagosome maturation in murine Raw 264.7 macrophages. *PLoS One* 5: e8769.

179. Vergne, I., R. A. Fratti, P. J. Hill, J. Chua, J. Belisle, and V. Deretic. 2004. Mycobacterium tuberculosis phagosome maturation arrest: mycobacterial phosphatidylinositol analog phosphatidylinositol mannoside stimulates early endosomal fusion. *Mol. Biol. Cell* 15: 751–760.

180. Mehra, A., A. Zahra, V. Thompson, N. Sirisaengtaksin, A. Wells, M. Porto, S. Köster, K. Penberthy, Y. Kubota, A. Dricot, D. Rogan, M. Vidal, D. E. Hill, A. J. Bean, and J. A. Philips. 2013. Mycobacterium tuberculosis type VII secreted effector EsxH targets host ESCRT to impair trafficking. *PLoS Pathog.* 9: e1003734.

181. Portal-Celhay, C., J. M. Tufariello, S. Srivastava, A. Zahra, T. Klevorn, P. S. Grace, A. Mehra, H. S. Park, J. D. Ernst, W. R. Jacobs, and J. A. Philips. 2016. Mycobacterium tuberculosis EsxH inhibits ESCRT-dependent CD4+ T-cell activation. *Nat. Microbiol.* 2: 16232.

182. Toei, M., R. Saum, and M. Forgac. 2010. Regulation and isoform function of the V-ATPases. *Biochemistry* 49: 4715–4723.

183. Wong, D., H. Bach, J. Sun, Z. Hmama, and Y. Av-Gay. 2011. Mycobacterium tuberculosis protein tyrosine phosphatase (PtpA) excludes host vacuolar-H +-ATPase to inhibit phagosome acidification. *Proc. Natl. Acad. Sci. U. S. A.* 108: 19371–19376.

184. Bach, H., K. G. Papavinasasundaram, D. Wong, Z. Hmama, and Y. Av-Gay. 2008. Mycobacterium tuberculosis virulence is mediated by PtpA dephosphorylation of human vacuolar protein sorting 33B. *Cell Host Microbe* 3: 316–322.

185. van der Wel, N., D. Hava, D. Houben, D. Fluitsma, M. van Zon, J. Pierson, M. Brenner, and P. J. Peters. 2007. M. tuberculosis and M. leprae translocate from the phagolysosome to the cytosol in myeloid cells. *Cell* 129: 1287–1298.

186. Simeone, R., A. Bobard, J. Lippmann, W. Bitter, L. Majlessi, R. Brosch, and J. Enninga. 2012. Phagosomal rupture by Mycobacterium tuberculosis results in toxicity and host cell death. *PLoS Pathog.* 8: e1002507.

187. Houben, D., C. Demangel, J. van Ingen, J. Perez, L. Baldeón, A. M. Abdallah, L. Caleechurn, D. Bottai, M. van Zon, K. de Punder, T. van der Laan, A. Kant, R. Bossers-de Vries, P. Willemsen, W. Bitter, D. van Soolingen, R. Brosch, N. van der Wel, and P. J. Peters. 2012. ESX-1-mediated translocation to the cytosol controls virulence of mycobacteria. *Cell. Microbiol.* 14: 1287–1298.

188. Conrad, W. H., M. M. Osman, J. K. Shanahan, F. Chu, K. K. Takaki, J. Cameron, D. Hopkinson-Woolley, R. Brosch, and L. Ramakrishnan. 2017. Mycobacterial ESX-1 secretion system mediates host cell lysis through bacterium contact-dependent gross membrane disruptions. *Proc. Natl. Acad. Sci. U. S. A.* 114: 1371–1376.

189. Gao, L. Y., S. Guo, B. McLaughlin, H. Morisaki, J. N. Engel, and E. J. Brown. 2004. A mycobacterial virulence gene cluster extending RD1 is required for cytolysis, bacterial spreading and ESAT-6 secretion. *Mol. Microbiol.* 53: 1677–1693.

190. Manzanillo, P. S., M. U. Shiloh, D. A. Portnoy, and J. S. Cox. 2012. Mycobacterium tuberculosis activates the DNA-dependent cytosolic surveillance pathway within macrophages. *Cell Host Microbe* 11: 469–480.

191. Sun, L., J. Wu, F. Du, X. Chen, and Z. J. Chen. 2013. Cyclic GMP-AMP synthase is a cytosolic DNA sensor that activates the type I interferon pathway. *Science* 339: 786–791.

192. Stanley, S. A., J. E. Johndrow, P. Manzanillo, and J. S. Cox. 2007. The type I IFN response to infection with Mycobacterium tuberculosis requires ESX-1-mediated secretion and contributes to pathogenesis. *J. Immunol.* 178: 3143–3152.

193. Watson, R. O., P. S. Manzanillo, and J. S. Cox. 2012. Extracellular M. tuberculosis DNA targets bacteria for autophagy by activating the host DNA-sensing pathway. *Cell* 150: 803–815.

194. Watson, R. O., S. L. Bell, D. A. MacDuff, J. M. Kimmey, E. J. Diner, J. Olivas, R. E. Vance, C. L. Stallings, H. W. Virgin, and J. S. Cox. 2015. The cytosolic sensor cGAS detects Mycobacterium tuberculosis DNA to induce type I interferons and activate autophagy. *Cell Host Microbe* 17: 811–819.

195. Nakagawa, I., A. Amano, N. Mizushima, A. Yamamoto, H. Yamaguchi, T. Kamimoto, A. Nara, J. Funao, M. Nakata, K. Tsuda, S. Hamada, and T. Yoshimori. 2004. Autophagy defends cells against invading group A Streptococcus. *Science* 306: 1037–1040.

196. Gatica, D., V. Lahiri, and D. J. Klionsky. 2018. Cargo recognition and degradation by selective autophagy. *Nat. Cell Biol.* 20: 233–242.

197. Kirkin, V., D. G. McEwan, I. Novak, and I. Dikic. 2009. A role for ubiquitin in selective autophagy. *Mol. Cell* 34: 259–269.

198. Franco, L. H., V. R. Nair, C. R. Scharn, R. J. Xavier, J. R. Torrealba, M. U. Shiloh, and B. Levine. 2017. The ubiquitin ligase Smurf1 functions in selective autophagy of Mycobacterium tuberculosis and anti-tuberculous host defense. *Cell Host Microbe* 21: 59–72.

199. Manzanillo, P. S., J. S. Ayres, R. O. Watson, A. C. Collins, G. Souza, C. S. Rae, D. S. Schneider, K. Nakamura, M. U. Shiloh, and J. S. Cox. 2013. The ubiquitin ligase parkin mediates resistance to intracellular pathogens. *Nature* 501: 512–516.

200. Tanida, I., T. Ueno, and E. Kominami. 2004. Human light chain 3/MAP1LC3B is cleaved at its carboxyl-terminal Met 121 to expose Gly120 for lipidation and targeting to autophagosomal membranes. *J. Biol. Chem.* 279: 47704–47710.

201. Hanada, T., N. N. Noda, Y. Satomi, Y. Ichimura, Y. Fujioka, T. Takao, F. Inagaki, and Y. Ohsumi. 2007. The Atg12-Atg5 conjugate has a novel E3-like activity for protein lipidation in autophagy. *J. Biol. Chem.* 282: 37298–37302.

202. Tanaka, Y., G. Guhde, A. Suter, E. L. Eskelinen, D. Hartmann, R. Lüllmann-Rauch, P. M. L. Janssen, J. Blanz, K. Von Figura, and P. Saftig. 2000. Accumulation of autophagic vacuoles and cardiomyopathy LAMP-2-deficient mice. *Nature* 406: 902–906.

203. Jäger, S., C. Bucci, I. Tanida, T. Ueno, E. Kominami, P. Saftig, and E. L. Eskelinen. 2004. Role for Rab7 in maturation of late autophagic vacuoles. *J. Cell Sci.* 117: 4837–4848.

204. Gwinn, D. M., D. B. Shackelford, D. F. Egan, M. M. Mihaylova, A. Mery, D. S. Vasquez, B. E. Turk, and R. J. Shaw. 2008. AMPK phosphorylation of raptor mediates a metabolic checkpoint. *Mol. Cell* 30: 214–226.

205. Inoki, K., T. Zhu, and K. L. Guan. 2003. TSC2 mediates cellular energy response to control cell growth and survival. *Cell* 115: 577–590.

206. Kim, J., M. Kundu, B. Viollet, and K. L. Guan. 2011. AMPK and mTOR regulate autophagy through direct phosphorylation of Ulk1. *Nat. Cell Biol.* 13: 132–141.

207. Wei, Y., S. Sinha, and B. Levine. 2008. Dual role of JNK1-mediated phosphorylation of Bcl-2 in autophagy and apoptosis regulation. *Autophagy* 4: 949–951.

208. Wei, Y., S. Pattingre, S. Sinha, M. Bassik, and B. Levine. 2008. JNK1-mediated phosphorylation of Bcl-2 regulates starvation-induced autophagy. *Mol. Cell* 30: 678–688.

209. Wei, Y., Z. An, Z. Zou, R. Sumpter, M. Su, X. Zang, S. Sinha, M. Gaestel, and B.

Levine. 2015. The stress-responsive kinases MAPKAPK2/MAPKAPK3 activate starvation-induced autophagy through Beclin 1 phosphorylation. *Elife* 4: e05289.

210. Saini, N. K., A. Baena, T. W. Ng, M. M. Venkataswamy, S. C. Kennedy, S. Kunnath-Velayudhan, L. J. Carreño, J. Xu, J. Chan, M. H. Larsen, W. R. Jacobs, and S. A. Porcelli. 2016. Suppression of autophagy and antigen presentation by Mycobacterium tuberculosis PE-PGRS47. *Nat. Microbiol.* 1: 16133.

211. Shin, D. M., B. Y. Jeon, H. M. Lee, H. S. Jin, J. M. Yuk, C. H. Song, S. H. Lee, Z. W. Lee, S. N. Cho, J. M. Kim, R. L. Friedman, and E. K. Jo. 2010. Mycobacterium tuberculosis eis regulates autophagy, inflammation, and cell death through redox-dependent signaling. *PLoS Pathog.* 6: e1001230.

212. Kim, K. H., D. R. An, J. Song, J. Y. Yoon, H. S. Kim, H. J. Yoon, H. N. Im, J. Kim, D. J. Kim, S. J. Lee, K. H. Kim, H. M. Lee, H. J. Kim, E. K. Jo, J. Y. Lee, and S. W. Suh. 2012. Mycobacterium tuberculosis Eis protein initiates suppression of host immune responses by acetylation of DUSP16/MKP-7. *Proc. Natl. Acad. Sci. U. S. A.* 109: 7729–7734.

213. Chandra, P., S. Ghanwat, S. K. Matta, S. S. Yadav, M. Mehta, Z. Siddiqui, A. Singh, and D. Kumar. 2015. Mycobacterium tuberculosis inhibits RAB7 recruitment to selectively modulate autophagy flux in macrophages. *Sci. Rep.* 5: 1–10.

214. Shui, W., C. J. Petzold, A. Redding, J. Liu, A. Pitcher, L. Sheu, T. Y. Hsieh, J. D. Keasling, and C. R. Bertozzi. 2011. Organelle membrane proteomics reveals differential influence of mycobacterial lipoglycans on macrophage phagosome maturation and autophagosome accumulation. *J.Proteome Res.* 10: 339–348.

215. Singh, S. B., A. S. Davis, G. A. Taylor, and V. Deretic. 2006. Human IRGM induces autophagy to eliminate intracellular mycobacteria. *Science* 313: 1438–1441.

216. Zhang, Q., J. Sun, Y. Wang, W. He, L. Wang, Y. Zheng, J. Wu, Y. Zhang, and X. Jiang. 2017. Antimycobacterial and anti-inflammatory mechanisms of baicalin via induced autophagy in macrophages infected with Mycobacterium tuberculosis. *Front. Microbiol.* 8: 2142.

217. Castillo, E. F., A. Dekonenko, J. Arko-Mensah, M. A. Mandell, N. Dupont, S. Jiang, M. Delgado-Vargas, G. S. Timmins, D. Bhattacharya, H. Yang, J. Hutt, C. R. Lyons, K. M. Dobos, and V. Deretic. 2012. Autophagy protects against active tuberculosis by suppressing bacterial burden and inflammation. *Proc. Natl. Acad. Sci. U. S. A.* 109: E3168.

218. Kim, J. J., H. M. Lee, D. M. Shin, W. Kim, J. M. Yuk, H. S. Jin, S. H. Lee, G. H. Cha, J. M. Kim, Z. W. Lee, S. J. Shin, H. Yoo, Y. K. Park, J. B. Park, J. Chung, T. Yoshimori, and E. K. Jo. 2012. Host cell autophagy activated by antibiotics is required for their effective antimycobacterial drug action. *Cell Host Microbe* 11: 457–468.

219. Giraud-Gatineau, A., J. M. Coya, A. Maure, A. Biton, M. Thomson, E. M. Bernard, J. Marrec, M. G. Gutierrez, G. Larrouy-Maumus, R. Brosch, B. Gicquel, and L. Tailleux.

2020. The antibiotic bedaquiline activates host macrophage innate immune resistance to bacterial infection. *Elife* 9: 1–29.

220. Tobin, D. M. 2015. Host-directed therapies for tuberculosis. *Cold Spring Harb. Perspect. Med.* 5: a021196.

221. Paik, S., J. K. Kim, C. Chung, and E.-K. Jo. 2019. Autophagy: a new strategy for host-directed therapy of tuberculosis. *Virulence* 10: 448–459.

222. Martin, C. J., M. G. Booty, T. R. Rosebrock, C. Nunes-Alves, D. M. Desjardins, I. Keren, S. M. Fortune, H. G. Remold, and S. M. Behar. 2012. Efferocytosis is an innate antibacterial mechanism. *Cell Host Microbe* 12: 289–300.

223. Schaible, U. E., F. Winau, P. A. Sieling, K. Fischer, H. L. Collins, K. Hagens, R. L. Modlin, V. Brinkmann, and S. H. E. Kaufmann. 2003. Apoptosis facilitates antigen presentation to T lymphocytes through MHC-I and CD1 in tuberculosis. *Nat. Med.* 9: 1039–1046.

224. Lee, J., M. Hartman, and H. Kornfeld. 2009. Macrophage apoptosis in tuberculosis. *Yonsei Med. J.* 50: 1–11.

225. Chung, E. Y., J. K. Sun, and J. M. Xiao. 2006. Regulation of cytokine production during phagocytosis of apoptotic cells. *Cell Res.* 16: 154–161.

226. Huynh, M.-L. N., V. A. Fadok, and P. M. Henson. 2002. Phosphatidylserine-dependent ingestion of apoptotic cells promotes TGF-β1 secretion and the resolution of inflammation. *J. Clin. Invest.* 109: 41–50.

227. Keane, J., H. G. Remold, and H. Kornfeld. 2000. Virulent Mycobacterium tuberculosis Strains Evade Apoptosis of Infected Alveolar Macrophages. *J. Immunol.* 164: 2016–2020.

228. Velmurugan, K., B. Chen, J. L. Miller, S. Azogue, S. Gurses, T. Hsu, M. Glickman, W. R. Jacobs, S. A. Porcelli, and V. Briken. 2007. Mycobacterium tuberculosis nuoG is a virulence gene that inhibits apoptosis of infected host cells. *PLoS Pathog.* 3: 0972–0980.

229. Hinchey, J., S. Lee, B. Y. Jeon, R. J. Basaraba, M. M. Venkataswamy, B. Chen, J. Chan, M. Braunstein, I. M. Orme, S. C. Derrick, S. L. Morris, W. R. Jacobs, and S. A. Porcelli. 2007. Enhanced priming of adaptive immunity by a proapoptotic mutant of Mycobacterium tuberculosis. *J. Clin. Invest.* 117: 2279–2288.

230. Poirier, V., H. Bach, and Y. Av-Gay. 2014. Mycobacterium tuberculosis promotes anti-apoptotic activity of the macrophage by PtpA protein-dependent dephosphorylation of host GSK3α. *J. Biol. Chem.* 289: 29376–29385.

231. Schaaf, K., S. R. Smith, A. Duverger, F. Wagner, F. Wolschendorf, A. O. Westfall, O. Kutsch, and J. Sun. 2017. Mycobacterium tuberculosis exploits the PPM1A signaling pathway to block host macrophage apoptosis. *Sci. Rep.* 7: 42101.

232. Wong, K. W., and W. R. Jacobs. 2011. Critical role for NLRP3 in necrotic death triggered by Mycobacterium tuberculosis. *Cell. Microbiol.* 13: 1371–1384.

233. Mishra, B. B., P. Moura-Alves, A. Sonawane, N. Hacohen, G. Griffiths, L. F. Moita, and E. Anes. 2010. Mycobacterium tuberculosis protein ESAT-6 is a potent activator of the NLRP3/ASC inflammasome. *Cell. Microbiol.* 12: 1046–1063.

234. Dorhoi, A., G. Nouailles, S. Jörg, K. Hagens, E. Heinemann, L. Pradl, D. Oberbeck-Müller, M. A. Duque-Correa, S. T. Reece, J. Ruland, R. Brosch, J. Tschopp, O. Gross, and S. H. E. Kaufmann. 2012. Activation of the NLRP3 inflammasome by *Mycobacterium tuberculosis* is uncoupled from susceptibility to active tuberculosis. *Eur. J. Immunol.* 42: 374–384.

235. Fremond, C. M., D. Togbe, E. Doz, S. Rose, V. Vasseur, I. Maillet, M. Jacobs, B. Ryffel, and V. F. J. Quesniaux. 2007. IL-1 receptor-mediated signal is an essential component of MyD88-dependent innate response to Mycobacterium tuberculosis infection. *J. Immunol.* 179: 1178–1189.

236. Beckwith, K. S., M. S. Beckwith, S. Ullmann, R. S. Sætra, H. Kim, A. Marstad, S. E. Åsberg, T. A. Strand, M. Haug, M. Niederweis, H. A. Stenmark, and T. H. Flo. 2020. Plasma membrane damage causes NLRP3 activation and pyroptosis during Mycobacterium tuberculosis infection. *Nat. Commun.* 11: 2270.

237. Sun, J., A. Siroy, R. K. Lokareddy, A. Speer, K. S. Doornbos, G. Cingolani, and M. Niederweis. 2015. The tuberculosis necrotizing toxin kills macrophages by hydrolyzing NAD. *Nat. Struct. Mol. Biol.* 22: 672–678.

238. Pajuelo, D., N. Gonzalez-Juarbe, U. Tak, J. Sun, C. J. Orihuela, and M. Niederweis. 2018. NAD+ depletion triggers macrophage necroptosis, a cell death pathway exploited by Mycobacterium tuberculosis. *Cell Rep.* 24: 429–440.

239. Galluzzi, L., O. Kepp, and G. Kroemer. 2014. MLKL regulates necrotic plasma membrane permeabilization. *Cell Res.* 24: 139–140.

240. Lee, Y. J., S. K. Han, J. H. Park, J. K. Lee, D. K. Kim, H. S. Chung, and E. Y. Heo. 2018. The effect of metformin on culture conversion in tuberculosis patients with diabetes mellitus. *Korean J. Intern. Med.* 33: 933–940.

241. Stanley, S. A., A. K. Barczak, M. R. Silvis, S. S. Luo, K. Sogi, M. Vokes, M. A. Bray, A. E. Carpenter, C. B. Moore, N. Siddiqi, E. J. Rubin, and D. T. Hung. 2014. Identification of host-targeted small molecules that restrict intracellular Mycobacterium tuberculosis growth. *PLoS Pathog.* 10: e1003946.

242. Choi, S. W., Y. Gu, R. S. Peters, P. Salgame, J. J. Ellner, G. S. Timmins, and V. Deretic. 2018. Ambroxol induces autophagy and potentiates rifampin antimycobacterial activity. *Antimicrob. Agents Chemother.* 62: e01019-18.

243. Singh, P., and S. Subbian. 2018. Harnessing the mTOR pathway for tuberculosis treatment. *Front. Microbiol.* 9: 70.

244. Kim, Y. C., and K. L. Guan. 2015. MTOR: A pharmacologic target for autophagy regulation. *J. Clin. Invest.* 125: 25–32.

245. Harrison, D. E., R. Strong, Z. D. Sharp, J. F. Nelson, C. M. Astle, K. Flurkey, N. L. Nadon, J. E. Wilkinson, K. Frenkel, C. S. Carter, M. Pahor, M. A. Javors, E. Fernandez, and R. A. Miller. 2009. Rapamycin fed late in life extends lifespan in genetically heterogeneous mice. *Nature* 460: 392–395.

246. Schiebler, M., K. Brown, K. Hegyi, S. M. Newton, M. Renna, L. Hepburn, C. Klapholz, S. Coulter, A. Obregón-Henao, M. Henao Tamayo, R. Basaraba, B. Kampmann, K. M. Henry, J. Burgon, S. A. Renshaw, A. Fleming, R. R. Kay, K. E. Anderson, P. T. Hawkins, D. J. Ordway, D. C. Rubinsztein, and R. A. Floto. 2015. Functional drug screening reveals anticonvulsants as enhancers of mTOR-independent autophagic killing of Mycobacterium tuberculosis through inositol depletion. *EMBO Mol. Med.* 7: 127–139.

247. Barber, G. N., S. Edelhoff, M. G. Katze, and C. M. Disteche. 1993. Chromosomal assignment of the interferon-inducible double-stranded RNA-dependent protein kinase (PRKR) to human chromosome 2p21-p22 and mouse chromosome 17 E2. *Genomics* 16: 765–767.

248. Taniuchi, S., M. Miyake, K. Tsugawa, M. Oyadomari, and S. Oyadomari. 2016. Integrated stress response of vertebrates is regulated by four eIF2α kinases. *Sci. Rep.* 6: 1–11.

249. Galabru, J., and A. Hovanessians. 1987. Autophosphorylation of the protein kinase dependent on double-stranded RNA. *J. Biol. Chem.* 262: 15538–15544.

250. Hull, C. M., and P. C. Bevilacqua. 2015. Mechanistic analysis of activation of the innate immune sensor PKR by bacterial RNA. *J. Mol. Biol.* 427: 3501–3515.

251. Bleiblo, F., P. Michael, D. Brabant, C. V Ramana, T. Tai, M. Saleh, J. E. Parrillo, A. Kumar, and A. Kumar. 2013. JAK kinases are required for the bacterial RNA and poly I:C induced tyrosine phosphorylation of PKR. *Int. J. Clin. Exp. Med.* 6: 16–25.

252. Dey, M., C. Cao, A. C. Dar, T. Tamura, K. Ozato, F. Sicheri, and T. E. Dever. 2005. Mechanistic link between PKR dimerization, autophosphorylation, and eIF2α substrate recognition. *Cell* 122: 901–913.

253. Zhang, F., P. R. Romano, T. Nagamura-Inoue, B. Tian, T. E. Dever, M. B. Mathews, K. Ozato, and A. G. Hinnebusch. 2001. Binding of double-stranded RNA to protein kinase PKR is required for dimerization and promotes critical autophosphorylation events in the activation loop. *J. Biol. Chem.* 276: 24946–24958.

254. Sudhakar, A., A. Ramachandran, S. Ghosh, S. E. Hasnain, R. J. Kaufman, and K. V. A.

Ramaiah. 2000. Phosphorylation of serine 51 in initiation factor 2α (eIF2α) promotes complex formation between eIF2α(P) and eIF2B and causes inhibition in the guanine nucleotide exchange activity of eIF2B. *Biochemistry* 39: 12929–12938.

255. Gordiyenko, Y., J. L. Llácer, and V. Ramakrishnan. 2019. Structural basis for the inhibition of translation through eIF2α phosphorylation. *Nat. Commun.* 10: 1–11.

256. García, M. A., J. Gil, I. Ventoso, S. Guerra, E. Domingo, C. Rivas, and M. Esteban. 2006. Impact of protein kinase PKR in cell biology: from antiviral to antiproliferative action. *Microbiol. Mol. Biol. Rev.* 70: 1032–1060.

257. Goh, K. C., M. J. DeVeer, and B. R. G. Williams. 2000. The protein kinase PKR is required for p38 MAPK activation and the innate immune response to bacterial endotoxin. *EMBO J.* 19: 4292–4297.

258. Horng, T., G. M. Barton, and R. Medzhitov. 2001. TIRAP: an adapter molecule in the Toll signaling pathway. *Nat. Immunol.* 2: 835–841.

259. Jiang, Z., M. Zamanian-Daryoush, H. Nie, A. M. Silva, B. R. G. Williams, and X. Li. 2003. Poly(dI·dC)-induced toll-like receptor 3 (TLR3)-mediated activation of NFκB and MAP kinase is through an interleukin-1 receptor-associated kinase (IRAK)-independent pathway employing the signaling components TLR3-TRAF6-TAK1-TAB2-PKR. *J. Biol. Chem.* 278: 16713–16719.

260. Deb, A., M. Zamanian-Daryoush, Z. Xu, S. Kadereit, and B. R. G. Williams. 2001. Protein kinase PKR is required for platelet-derived growth factor signaling of c-fos gene expression via Erks and Stat3. *EMBO J.* 20: 2487–2496.

261. Deb, A., S. J. Haque, T. Mogensen, R. H. Silverman, and B. R. G. Williams. 2001. RNA-dependent protein kinase PKR is required for activation of NF-κB by IFN-γ in a STAT1-independent pathway. *J. Immunol.* 166: 6170–6180.

262. Yang, Y. L., L. F. L. Reis, J. Paylovic, S. Aguzzi, R. Schäfer, A. Kumar, B. R. G. Williams, M. Aguet, and C. Weissmann. 1995. Deficient signaling in mice devoid of double-stranded RNA-dependent protein kinase. *EMBO J.* 14: 6095–6106.

263. Kuhen, K. L., and C. E. Samuel. 1997. Isolation of the interferon-inducible RNA-dependent protein kinase Pkr promoter and identification of a novel DNA element within the 5'-flanking region of human and mouse Pkr genes. *Virology* 227: 119–130.

264. Rouillard, A. D., G. W. Gundersen, N. F. Fernandez, Z. Wang, C. D. Monteiro, M. G. McDermott, and A. Ma'ayan. 2016. The harmonizome: a collection of processed datasets gathered to serve and mine knowledge about genes and proteins. *Database (Oxford)* 2016: baw100.

265. Zhang, P., J. O. Langland, B. L. Jacobs, and C. E. Samuel. 2009. Protein kinase PKR-dependent activation of mitogen-activated protein kinases occurs through mitochondrial

adapter IPS-1 and is antagonized by vaccinia virus E3L. *J. Virol.* 83: 5718–5725.

266. Silva, A. M., M. Whitmore, Z. Xu, Z. Jiang, X. Li, and B. R. G. Williams. 2004. Protein kinase R (PKR) interacts with and activates mitogen-activated protein kinase kinase 6 (MKK6) in response to double-stranded RNA stimulation. *J. Biol. Chem.* 279: 37670–37676.

267. Cheung, B. K. W., D. C. W. Lee, J. C. B. Li, Y.-L. Lau, and A. S. Y. Lau. 2005. A role for double-stranded RNA-activated protein kinase PKR in Mycobacterium-induced cytokine expression. *J. Immunol.* 175: 7218–7225.

268. Roman-Blas, J. A., and S. A. Jimenez. NF-kappaB as a potential therapeutic target in osteoarthritis and rheumatoid arthritis. *Osteoarthritis Cartilage.* 14: 839–848.

269. Gil, J., J. Alcamí, and M. Esteban. 2000. Activation of NF-κB by the dsRNA-dependent protein kinase, PKR involves the IκB kinase complex. *Oncogene* 19: 1369–1378.

270. Bonnet, M. C., R. Weil, E. Dam, A. G. Hovanessian, and E. F. Meurs. 2000. PKR stimulates NF-κB irrespective of its kinase function by interacting with the IκB kinase complex. *Mol. Cell. Biol.* 20: 4532–4542.

271. Kumar, A., Y. L. Yang, V. Flati, S. Der, S. Kadereit, A. Deb, J. Haque, L. Reis, C. Weissmann, and B. R. G. Williams. 1997. Deficient cytokine signaling in mouse embryo fibroblasts with a targeted deletion in the PKR gene: role of IRF-1 and NF-κB. *EMBO J.* 16: 406–416.

272. Zhang, P., and C. E. Samuel. 2007. Protein kinase PKR plays a stimulus- and virus-dependent role in apoptotic death and virus multiplication in human cells. *J. Virol.* 81: 8192–8200.

273. Alexopoulou, L., A. C. Holt, R. Medzhitov, and R. A. Flavell. 2001. Recognition of double-stranded RNA and activation of NF-κB by toll-like receptor 3. *Nature* 413: 732–738.

274. Nakayama, Y., E. H. Plisch, J. Sullivan, C. Thomas, C. J. Czuprynski, B. R. G. Williams, and M. Suresh. 2010. Role of PKR and type I IFNs in viral control during primary and secondary infection. *PLoS Pathog.* 6: e1000966.

275. Baltzis, D., L.-K. Qu, S. Papadopoulou, J. D. Blais, J. C. Bell, N. Sonenberg, and A. E. Koromilas. 2004. Resistance to vesicular stomatitis virus infection requires a functional cross talk between the eukaryotic translation initiation factor 2α kinases PERK and PKR. *J. Virol.* 78: 12747–12761.

276. Samuel, M. A., K. Whitby, B. C. Keller, A. Marri, W. Barchet, B. R. G. Williams, R. H. Silverman, M. Gale, and M. S. Diamond. 2006. PKR and RNase L contribute to protection against lethal West Nile virus infection by controlling early viral spread in the periphery and replication in neurons. *J. Virol.* 80: 7009–7019.

277. Balachandran, S., C. N. Kim, W. C. Yeh, T. W. Mak, K. Bhalla, and G. N. Barber. 1998. Activation of the dsRNA-dependent protein kinase, PKR, induces apoptosis through FADD-mediated death signaling. *EMBO J.* 17: 6888–6902.

278. Von Roretz, C., and I. E. Gallouzi. 2010. Protein kinase RNA/FADD/caspase-8 pathway mediates the proapoptotic activity of the RNA-binding protein human antigen R (HuR). *J. Biol. Chem.* 285: 16806–16813.

279. Gil, J., J. Alcamí, and M. Esteban. 1999. Induction of apoptosis by double-stranded-RNA-dependent protein kinase (PKR) involves the α subunit of eukaryotic translation initiation factor 2 and NF-κB. *Mol. Cell. Biol.* 19: 4653–4663.

280. Munir, M., and M. Berg. 2013. The multiple faces of protein kinase R in antiviral defense. *Virulence* 4: 85–89.

281. Schulz, O., A. Pichlmair, J. Rehwinkel, N. C. Rogers, D. Scheuner, H. Kato, O. Takeuchi, S. Akira, R. J. Kaufman, and C. R. E Sousa. 2010. Protein kinase R contributes to immunity against specific viruses by regulating interferon mRNA integrity. *Cell Host Microbe* 7: 354–361.

282. Tallóczy, Z., W. Jiang, H. W. Virgin IV, D. A. Leib, D. Scheuner, R. J. Kaufman, E. L. Eskelinen, and B. Levine. 2002. Regulation of starvation- and virus-induced autophagy by the elF2α kinase signaling pathway. *Proc. Natl. Acad. Sci. U. S. A.* 99: 190–195.

283. Tallóczy, Z., H. W. Virgin IV, and B. Levine. 2006. PKR-dependent autophagic degradation of herpes simplex virus type 1. *Autophagy* 2: 24–29.

284. Faria, M. S., T. C. Calegari-Silva, A. De Carvalho Vivarini, J. C. Mottram, U. G. Lopes, and A. P. C. A. Lima. 2014. Role of protein kinase R in the killing of Leishmania major by macrophages in response to neutrophil elastase and TLR4 via TNFα and IFNβ. *FASEB J.* 28: 3050–3063.

285. Pereira, R. M. S., K. L. Dias Teixeira, V. Barreto-de-Souza, T. C. Calegari-Silva, L. D. B. De-Melo, D. C. Soares, D. C. Bou-Habib, A. M. Silva, E. M. Saraiva, and U. G. Lopes. 2010. Novel role for the double-stranded RNA-activated protein kinase PKR: modulation of macrophage infection by the protozoan parasite Leishmania. *FASEB J.* 24: 617–626.

286. Ogolla, P. S., J.-A. C. Portillo, C. L. White, K. Patel, B. Lamb, G. C. Sen, and C. S. Subauste. 2013. The protein kinase double-stranded RNA-dependent (PKR) enhances protection against disease caused by a non-viral pathogen. *PLoS Pathog.* 9: e1003557.

287. Hsu, L. C., J. M. Park, K. Zhang, J. L. Luo, S. Maeda, R. J. Kaufman, L. Eckmann, D. G. Guiney, and M. Karin. 2004. The protein kinase PKR is required for macrophage apoptosis after activation of toll-like receptor 4. *Nature* 428: 341–345.

288. Lu, B., T. Nakamura, K. Inouye, J. Li, Y. Tang, P. Lundbäck, S. I. Valdes-Ferrer, P. S. Olofsson, T. Kalb, J. Roth, Y. Zou, H. Erlandsson-Harris, H. Yang, J. P. Y. Ting, H. Wang,

U. Andersson, D. J. Antoine, S. S. Chavan, G. S. Hotamisligil, and K. J. Tracey. 2012. Novel role of PKR in inflammasome activation and HMGB1 release. *Nature* 488: 670–674.

289. Ranjbar, S., V. Haridas, A. Nambu, L. D. Jasenosky, S. Sadhukhan, T. S. Ebert, V. Hornung, G. H. Cassell, J. V. Falvo, and A. E. Goldfeld. 2019. Cytoplasmic RNA sensor pathways and nitazoxanide broadly inhibit intracellular Mycobacterium tuberculosis growth. *iScience* 22: 299–313.

290. Wu, K., J. Koo, X. Jiang, R. Chen, S. N. Cohen, and C. Nathan. 2018. Correction: Improved control of tuberculosis and activation of macrophages in mice lacking protein kinase R. *PLoS One* 13: e0205424.

291. Marchal, J. A., G. J. Lopez, M. Peran, A. Comino, J. R. Delgado, J. A. García-García, V. Conde, F. M. Aranda, C. Rivas, M. Esteban, and M. A. Garcia. 2014. The impact of PKR activation: from neurodegeneration to cancer. *FASEB J.* 28: 1965–1974.

292. Jammi, N. V., L. R. Whitby, and P. A. Beal. 2003. Small molecule inhibitors of the RNA-dependent protein kinase. *Biochem. Biophys. Res. Commun.* 308: 50–57.

293. Hu, Y., and T. W. Conway. 1993. 2-aminopurine inhibits the double-stranded RNA-dependent protein kinase both in vitro and in vivo. *J. Interferon Res.* 13: 323–328.

294. Watanabe, T., T. Imamura, and Y. Hiasa. 2018. Roles of protein kinase R in cancer: potential as a therapeutic target. *Cancer Sci.* 109: 919–925.

295. Marchal, J. A., E. Carrasco, A. Ramirez, G. Jiménez, C. Olmedo, M. Peran, A. Agil, A. Conejo-García, O. Cruz-López, J. M. Campos, and M. Á. García. 2013. Bozepinib, a novel small antitumor agent, induces PKR-mediated apoptosis and synergizes with IFNα triggering apoptosis, autophagy and senescence. *Drug Des. Devel. Ther.* 7: 1301–1313.

296. López-Cara, L. C., A. Conejo-García, J. A. Marchal, G. MacChione, O. Cruz-López, H. Boulaiz, M. A. García, F. Rodríguez-Serrano, A. Ramírez, C. Cativiela, A. I. Jiménez, J. M. García-Ruiz, D. Choquesillo-Lazarte, A. Aránega, and J. M. Campos. 2011. New (RS)-benzoxazepin-purines with antitumour activity: the chiral switch from (RS)-2,6-dichloro-9-[1-(p-nitrobenzenesulfonyl)-1,2,3,5-tetrahydro-4,1- benzoxazepin-3-yl]-9H-purine. *Eur. J. Med. Chem.* 46: 249–258.

297. Elazar, M., M. Liu, S. A. McKenna, P. Liu, E. A. Gehrig, J. D. Puglisi, J. F. Rossignol, and J. S. Glenn. 2009. The anti-hepatitis C agent nitazoxanide induces phosphorylation of eukaryotic initiation factor 2α via protein kinase activated by double-stranded RNA activation. *Gastroenterology* 137: 1827–1835.

298. Ashiru, O., J. D. Howe, and T. D. Butters. 2014. Nitazoxanide, an antiviral thiazolide, depletes ATP-sensitive intracellular Ca(2+) stores. *Virology* 462–463: 135–148.

299. Shigyo, K., O. Ocheretina, Y. M. Merveille, W. D. Johnson, J. W. Pape, C. F. Nathan, and D. W. Fitzgerald. 2013. Efficacy of nitazoxanide against clinical isolates of

Mycobacterium tuberculosis. *Antimicrob. Agents Chemother.* 57: 2834–2837.

300. Walsh, K. F., K. McAulay, M. H. Lee, S. C. Vilbrun, L. Mathurin, D. J. Francois, M. Zimmerman, F. Kaya, N. Zhang, K. Saito, O. Ocheretina, R. Savic, V. Dartois, W. D. Johnson, J. W. Pape, C. Nathan, and D. W. Fitzgerald. 2020. Early bactericidal activity trial of nitazoxanide for pulmonary tuberculosis. *Antimicrob. Agents Chemother.* 64: e01956-19.

301. Hu, W., W. Hofstetter, X. Wei, W. Guo, Y. Zhou, A. Pataer, H. Li, B. Fang, and S. G. Swisher. 2009. Double-stranded RNA-dependent protein kinase-dependent apoptosis induction by a novel small compound. *J. Pharmacol. Exp. Ther.* 328: 866–872.

302. Bai, H., T. Chen, J. Ming, H. Sun, P. Cao, D. N. Fusco, R. T. Chung, M. Chorev, Q. Jin, and B. H. Aktas. 2013. Dual activators of protein kinase R (PKR) and protein kinase R-like kinase (PERK) identify common and divergent catalytic targets. *ChemBioChem* 14: 1255–1262.

303. Morrison, J., M. Pai, and P. C. Hopewell. 2008. Tuberculosis and latent tuberculosis infection in close contacts of people with pulmonary tuberculosis in low-income and middle-income countries: a systematic review and meta-analysis. *Lancet Infect. Dis.* 8: 359–368.

304. Behar, S. M., M. Divangahi, and H. G. Remold. 2010. Evasion of innate immunity by mycobacterium tuberculosis: Is death an exit strategy? *Nat. Rev. Microbiol.* 8: 668–674.

305. Wu, K., J. Koo, X. Jiang, R. Chen, S. N. Cohen, and C. Nathan. 2012. Improved control of tuberculosis and activation of macrophages in mice lacking protein kinase R. *PLoS One* 7: e30512.

306. Thapa, R. J., S. Nogusa, P. Chen, J. L. Maki, A. Lerro, M. Andrake, G. F. Rall, A. Degterev, and S. Balachandran. 2013. Interferon-induced RIP1/RIP3-mediated necrosis requires PKR and is licensed by FADD and caspases. *Proc. Natl. Acad. Sci. U. S. A.* 110: E3109.

307. Sun, J., K. Schaaf, A. Duverger, F. Wolschendorf, A. Speer, F. Wagner, M. Niederweis, and O. Kutsch. 2016. Protein phosphatase, Mg2+/Mn2+-dependent 1A controls the innate antiviral and antibacterial response of macrophages during HIV-1 and Mycobacterium tuberculosis infection. *Oncotarget* 7: 15394–15409.

308. Chen, B., L. A. Gilbert, B. A. Cimini, J. Schnitzbauer, W. Zhang, G. W. Li, J. Park, E. H. Blackburn, J. S. Weissman, L. S. Qi, and B. Huang. 2013. Dynamic imaging of genomic loci in living human cells by an optimized CRISPR/Cas system. *Cell* 155: 1479–1491.

309. Sanjana, N. E., O. Shalem, and F. Zhang. 2014. Improved vectors and genome-wide libraries for CRISPR screening. *Nat. Methods* 11: 783–784.

310. Livak, K. J., and T. D. Schmittgen. 2001. Analysis of relative gene expression data using real-time quantitative PCR and the 2-ΔΔCT method. *Methods* 25: 402–408.

311. Maeß, M. B., S. Sendelbach, and S. Lorkowski. 2010. Selection of reliable reference genes during THP-1 monocyte differentiation into macrophages. *BMC Mol. Biol.* 11: 90.

312. Cao, X. mei, X. guang Luo, J. hong Liang, C. Zhang, X. ping Meng, and D. wei Guo. 2012. Critical selection of internal control genes for quantitative real-time RT-PCR studies in lipopolysaccharide-stimulated human THP-1 and K562 cells. *Biochem. Biophys. Res. Commun.* 427: 366–372.

313. Jain, P., T. Hsu, M. Arai, K. Biermann, D. S. Thaler, A. Nguyen, P. A. González, J. M. Tufariello, J. Kriakov, B. Chen, M. H. Larsen, and W. R. Jacobs. 2014. Specialized transduction designed for precise high-throughput unmarked deletions in Mycobacterium tuberculosis. *MBio* 5: e01245-14.

314. Mouton, J. M., T. Heunis, A. Dippenaar, J. L. Gallant, L. Kleynhans, and S. L. Sampson. 2019. Comprehensive characterization of the attenuated double auxotroph Mycobacterium tuberculosisΔleuDΔpanCD as an alternative to h37Rv. *Front. Microbiol.* 10: 1922.

315. Shrestha, N., W. Bahnan, D. J. Wiley, G. Barber, K. A. Fields, and K. Schesser. 2012. Eukaryotic initiation factor 2 (eIF2) signaling regulates proinflammatory cytokine expression and bacterial invasion. *J. Biol. Chem.* 287: 28738–28744.

316. Mundhra, S., R. Bryk, N. Hawryluk, T. Zhang, X. Jiang, and C. F. Nathan. 2018. Evidence for dispensability of protein kinase R in host control of tuberculosis. *Eur. J. Immunol.* 48: 612–620.

317. Sun, J., A. Lau, X. Wang, T. Y. A. Liao, A. Zoubeidi, and Z. Hmama. 2009. A broad-range of recombination cloning vectors in mycobacteria. *Plasmid* 62: 158–165.

318. Sorrentino, F., R. G. Del Rio, X. Zheng, J. P. Matilla, P. T. Gomez, M. M. Hoyos, M. E. P. Herran, A. M. Losana, and Y. Av-Gay. 2016. Development of an intracellular screen for new compounds able to inhibit Mycobacterium tuberculosis growth in human macrophages. *Antimicrob. Agents Chemother.* 60: 640–645.

319. Snewin, V. A., M. P. Gares, P. Ó Gaora, Z. Hasan, I. N. Brown, and D. B. Young. 1999. Assessment of immunity to mycobacterial infection with luciferase reporter constructs. *Infect. Immun.* 67: 4586–4593.

320. Upadhyay, R., A. Sanchez-Hidalgo, C. J. Wilusz, A. J. Lenaerts, J. Arab, J. Yeh, K. Stefanisko, N. I. Tarasova, and M. Gonzalez-Juarrero. 2018. Host directed therapy for chronic tuberculosis via intrapulmonary delivery of aerosolized peptide inhibitors targeting the IL-10-STAT3 Pathway. *Sci. Rep.* 8: 16610.

321. Jayaraman, P., I. Sada-Ovalle, T. Nishimura, A. C. Anderson, V. K. Kuchroo, H. G. Remold, and S. M. Behar. 2013. IL-1β promotes antimicrobial immunity in macrophages by regulating TNFR signaling and caspase-3 activation. *J. Immunol.* 190: 4196–4204.

322. Chu, L. Y., Y. C. Hsueh, H. L. Cheng, and K. K. Wu. 2017. Cytokine-induced autophagy promotes long-term VCAM-1 but not ICAM-1 expression by degrading late-phase IκBα. *Sci. Rep.* 7.

323. Palucci, I., B. Battah, A. Salustri, F. De Maio, L. Petrone, F. Ciccosanti, M. Sali, V. Bondet, D. Duffy, G. M. Fimia, D. Goletti, and G. Delogu. 2019. IP-10 contributes to the inhibition of mycobacterial growth in an ex vivo whole blood assay. *Int. J. Med. Microbiol.* 309: 299–306.

324. Daigneault, M., J. A. Preston, H. M. Marriott, M. K. B. Whyte, and D. H. Dockrell. 2010. The identification of markers of macrophage differentiation in PMA-stimulated THP-1 cells and monocyte-derived macrophages. *PLoS One* 5: e8668.

325. Gazzinelli, R. T., I. P. Oswald, S. L. James, and A. Sher. 1992. IL-10 inhibits parasite killing and nitrogen oxide production by IFN-gamma-activated macrophages. *J. Immunol.* 148: 1792–1796.

326. Yamamoto, A., Y. Tagawa, T. Yoshimori, Y. Moriyama, R. Masaki, and Y. Tashiro. 1998. Bafilomycin A1 prevents maturation of autophagic vacuoles by inhibiting fusion between autophagosomes and lysosomes in rat hepatoma cell line, H-4-II-E cells. *Cell Struct. Funct.* 23: 33–42.

327. Yoshii, S. R., and N. Mizushima. 2017. Monitoring and measuring autophagy. *Int. J. Mol. Sci.* 18: 1865.

328. Matsumoto, G., K. Wada, M. Okuno, M. Kurosawa, and N. Nukina. 2011. Serine 403 phosphorylation of p62/SQSTM1 regulates selective autophagic clearance of ubiquitinated proteins. *Mol. Cell* 44: 279–289.

329. Eissenberg, L. G., and W. E. Goldman. 1988. Fusion of lysosomes with phagosomes containing Histoplasma capsulatum: use of fluoresceinated dextran. *Adv. Exp. Med. Biol.* 239: 53–61.

330. Limame, R., A. Wouters, B. Pauwels, E. Fransen, M. Peeters, F. Lardon, O. de Wever, and P. Pauwels. 2012. Comparative analysis of dynamic cell viability, migration and invasion assessments by novel real-time technology and classic endpoint assays. *PLoS One* 7: e46536.

331. Fallahi-Sichani, M., D. E. Kirschner, and J. J. Linderman. 2012. NF-κB signaling dynamics play a key role in infection control in tuberculosis. *Front. Physiol.* 3: 170.

332. Ladiges, W., J. Morton, H. Hopkins, R. Wilson, G. Filley, C. Ware, and M. Gale. 2002. Expression of human PKR protein kinase in transgenic mice. *J. Interf. Cytokine Res.* 22: 329–334.

333. Napier, R. J., W. Rafi, M. Cheruvu, K. R. Powell, M. A. Zaunbrecher, W. Bornmann, P. Salgame, T. M. Shinnick, and D. Kalman. 2011. Imatinib-sensitive tyrosine kinases

regulate mycobacterial pathogenesis and represent therapeutic targets against tuberculosis. *Cell Host Microbe* 10: 475–485.

334. Posti, K., S. Leinonen, S. Tetri, S. Kottari, P. Viitala, O. Pelkonen, and H. Raunio. 1999. Modulation of murine phenobarbital-inducible CYP2A5, CYP2B10 and CYP1A enzymes by inhibitors of protein kinases and phosphatases. *Eur. J. Biochem.* 264: 19–26.

335. Yim, H. C. H., D. Wang, L. Yu, C. L. White, P. W. Faber, B. R. G. Williams, and A. J. Sadler. 2016. The kinase activity of PKR represses inflammasome activity. *Cell Res.* 26: 367–379.

336. Novikov, A., M. Cardone, R. Thompson, K. Shenderov, K. D. Kirschman, K. D. Mayer-Barber, T. G. Myers, R. L. Rabin, G. Trinchieri, A. Sher, and C. G. Feng. 2011. Mycobacterium tuberculosis triggers host type I IFN signaling to regulate IL-1β production in human macrophages. *J. Immunol.* 187: 2540–2547.

337. Kaufman, R. J. 1999. Double-stranded RNA-activated protein kinase mediates virus-induced apoptosis: a new role for an old actor. *Proc. Natl. Acad. Sci. U. S. A.* 96: 11693–11695.

338. Der, S. D., Y. L. Yang, C. Weissmann, and B. R. G. Williams. 1997. A double-stranded RNA-activated protein kinase-dependent pathway mediating stress-induced apoptosis. *Proc. Natl. Acad. Sci. U. S. A.* 94: 3279–3283.

339. Yeung, M. C., J. Liu, and A. S. Lau. 1996. An essential role for the interferon-inducible, double-stranded RNA-activated protein kinase PKR in the tumor necrosis factor-induced apoptosis in U937 cells. *Proc. Natl. Acad. Sci. U. S. A.* 93: 12451–12455.

340. Balcewicz-Sablinska, M. K., J. Keane, H. Kornfeld, and H. G. Remold. 1998. Pathogenic Mycobacterium tuberculosis evades apoptosis of host macrophages by release of TNF-R2, resulting in inactivation of TNF-alpha. *J. Immunol.* 161: 2641.

341. Gil, J., and M. Esteban. 2000. The interferon-induced protein kinase (PKR), triggers apoptosis through FADD-mediated activation of caspase 8 in a manner independent of Fas and TNF-α receptors. *Oncogene* 19: 3665–3674.

342. Yanti, B., M. Mulyadi, M. Amin, H. Harapan, N. M. Mertaniasih, and S. Soetjipto. 2020. The role of Mycobacterium tuberculosis complex species on apoptosis and necroptosis state of macrophages derived from active pulmonary tuberculosis patients. *BMC Res. Notes* 13: 415.

343. Fan, L., X. Wu, C. Jin, F. Li, S. Xiong, and Y. Dong. 2018. MptpB promotes mycobacteria survival by inhibiting the expression of inflammatory mediators and cell apoptosis in macrophages. *Front. Cell. Infect. Microbiol.* 8: 171.

344. Hett, E. C., L. H. Slater, K. G. Mark, T. Kawate, B. G. Monks, A. Stutz, E. Latz, and D. T. Hung. 2013. Chemical genetics reveals a kinase-independent role for protein kinase R in

pyroptosis. *Nat. Chem. Biol.* 9: 398–405.

345. He, Y., L. Franchi, and G. Núñez. 2013. The protein kinase PKR is critical for LPS-induced iNOS production but dispensable for inflammasome activation in macrophages. *Eur. J. Immunol.* 43: 1147–1152.

346. Kayagaki, N., S. Warming, M. Lamkanfi, L. Vande Walle, S. Louie, J. Dong, K. Newton, Y. Qu, J. Liu, S. Heldens, J. Zhang, W. P. Lee, M. Roose-Girma, and V. M. Dixit. 2011. Non-canonical inflammasome activation targets caspase-11. *Nature* 479: 117–121.

347. Endo, M., M. Mori, S. Akira, and T. Gotoh. 2006. C/EBP homologous protein (CHOP) is crucial for the induction of caspase-11 and the pathogenesis of lipopolysaccharide-induced inflammation. *J. Immunol.* 176: 6245–6253.

348. Wassermann, R., M. F. Gulen, C. Sala, S. G. Perin, Y. Lou, J. Rybniker, J. L. Schmid-Burgk, T. Schmidt, V. Hornung, S. T. Cole, and A. Ablasser. 2015. Mycobacterium tuberculosis differentially activates cGAS- and inflammasome-dependent intracellular immune responses through ESX-1. *Cell Host Microbe* 17: 799–810.

349. Collins, A. C., H. Cai, T. Li, L. H. Franco, X. D. Li, V. R. Nair, C. R. Scharn, C. E. Stamm, B. Levine, Z. J. Chen, and M. U. Shiloh. 2015. Cyclic GMP-AMP synthase is an innate immune DNA sensor for Mycobacterium tuberculosis. *Cell Host Microbe* 17: 820–828.

350. Marinho, F. V., S. Benmerzoug, S. Rose, P. C. Campos, J. T. Marques, A. Báfica, G. Barber, B. Ryffel, S. C. Oliveira, and V. F. J. Quesniaux. 2018. The cGAS/STING pathway is important for dendritic cell activation but is not essential to induce protective immunity against Mycobacterium tuberculosis infection. *J. Innate Immun.* 10: 239–252.

351. Cheng, Y., and J. S. Schorey. 2018. Mycobacterium tuberculosis-induced IFN-β production requires cytosolic DNA and RNA sensing pathways. *J. Exp. Med.* 215: 2919–2935.

352. Hu, S., H. Sun, L. Yin, J. Li, S. Mei, F. Xu, C. Wu, X. Liu, F. Zhao, D. Zhang, Y. Huang, L. Ren, S. Cen, J. Wang, C. Liang, and F. Guo. 2019. PKR-dependent cytosolic cGAS foci are necessary for intracellular DNA sensing. *Sci. Signal.* 12: eaav7934.

353. Tanaka, Y., and Z. J. Chen. 2012. STING specifies IRF3 phosphorylation by TBK1 in the cytosolic DNA signaling pathway. *Sci. Signal.* 5: ra20.

354. Ward, S. V., and C. E. Samuel. 2002. Regulation of the interferon-inducible PKR kinase gene: the KCS element is a constitutive promoter element that functions in concert with the interferon-stimulated response element. *Virology* 295: 136–146

355. Hsu, T., S. M. Hingley-Wilson, B. Chen, M. Chen, A. Z. Dai, P. M. Morin, C. B. Marks, J. Padiyar, C. Goulding, M. Gingery, D. Eisenberg, R. G. Russell, S. C. Derrick, F. M. Collins, S. L. Morris, C. H. King, and W. R. Jacobs. 2003. The primary mechanism of

attenuation of bacillus Calmette-Guérin is a loss of secreted lytic function required for invasion of lung interstitial tissue. *Proc. Natl. Acad. Sci. U. S. A.* 100: 12420–12425.

356. Perkins, D. J., and S. N. Vogel. 2015. Space and time: New considerations about the relationship between toll-like receptors (TLRs) and type I interferons (IFNs). *Cytokine* 74: 171–174.

357. Falvo, J. V., S. Ranjbar, L. D. Jasenosky, and A. E. Goldfeld. 2011. Arc of a vicious circle: pathways activated by Mycobacterium tuberculosis that target the HIV-1 long terminal repeat. *Am. J. Respir. Cell Mol. Biol.* 45: 1116–1124.

358. Shen, S., M. Niso-Santano, S. Adjemian, T. Takehara, S. A. Malik, H. Minoux, S. Souquere, G. Mariño, S. Lachkar, L. Senovilla, L. Galluzzi, O. Kepp, G. Pierron, M. C. Maiuri, H. Hikita, R. Kroemer, and G. Kroemer. 2012. Cytoplasmic STAT3 represses autophagy by inhibiting PKR activity. *Mol. Cell* 48: 667–680.

359. Matsuzawa, T., E. Fujiwara, and Y. Washi. 2014. Autophagy activation by interferon-γ via the p38 mitogen-activated protein kinase signalling pathway is involved in macrophage bactericidal activity. *Immunology* 141: 61–69.

360. Pattingre, S., A. Tassa, X. Qu, R. Garuti, H. L. Xiao, N. Mizushima, M. Packer, M. D. Schneider, and B. Levine. 2005. Bcl-2 antiapoptotic proteins inhibit Beclin 1-dependent autophagy. *Cell* 122: 927–939.

361. Goh, K. C. 2000. The protein kinase PKR is required for p38 MAPK activation and the innate immune response to bacterial endotoxin. *EMBO J.* 19: 4292–4297.

362. Gupta, A., G. Pant, K. Mitra, J. Madan, M. K. Chourasia, and A. Misra. 2014. Inhalable particles containing rapamycin for induction of autophagy in macrophages infected with Mycobacterium tuberculosis. *Mol. Pharm.* 11: 1201–1207.

363. Rossignol, J. F. A., A. Ayoub, and M. S. Ayers. 2001. Treatment of diarrhea caused by Cryptosporidium parvum: A prospective randomized, double-blind, placebo-controlled study of nitazoxanide. *J. Infect. Dis.* 184: 103–106.

364. Ortiz, J. J., A. Ayoub, G. Gargala, N. L. Chegne, and L. Favennec. 2001. Randomized clinical study of nitazoxanide compared to metronidazole in the treatment of symptomatic giardiasis in children from Northern Peru. *Aliment. Pharmacol. Ther.* 15: 1409–1415.

365. Lam, K. K. Y., X. Zheng, R. Forestieri, A. D. Balgi, M. Nodwell, S. Vollett, H. J. Anderson, R. J. Anderson, Y. Av-Gay, and M. Roberge. 2012. Nitazoxanide stimulates autophagy and inhibits mTORC1 signaling and intracellular proliferation of Mycobacterium tuberculosis. *PLoS Pathog.* 8: 1002691.

366. De Carvalho, L. P. S., G. Lin, X. Jiang, and C. Nathan. 2009. Nitazoxanide kills replicating and nonreplicating Mycobacterium tuberculosis and evades resistance. *J. Med. Chem.* 52: 5789–5792.

367. Anderson, E., W. S. Pierre-Louis, C. J. Wong, J. W. Lary, and J. L. Cole. 2011. Heparin activates PKR by inducing dimerization. *J. Mol. Biol.* 413: 973–984.

368. Hickson, S. E., D. Margineantu, D. M. Hockenbery, J. A. Simon, and A. P. Geballe. 2018. Inhibition of vaccinia virus replication by nitazoxanide. *Virology* 518: 398–405.

369. Pai, M., M. A. Behr, D. Dowdy, K. Dheda, M. Divangahi, C. C. Boehme, A. Ginsberg, S. Swaminathan, M. Spigelman, H. Getahun, D. Menzies, and M. Raviglione. 2016. Tuberculosis. *Nat. Rev. Dis. Prim.* 2: 1–23.

370. Queval, C. J., R. Brosch, and R. Simeone. 2017. The macrophage: A disputed fortress in the battle against Mycobacterium tuberculosis. *Front. Microbiol.* 8: 23.

6. CONTRIBUTIONS OF COLLABORATORS

I performed all the experiments presented in this thesis, with the exception of the western blot shown in Figure 19B, which was performed by Dr. Stefania Berton. All data collection and data analyses were performed by me, with help from Dr. Sun and Dr. Berton. Nusrah Rajabalee performed the required modifications to optimize the lentiCRISPR v2 plasmid that I later used to generate the PKR knockout cells. I received extensive feedback from Dr. Sun throughout my master's project and during the writing process of this thesis.

Dr. William Jacobs provided *M. tuberculosis* $mc^2$6206, and Dr. Zakaria Hmama provided the pSMT3 luciferase plasmid. The *Salmonella enterica* serovar Typhimurium and *Listeria monocytogenes* bacterial strains were provided by Dr. Subash Sad. Parts of the work were performed in the University of Ottawa Common Equipment and Technical Service Core and the Cell Biology and Image Acquisition Core.

7. CURRICULUM VITAE

Education

- **University of Ottawa –** MSc in Microbiology and Immunology (2018 – 2021)
- **Queen's University –** BSc in Life Sciences with research specialization in Biomedical Sciences (2014 – 2018)

Scholarships & Awards

- Ontario Graduate Scholarship (2019; 2020 – declined)
- Queen Elizabeth II Graduate Scholarship in Science and Technology (2019 – declined)
- University of Ottawa Excellence Scholarship (2019)
- University of Ottawa Admission Scholarship (2018)
- Queen's University Principal's Scholarship (2014, renewed in 2015)
- University of Ottawa Poster Day Award, 2nd place (2019)
- Microbiology and Immunology Undergraduate Research Award (2018)

Publications

Smyth, R., Berton, S., Rajabalee, N., Chan, T., Sun, J. 2021. Protein Kinase R restricts the intracellular survival of *Mycobacterium tuberculosis* by promoting selective autophagy. *Front. Microbiol.* 11: 613963.

Kourko, O., **Smyth, R**., Cino, D., Seaver, K., Petes, C., Eo Young, S., Basta, S., and K. Gee. 2019. Poly(I:C)-mediated death of human prostate cancer cell lines is induced by interleukin-27 treatment. *J Interferon Cytokine Res* 39: 483-494.

Poster Presentations

Smyth, R., Sun, J. "Regulation of cell death by PKR during *Mycobacterium tuberculosis* infection". University of Ottawa BMI Poster Day, May 2019.

Smyth, R., Petes, C., Odoardi, N., Kourko, O., Gee, K. "Investigating the Effects of IL-27 on Immune-Regulation of Human Prostate Cancer Cells". Queen's University 499 Research Poster Day, March 2018.

Employment

- University of Ottawa (Sun lab) – Undergraduate Research Assistant (2018)
- Donald Family Medicine Clinic – Medical Office Assistant (2017 – 2018)
- The Chandlery Marine Supplies – Retail Associate (2010 – 2018)

Extra-curriculars & Volunteer Experience

- BMI Graduate Student Association – VP Archives (2019 – 2020)
- U of O Student Emergency Response Team – Volunteer first responder (2019 – 2020)
- Woodroffe High School – Volunteer teaching assistant (2018 – 2020)
- Children's Hospital of Eastern Ontario – Volunteer (2012 – 2019)
- ASUS Crohn's and Colitis Committee – Sponsorship Director (2016 – 2018)